BOB WILLIAMS

Engineering Biomechanics of Human Motion

on-line NotesBook Supplement

Engineering Biomechanics of Human Motion

Dr. Robert L. Williams II
Mechanical/Biomedical Engineering
Ohio University

NotesBook Supplement for
ME 4670 / 5670 Engineering Biomechanics of Human Motion

williar4@ohio.edu

www.ohio.edu/mechanical-faculty/williams

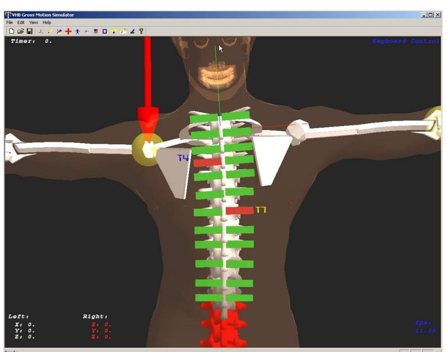

These notes supplement the ME 4670 / ME 5670 NotesBook by Dr. Bob

This document presents supplemental notes to accompany the ME 4670 / 5670 NotesBook. The outline given in the Table of Contents on the next page dovetails with and augments the ME 4670 / 5670 NotesBook outline and thus is incomplete here.

ME 4670 / 5670 Supplement Table of Contents

1. Additional Introductory Material

Some Perspective

Is the study of human biomechanics/kinesiology significant? As human engineers we answer, of course! But let us provide some perspective in terms of the natural history of the universe.

The age of the Universe is approximately 14 billion years (14,000,000,000 years). For convenient scale, let the entire age of the Universe be represented by 14 years. Then:

- The Big Bang happened 14 years ago.
- The Earth is 5 years old.
- Large complex creatures have existed on Earth for the past 7 months.
- The dinosaurs became extinct 3 weeks ago.
- The entire recorded history of human beings covers the past 3 minutes.
- The industrial revolution occurred 6 seconds ago.

So the time humans have been around is insignificant relative to the age of the Earth and the Universe.

An unrelated shocker: during the 20th century, due to advances in mechanized warfare, 3 times the number of soldiers were killed in battle than in the previous 20 centuries combined!

Vitruvian Man

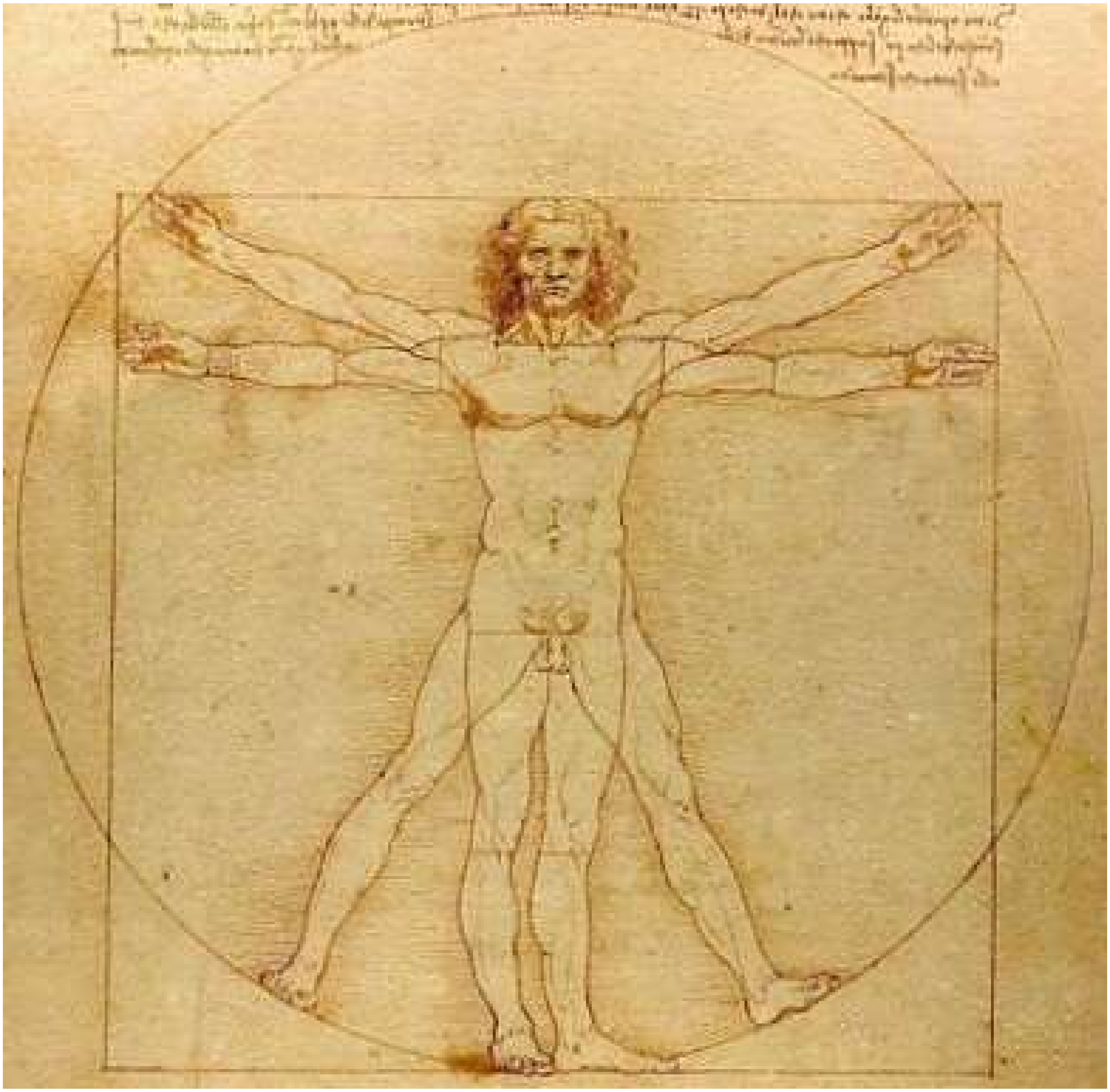

Vitruvian Man, Leonardo da Vinci

"According to Leonardo da Vinci's notes in the accompanying text, written in mirror writing, it was made as a study of the proportions of the (male) human body as described in a treatise by the Ancient Roman architect Vitruvius, who wrote that in the human body:

- a palm is the width of 4 fingers
- a foot is the width of 4 palms
- a cubit[1] is the width of 6 palms
- a man's height is 4 cubits (and thus 24 palms)
- a pace is 4 cubits
- the length of a man's outspread arms is equal to his height
- the distance from the hairline to the bottom of the chin is 1/10 of a man's height
- the distance from the top of the head to the bottom of the chin is 1/8 of the height
- the maximum width of the shoulders is 1/4 of a man's height
- the distance from the elbow to the tip of the hand is 1/5 of a man's height
- the distance from the elbow to the armpit is 1/8 of a man's height
- the length of the hand is 1/10 of a man's height
- the distance from the bottom of the chin to the nose is 1/3 of the head length
- the distance from the hairline to the eyebrows is 1/3 of the length of the face
- the length of the ear is 1/3 of the length of the face

Leonardo da Vinci is clearly illustrating Vitruvius De Architectura 3.1.3 which reads:

The navel is naturally placed in the centre of the human body, and, if in a man lying with his face upward, and his hands and feet extended, from his navel as the centre, a circle be described, it will touch his fingers and toes. It is not alone by a circle, that the human body is thus circumscribed, as may be seen by placing it within a square. For measuring from the feet to the crown of the head, and then across the arms fully extended, we find the latter measure equal to the former; so that lines at right angles to each other, enclosing the figure, will form a square."

leonardo-davinci.org

[1] The **cubit** is the earliest known unit of length, which originated between 2800 and 2300 BCE. A cubit is approximately 43 to 56 cm (17 to 22 in) long, which is about the length of the human forearm measured from the tip of the middle finger to the elbow. Microsoft Encarta Encyclopedia on-line.

Vitruvian Man Parodies

Vitruvian Jam

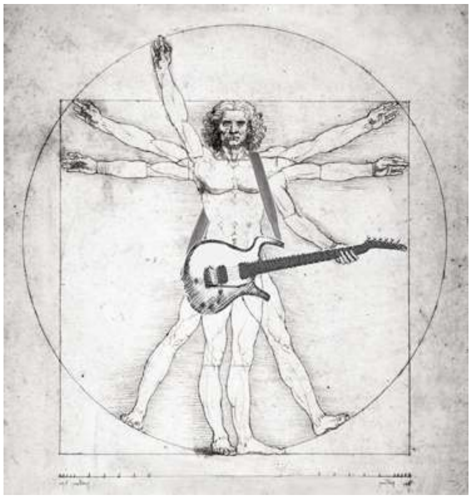

Vitruvian Homer

Vitruvian Astronaut

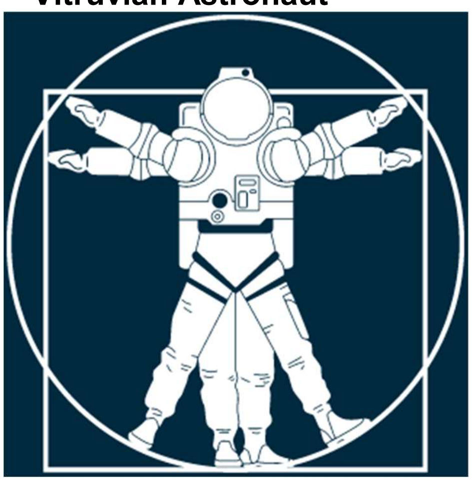

Vitruvian Storm Trooper

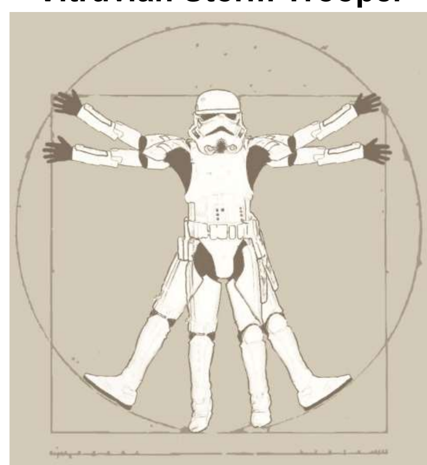

Vitruvian TMNT

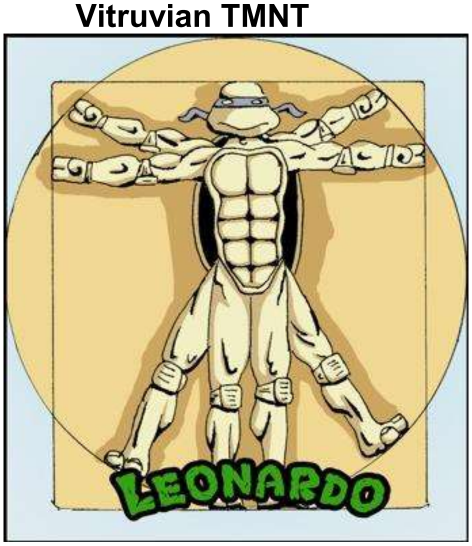

Vitruvian Badger

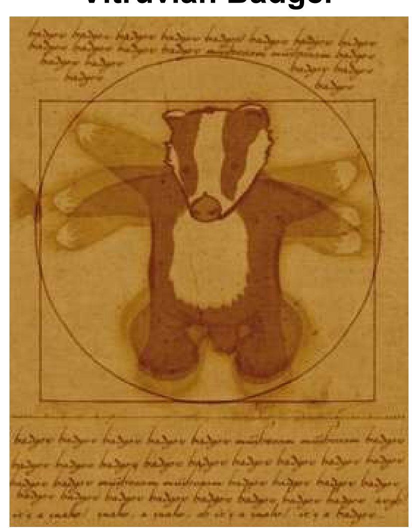


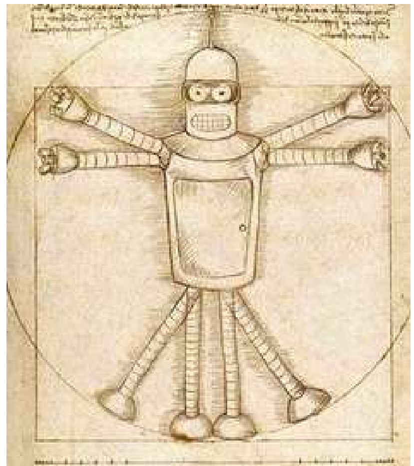
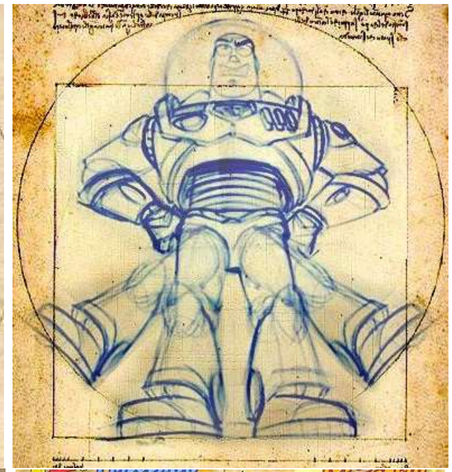
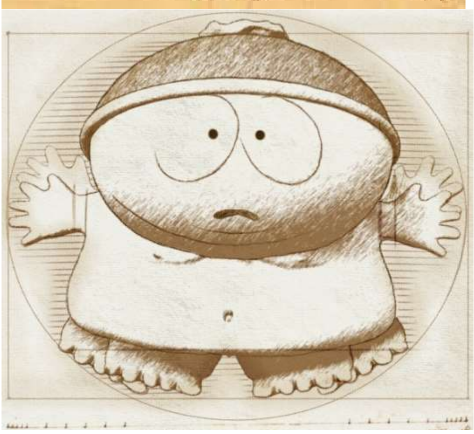
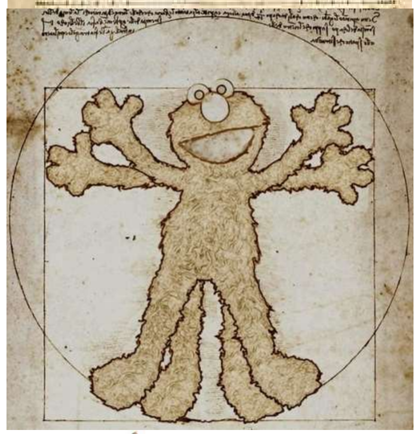
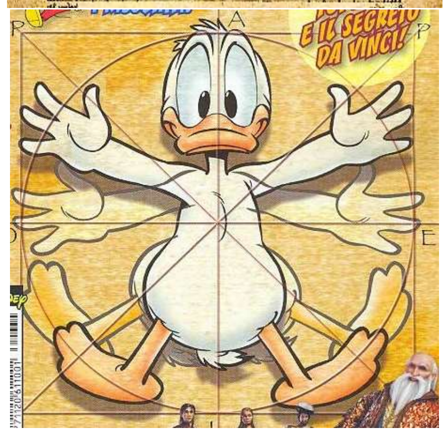
E IL SEGRETO DA VINCI!
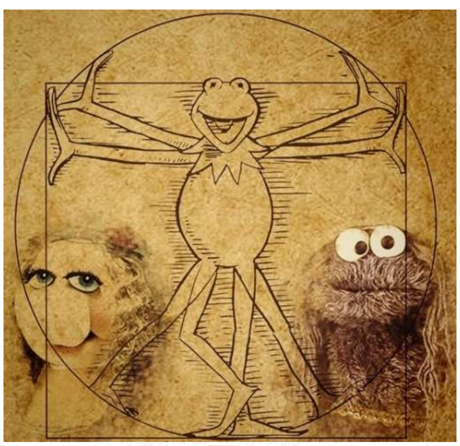
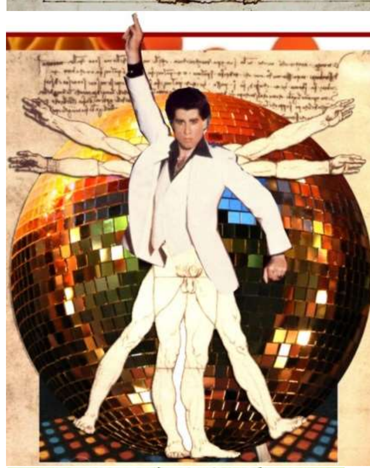
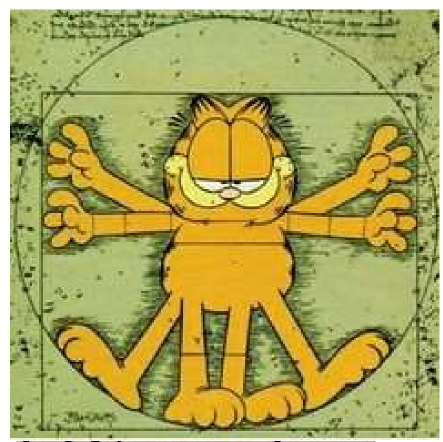
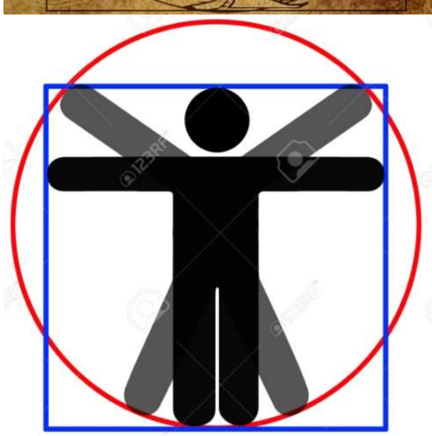
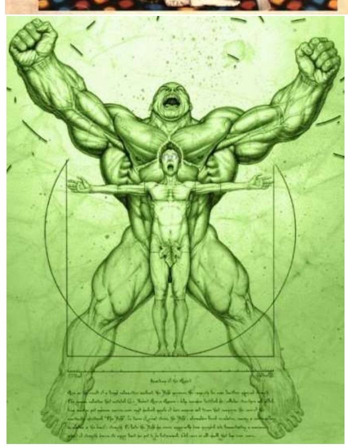

Vitruvian
Hello Kitty

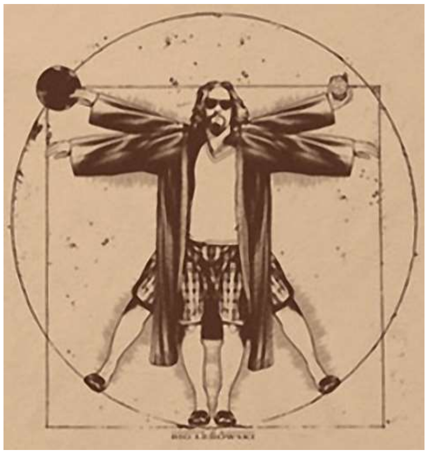

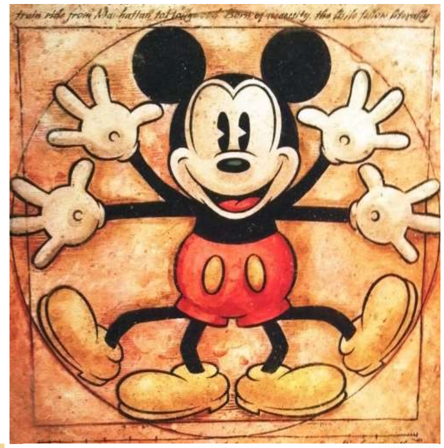
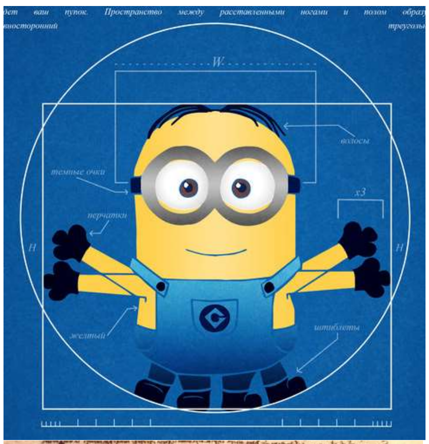
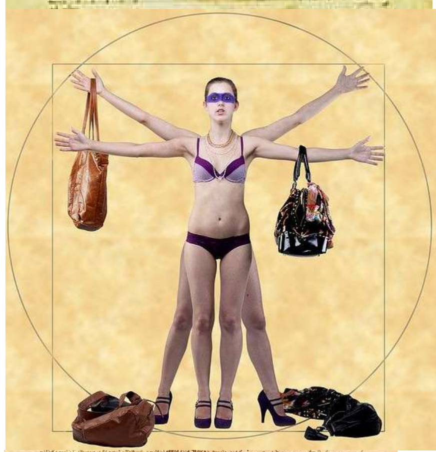
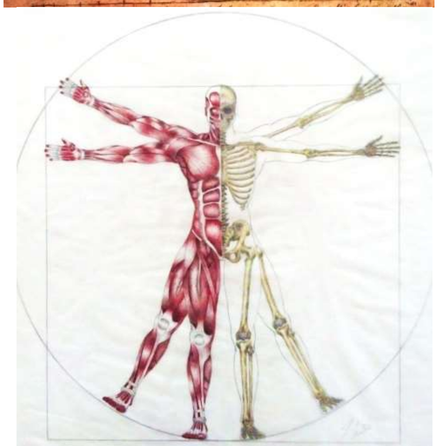
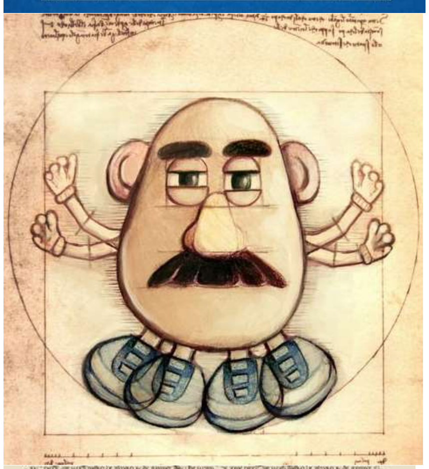
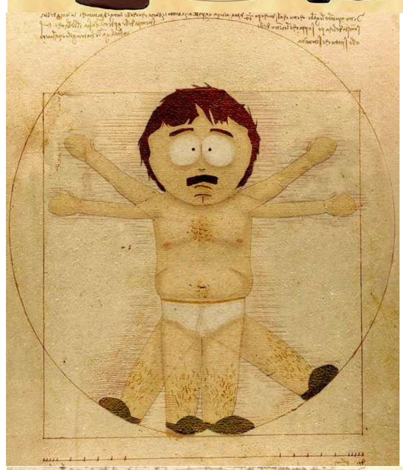

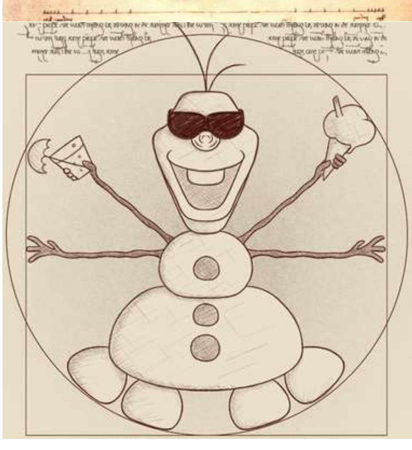
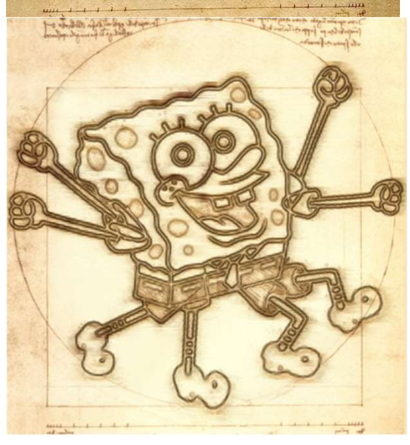
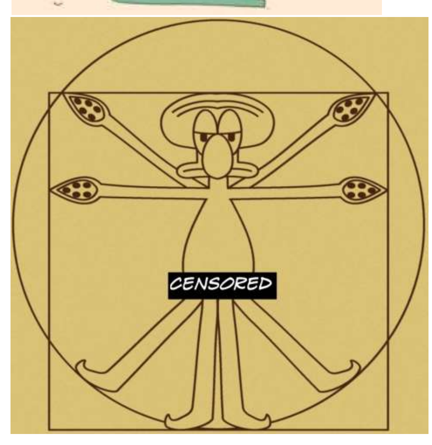
CENSORED

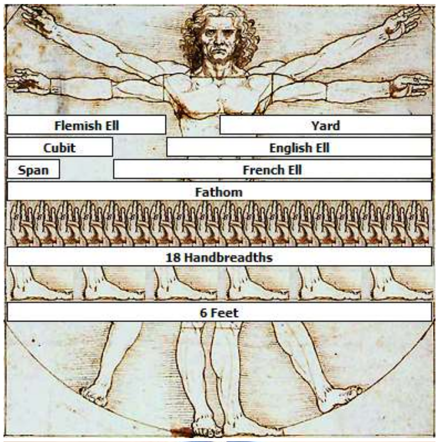
Flemish Ell
Yard
Cubit
English Ell
Span
French Ell
Fathom
18 Handbreadths
6 Feet

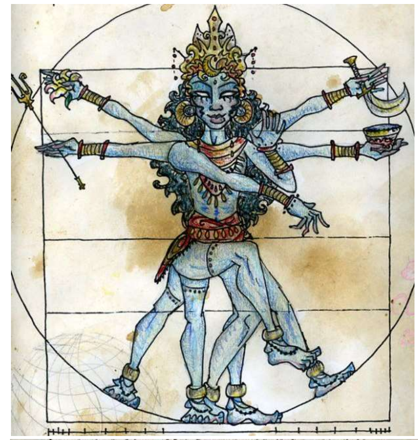

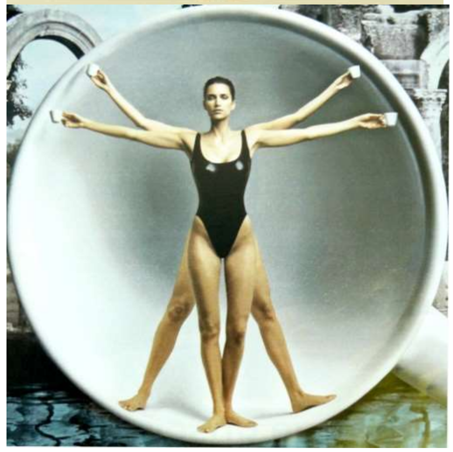

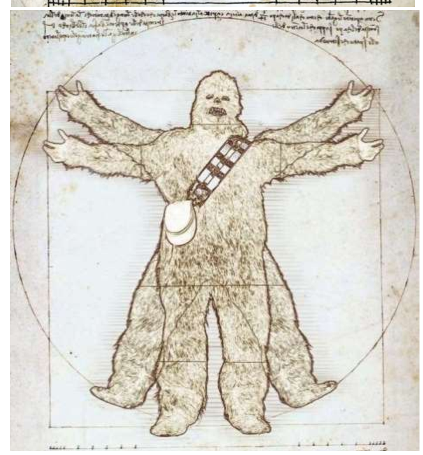

Anatomy Art by Leonardo da Vinci

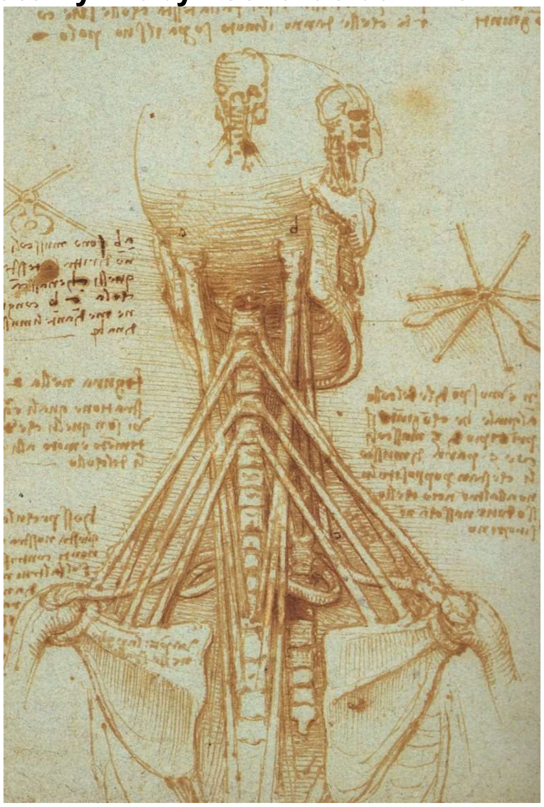

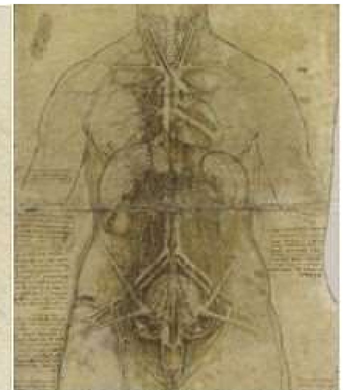

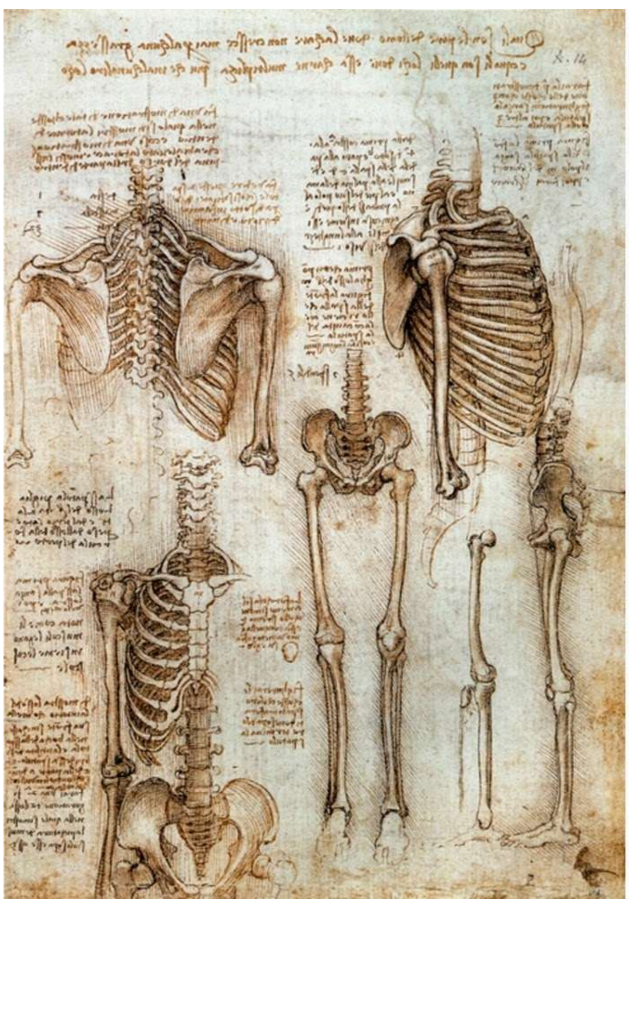

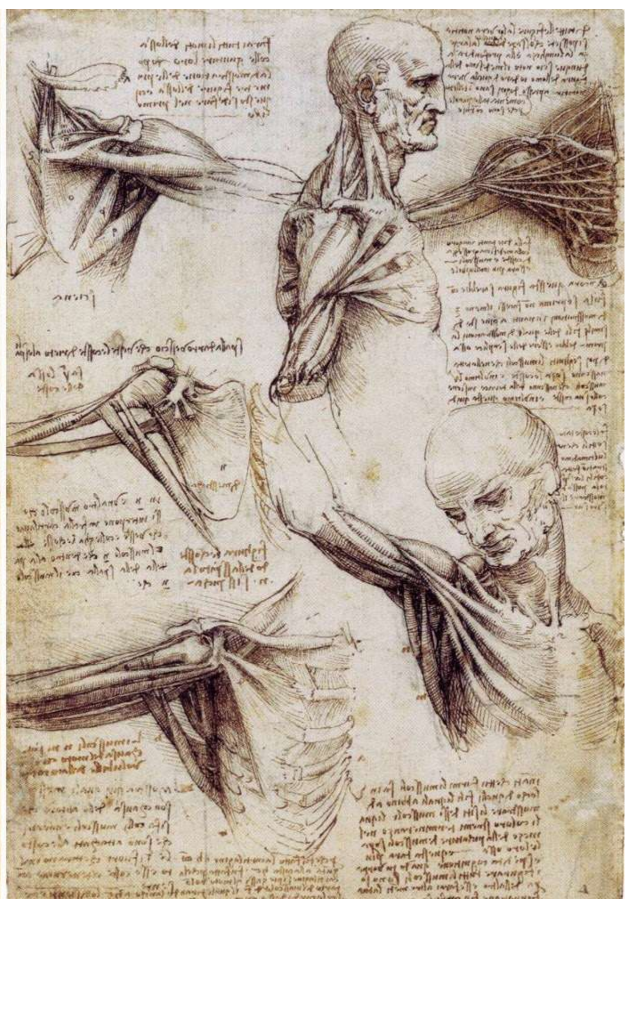

Bodies: The Exhibition – Images

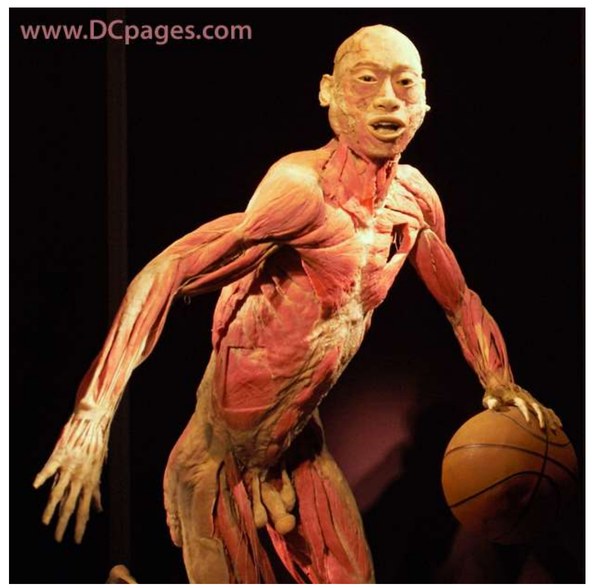

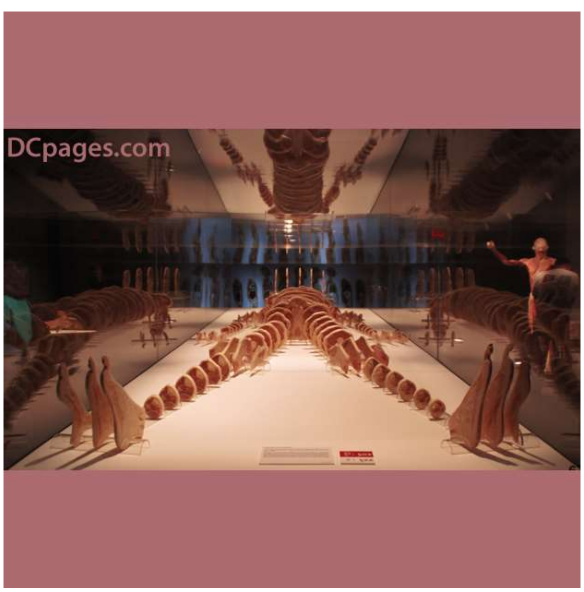

Interesting Human Facts

Human **bone** is 5 times stronger than steel by weight. Yet it is flexible, self-healing, and it provides many useful functions in addition to structural support. How is it so strong?

Tendons are up to 500 times stronger than the skeletal muscles they connect to the bones. They protect their muscles from ripping.

Cardiac **muscles** work autonomously and rest only in between beats. They pump an average of 3,027,456,000 times during an 80-year lifespan, assuming 72 bpm (The Grateful Dead, 'U.S. Blues'). The heart provides life-giving oxygen and fuel to all cells, none of which are more than a few microns from a blood vessel. This system also collects wastes and CO_2.

Synovial fluid in our joints has very low friction. Engineers are trying to duplicate it synthetically for lubricating machines.

The **human body** is the most amazing, complex, interconnected, efficient machine ever devised by (choose one) ________________________.

a. Evolution
b. The Creator
c. Intelligent Design
d. Random Happenstance

Arthrokinematics is the study of the movement of bone surfaces within a joint.

Amazing Brain Facts

- The human brain is faster, more powerful, and more capable than the best computer (100 trillion instructions per second; the fastest computer currently measures in MIPS, 2008).
- The brain weighs 3-4 lbs. and consumes 1/5 of our caloric intake.
- 70% of the brain is dedicated to vision (RGB cones see 10M colors; B&W rods detect motion; the human is capable of 180 *deg* eye motion in ¼ *sec*). Blind persons adapt this power to increased sensitivity for hearing and touch.
- The human brain is 2/3 fat. The protective sheath covering neurons is 70% fat. Eating fatty fish, green leafy vegetables, olive oil, avocados, chia seeds, flax seeds, and nuts replenish your neurons and brain cells.
- Loss of fatty acids EPA and DHA are linked to depression, plus Parkinson's and Alzheimer's diseases.
- You have 70,000 thoughts per day (for males, we know what 60,000 of these thoughts are!).
- The conscious mind only controls 5% of the brain during the day, while the subconscious mind controls 95% of our thoughts.
- Thoughts cause biological and physiological effects. That is, mental input is physically real to the body.
- Listening to music has been proven to strengthen the brain and physically change brain structure.
- Meditation is proven to increase IQ, relieve stress, and enable higher learning.
- Engineers have imaged the mouse brain to unprecedented resolution in 2014, requiring 450,000 terabytes of storage. A single human brain imaged at the same resolution would require 1.3B terabytes. The global digital storage in 2012 was 2.7B terabytes! (NGM, February 2014)

Human Brain Grows and Shrinks Over Lifetime

The human brain volume and mass change over years of life. This is shown in the images below, averaged over 120,000 MRI brain scans. The next two images present preliminary results, as of April 2022.

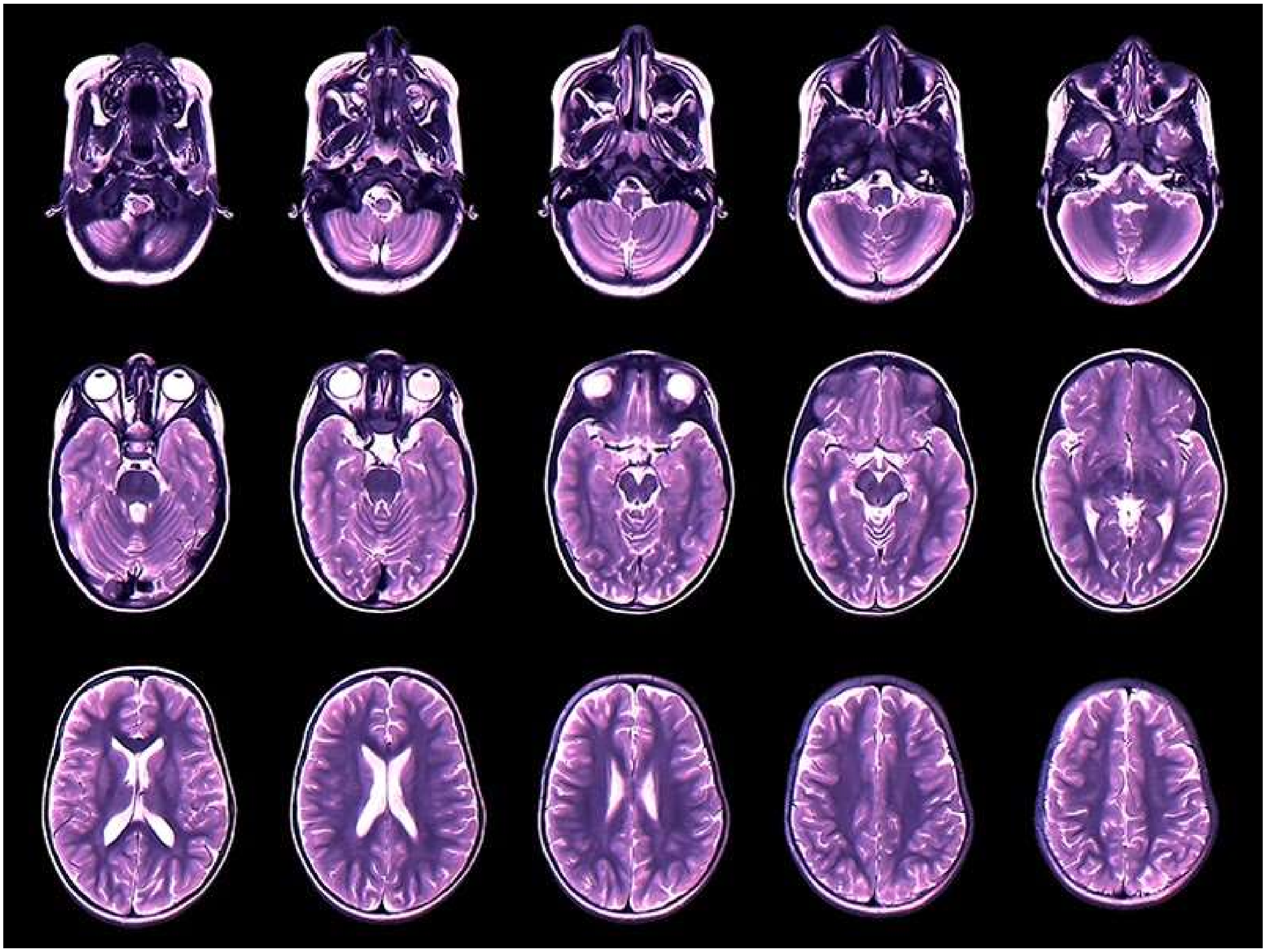

Human Brain Growth Images

https://www.nature.com/articles/d41586-022-00971-1?utm_source=join1440&utm_medium=email

In a regrettable oversight, this reference failed to provide the age legend for the above images. It appears that the top row (before the eyes appear) is from in-utero data. See the next page, from the same reference, for a much better handle on the lifetime ages involved.

BRAIN CHANGE

Researchers analysed more than 120,000 brain scans to assemble the most comprehensive growth chart of the brain so far. White- and grey-matter volume and mean cortical thickness (the width of the grey matter) increase rapidly early in development, whereas ventricular volume (the amount of cerebrospinal fluid in the brain) increases rapidly later in life.

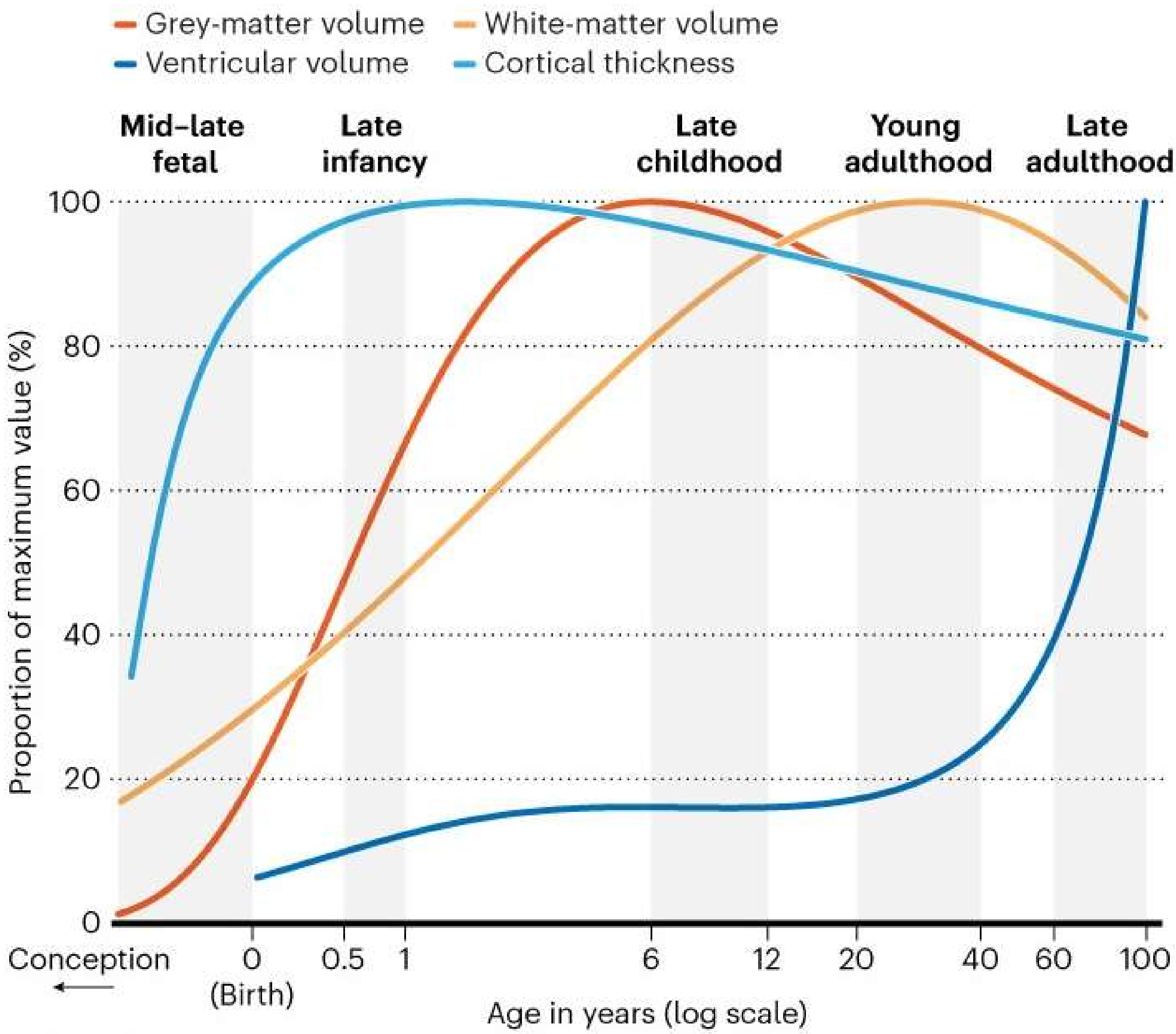

Data shown are median values.

https://www.nature.com/articles/d41586-022-00971-1?utm_source=join1440&utm_medium=email

Brain-Controlled Exoskeleton for Paraplegics

"People with spinal cord injuries can't move because the brain and body no longer communicate. Scientists hope to restore motion with a mechanical skeleton controlled by the wearer's thoughts. It's a daunting challenge: Hundreds of sensors must be implanted in the brain to send commands to the exoskeleton. Signals must also travel in reverse, from touch sensors telling the brain where the body is in space."

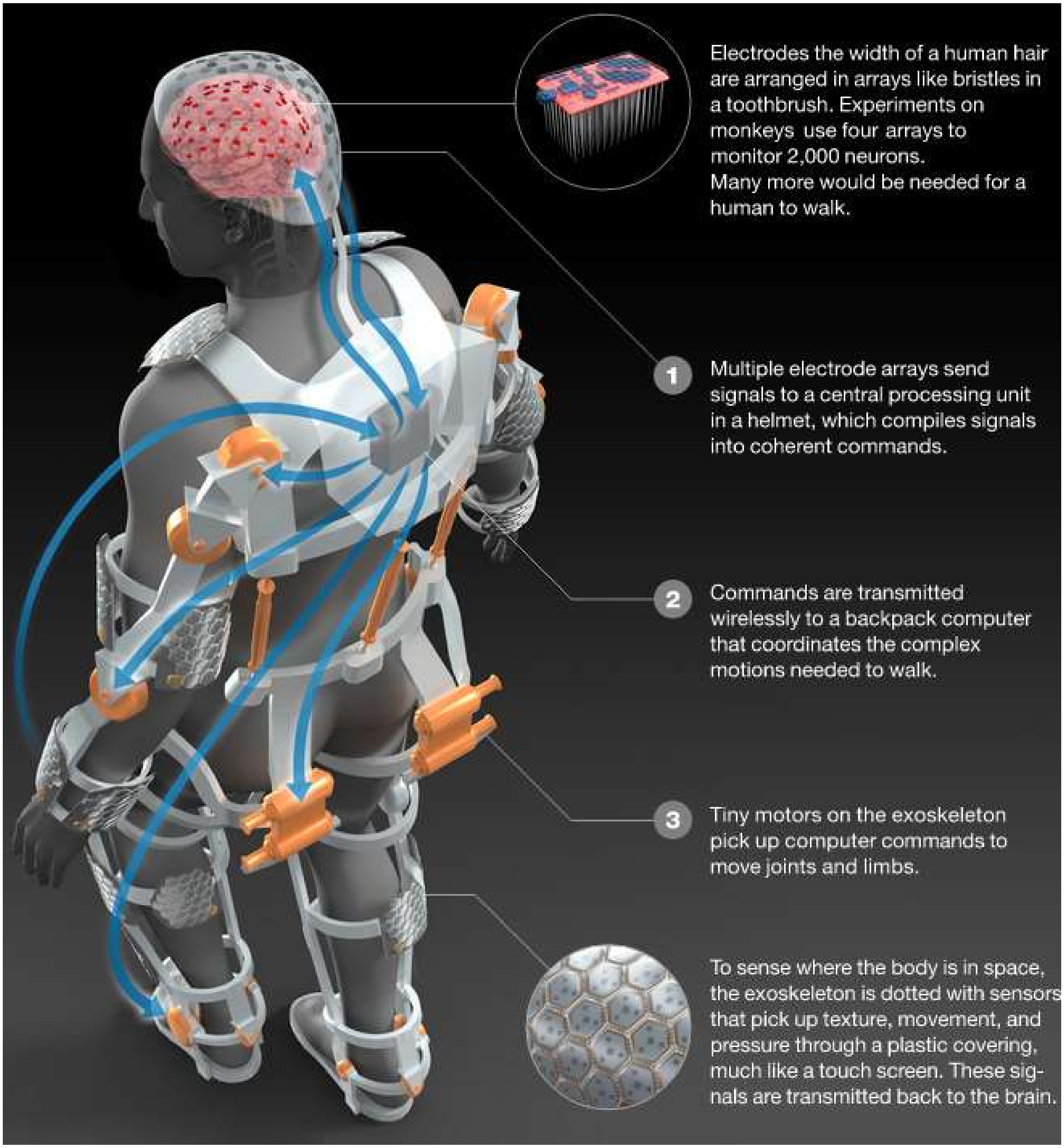

National Geographic Magazine, February 2014

Walk Again Project

Miguel Nicolelis' lab of Duke University plans to have a paralyzed teenager perform the opening kick for the 2014 World Cup in Brazil.

virtualreality.duke.edu

Did You Know?

- A human being loses an average of 40 to 100 strands of hair a day.
- A cough releases an explosive charge of air that moves at speeds up to 60 mph.
- Every time you lick a stamp, you consume 1/10 of a calorie.
- A fetus acquires fingerprints at the age of three months.
- A sneeze can exceed the speed of 100 mph.
- Every person has a unique tongue print.
- The risk of heart attack is higher on Monday than any other day of the week.
- After spending hours working at a computer display, look at a blank piece of white paper. It will probably appear pink.
- An average human drinks about 16,000 gallons of water in a lifetime.
- A fingernail or toenail takes about 6 months to grow from base to tip.
- An average human scalp has 100,000 hairs.
- It takes 17 muscles to smile and 43 to frown.
- Babies are born with 300 bones, but by adulthood we have only 206 in our bodies.
- Beards are the fastest growing hairs on the human body. If the average man never trimmed his beard, it would grow to nearly 30 feet long in his lifetime.
- Each square inch of human skin consists of twenty feet of blood vessels.
- Every square inch of the human body has an average of 32 million bacteria on it.
- Fingernails grow faster than toenails.
- Humans shed about 600,000 particles of skin every hour - about 1.5 pounds a year. By 70 years of age, an average person will have lost 105 pounds of skin.
- The **External Auditory Meatus** is the tube from the outer ear to the middle ear (*meatus* is Latin for passage).

Amazing Lung Facts

- At rest, a person breathes about 14 to 16 times per minute. After exercise it could increase to over 60 times per minute.
- New babies at rest breathe between 40 and 50 times per minute. By age five it decreases to around 25 times per minute.
- The total surface area of the alveoli (tiny air sacs in the lungs) is the size of a tennis court.
- The lungs are the only organ in the body that can float on water.
- The lungs produce a detergent-like substance which reduces the surface tension of the fluid lining, allowing air in.

Amazing Heart Facts

- Your heart is about the same size as your fist.
- An average adult body contains about five quarts of blood.
- All the blood vessels in the body joined end to end would stretch 62,000 miles (2½ times around the earth).
- The heart circulates the body's blood supply about 1,000 times each day.
- The heart pumps the equivalent of 5,000 to 6,000 quarts of blood each day.

Bodies: The Exhibition

Facts regarding the Five Senses

These are all adapted from Parade Magazine, July 29, 2012.

Sight

- 20/20 vision, the standard for normal sight ability, means one can see a reference image clearly at 20 feet. 20/100 vision means another person must stand 5 times closer, i.e. 4 feet, to see the same image.
- The world record for vision was set by Dennis Levi in 1985, identifying a bright line ¼” thick from a distance of one mile.
- Sitting too close to the TV or reading in dim light will not damage your vision. Wrong again, mom!
- One in 20 men is at least partially colorblind. Colorblindness is 10 times more common in men than in women. All babies are color-blind at birth.

Hearing

- Even small noises cause the pupil to dilate, blurring vision temporarily.
- A large meal temporarily reduces hearing acuity.
- Human hearing is good at detecting the direction of sounds, but not as good at detecting the distance of sounds.
- Most humans can detect sounds from the front more easily than from the back.
- 90% of a young child’s knowledge comes from hearing background conversation. Over one third of children with even a slight hearing loss will fail at least one grade in school.
- Tinnitus is a buzzing or ringing sound in the ears that affects 15% of the U.S. population. It is first described on clay tablets from Assyria.

Touch

- The skin is the human body’s largest organ and contains over 4 million sensory receptors.
- The most sensitive areas include the lips, back of the neck, fingertips, and soles of the feet. The least sensitive is the middle of the back.
- Being touched can reduce stress by lowering levels of hormones such as cortisol.
- Pain is the body’s warning system. Humans have more pain receptors than for any other sensation.
- Thermoreceptors stop being stimulated when the surface skin temperature is below 41 deg F (why your body feels numb in the cold) or is above 113 deg F (when pain receptors take over to avoid burns).

Taste

- The tongue taste map where specific tastes (sweet, bitter, salty, sour) have receptors in specific locations (tip, back, and sides, respectively) is a myth. Receptors for these specific tastes exist, but they are distributed across the tongue.
- Phillipe Besnard recently discovered that some taste buds respond to the flavor of fat (no shit!).
- About ¼ of Americans are super-tasters and another ¼ are non-tasters. Super-tasters have more taste buds and are sensitive bitter foods. Non-tasters have fewer taste buds and have a high tolerance for spicy foods.
- Taste buds die and regenerate every 10 days. Aging cause this cycle to slow down, dulling the ability to taste. Some older people tend to like foods saltier and spicier.

Smell

- Taste is strongly linked to smell – taste is about 75% smell.
- The sense of smell is weakest in the morning and gets stronger as the day progresses.
- A recent study showed people in a citrus-scented room cooperated more in trust experiments and even offered to make charitable donations.
- Your sense of smell becomes more acute when you are hungry.
- The ability to detect scents is boosted by estrogen, which is why women (especially pregnant women) tend to have more sensitive noses than men.
- Astronauts in space tend to lose their sense of smell and taste. Due to the lack of gravity, their sinuses fill up with fluid, causing stuffiness which interferes with the smell receptors in the nose.

Ten ways to sharpen your senses

1. Use sunglasses with 100% UV blocking to protect your eyes from cataracts and macular degeneration.
2. Take regular breaks from activities that require prolonged staring. Otherwise your eyes can dry out and cause blurred vision.
3. Relax your jaw or smile to hear faint sounds.
4. Practice listening to identify all sounds around you and where they came from.
5. Close your eyes to sharpen hearing, since vision takes up so much brainpower.
6. Spend an hour in a completely silent place (and that would be where?!?).
7. Breathe in warm moist air before eating to clear your nasal passages and enable smell receptors to enhance the tasting of flavors.
8. Alternate foods with each bite to keep your palate awake.
9. Limit salt and sugar since one can become desensitized to these flavors.
10. Quit smoking since cigarettes damage your taste buds.

The Sixth Sense?

Any second-grader will tell you there are five human senses: **sight**, **hearing**, **touch**, **taste**, and **smell**. But should there be a sixth sense? No, I am not referring to ESP or intuition:

The Sense of Motion

Humans sense position and velocity of motion via sight. Healthy humans have a keen sense of acceleration via the semicircular canals in both ears. This is the **vestibular system**. It could be considered a haptic (i.e. touch) sense, but perhaps it should be identified as its own sense. Tiny clumps of hairs in the inner hear play a major role in the vestibular system sensing.

The semicircular canals have 3 perpendicular axes for sensing angular roll, pitch, and yaw in 3D.

The inner ear otoliths (literally, ear-stones) have 2 planes for sensing translational motion in 3D.

See Section 4.1.5 in the ME 4670 / 5670 NotesBook for more information regarding the human acceleration sensing system.

1. Holding your head fixed, track your hand as it moves quickly side to side.

2. Now reverse this (hold your hand fixed and move your head quickly side to side, either translating or rotating will work). What do you observe and how is it different from 1?

Spin a volunteer vigorously on a rotating chair for 10 seconds. Freeze the subject and then observe their eyes. What happens? **Nystagmus**.

50 Interesting Human Body Attributes

The following made the rounds of the Internet and e-mail in October 2012.

The Human Body is a treasure trove of mysteries, one that still confounds doctors and scientists about its working details. It is not an overstatement to say that every part of your body is interesting. Here are fifty facts about your body.

1. It is possible for your body to survive without a surprisingly large fraction of its internal organs. Even if you lose your stomach, your spleen, 75% of your liver, 80% of your intestines, one kidney, one lung, and virtually every organ from your pelvic and groin area, you wouldn't be very healthy, but you would live.

2. During your lifetime, you will produce enough saliva to fill two swimming pools. Actually, saliva is more important than you realize: if your saliva cannot dissolve something, you cannot taste it.

3. The largest cell in the human body is the female egg and the smallest is the male sperm. The egg is the only cell in the body that is visible by the naked eye.

4. The strongest muscle in the human body is the tongue and the hardest bone is the jawbone.

5. Human feet have 52 bones, accounting for one quarter of all the human body's bones.

6. Feet have 500,000 sweat glands and can produce more than a pint of sweat a day.

7. The acid in your stomach is strong enough to dissolve razor blades. The reason it doesn't eat away at your stomach is that the cells of your stomach wall renew themselves so frequently that you get a new stomach lining every three to four days.

8. The human lungs contain approximately 2,400 km (1,500 mi) of airways and 300 to 500 million hollow cavities, having a total surface area of about 70 m^2, the area of one side of a tennis court. If all of the capillaries that surround the lung cavities were unwound and laid end to end, they would extend for 992 km. Your left lung is smaller than your right lung to make room for your heart.

9. Sneezes regularly exceed 100 mph, while coughs clock in at about 60 mph.

10. Your body gives off enough heat in 30 minutes to bring half a gallon of water to a boil.

11. Your body has enough iron in it to make a nail 3 inches long.

12. Earwax production is necessary for good ear health. It protects the delicate inner ear from bacteria, fungus, dirt and even insects. It also cleans and lubricates the ear canal.

13. Everyone has a unique smell, except for identical twins, who smell the same.

14. Your teeth start growing 6 months before you are born. This is why one out of every 2,000 newborn infants has a tooth when they are born.

15. A baby's head is ¼ of its total length, but by the age of 25 will only be one-eighth of its total length. This is because people's heads grow at a much slower rate than the rest of their bodies.

16. Babies are born with 300 bones, but by adulthood the number is reduced to 206. Some of the bones, like skull bones, get fused into each other, bringing down the total number.

17. It is not possible to tickle yourself. This is because when you attempt to tickle yourself you are totally aware of the exact time and manner in which the tickling will occur, unlike when someone else tickles you.

18. Less than one third of the human race has 20-20 vision. This means that two out of three people cannot see perfectly.

19. Your nose can remember 50,000 different scents. But if you are a woman, you are a better smeller than men, and will remain a better smeller throughout your life. Not to mention you will smell better.

20. The human body is estimated to have 60,000 miles of blood vessels.

21. The three things pregnant women dream most of during their first trimester are frogs, worms and potted plants. Scientists have no idea why this is so, but attribute it to the growing imbalance of hormones in the body during pregnancy.

22. The life span of a human hair is 3 to 7 years on average. Every day the average person loses 60-100 strands of hair. But don't worry, you must lose over 50% of your scalp hairs before it is apparent to anyone.

23. The human brain cell can hold 5 times as much information as an encyclopedia. Your brain uses 20% of the oxygen that enters your bloodstream, and is itself made up of 80% water. Though it interprets pain signals from the rest of the body, the brain itself cannot feel pain.

24. The tooth is the only part of the human body that can't repair itself.

25. Your eyes are always the same size from birth but your nose and ears never stop growing.

26. By 60 years of age, 60% of men and 40% of women will snore.

27. We are about 1 cm taller in the morning than in the evening, because during normal activities during the day, the cartilage in our knees, spine, and other areas slowly compress.

28. The brain operates on the same amount of power as 10-watt light bulb, even while you are sleeping. In fact, the brain is much more active at night than during the day.

29. Nerve impulses to and from the brain travel as fast as 170 miles per hour. Neurons continue to grow throughout human life. Information travels at different speeds within different types of neurons.

30. It is a fact that people who dream more often and more vividly, on an average have a higher IQ.

31. The fastest growing nail is on the middle finger.

32. Facial hair grows faster than any other hair on the body. This is true for men as well as women.

33. There are as many hairs per square inch on your body as a chimpanzee has.

34. A human fetus acquires fingerprints at the age of three months.

35. By the age of 60, most people will have lost about half their taste buds.

36. About 32 million bacteria call every inch of your skin home. But don’t worry, a majority of these are harmless or even helpful bacteria.

37. The colder the room you sleep in, the higher the chances are that you’ll have a bad dream.

38. Human lips have a reddish color because of the great concentration of tiny capillaries just below the skin.

39. Three hundred million cells die in the human body every minute.

40. Like fingerprints, every individual has a unique tongue print that can be used for identification.

41. A human head remains conscious for about 15 to 20 seconds after it has been decapitated.

42. It takes 17 muscles to smile and 43 to frown.

43. Humans can make do longer without food than without sleep. With water, the average human can survive 1-2 months without food depending on body fat and other factors. Sleep-deprived people, however, start experiencing radical personality and psychological changes after only a few sleepless days. The longest time anyone has ever gone without sleep is 11 days, at the end of which the experimenter was awake, but stumbled over words, hallucinated and often forgot what he was doing.

44. The most common blood type in the world is Type O. The rarest blood type, A-H or Bombay blood, due to the location of its discovery, has been found in less than hundred people since it was discovered.

45. Every human spent about half an hour after being conceived as a single cell. Shortly afterward, the cells begin rapidly dividing and begin forming the components of a tiny embryo.

46. Right-handed people live, on average, nine years longer than left-handed people do. This is largely due to the fact that a majority of the machines and tools we use on a daily basis are designed for those who are right handed, making them somewhat dangerous for lefties to use and resulting in thousands of accidents and deaths each year.

47. Your ears secrete more earwax when you are afraid than when you aren't.

48. Koalas and primates are the only animals with unique fingerprints.

49. Humans are the only animals to produce emotional tears.

50. The human heart creates enough pressure to squirt blood 30 feet in the air.

Human Microbiology

- There are about **10,000,000,000,000** (ten trillion, 1×10^{13}) **cells** in the adult human body.

- Of this number, **only 10% are human cells!** That is, 90% are foreign microbes, most of which are harmless or beneficial. This amazing percentage is by number of cells, not by weight or volume (muscle and bone cells are all human and relatively heavy).

- In an average adult human all foreign microbes can weigh as much as their brain, about 3-4 pounds.

- Most of these **symbiotic microbes** are on the skin surface, in orifices, or in the digestive tract. The human internal organs and bloodstream are generally a sterile environment, with 100% human cells (nominally).

- The adult human **stool** (feces, aka poop, dung, guano, excrement, shit, merde, solid waste, caca, number 2, etc.) is composed of 70% dead foreign digestive microbes by dry weight. These regenerate, reproducing every 20 minutes.

- People who **overwash & scrub** to stay germ-free may actually be doing themselves a disservice, as they kill the good germs on their skin along with any bad ones.

- **Antibiotics** have saved millions of lives during the past century; however, today they are being overused. The bad bacterial targets of antibiotics can quickly evolve to resist antibiotics. Some patients may not complete the full course of medicine. Also, antibiotics kill the good microbes along with the bad – this is why stomach problems may be a side-effect of antibiotics. For example, the disorder C-diff (clostridium difficile colitis) is the death of the digestive bacteria C-difficile, which can even lead to death!

- **Probiotics** is a diet supplementary tool to replenish the good microbes in your digestive tract.

- New research is suggesting the human body and its symbiotic foreign microbes be approached as an **ecosystem** as a better means of maintaining balance and health. Previously medical science has largely ignored these bacteria (or interpreted harmless or beneficial interactions as bad) as they only add up to a few pounds of body weight.

- The number of non-human bacteria each human being contains is about equal to 1000 times the number of humans currently living on earth.

Gears found in nature for the first time

In Section 1.4 of the ME 4670 / 5670 NotesBook it states that the only simple machine found in the human body is the lever (all three classes appear). Some physiologists also consider pulley systems to exist at the human knee and fingers.

For the first time in 2013 it was discovered that a certain tiny jumping insect has evolved biological gears to enable extreme (powerful, high acceleration) jumping during its juvenile period.

According to scientists at the University of Cambridge[2], the juvenile ***Issus*** insect has hind-leg joints with curved cog-like strips of opposing teeth that mesh, rotating like mechanical gears to synchronize the animal's legs when it launches. Both sides have 10-12 teeth for a 1:1 gear ratio. The gears ensure that both hind legs move at the same angular velocities to propel the body without yaw rotation, to avoid catastrophic loss of control.

The Issus, a plant-hopping insect found in gardens across Europe, loses this feature at adulthood, possibly because if a tooth is damaged while young, the next molt can repair it, which is impossible after adulthood.

Juvenile Issus Insect

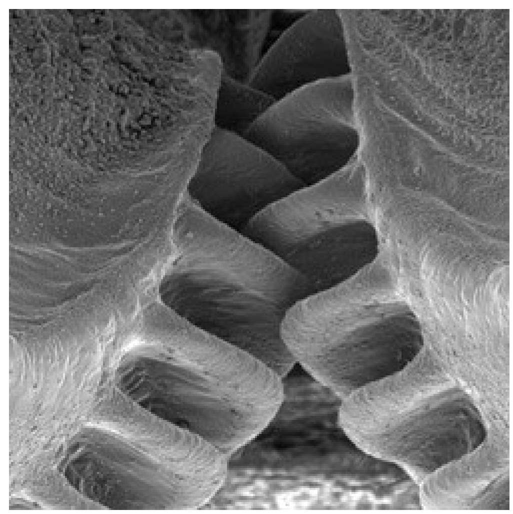

Biological Hind-leg Gears

[2] M. Burrows and G. Sutton, 2013, Interacting Gears Synchronize Propulsive Leg Movements in a Jumping Insect, Science, 341 (6151): 1254-1256.

Parrotfish jaw has 4-bar mechanism for bite force amplification

Parrotfish are found in shallow tropical waters around coral reefs. They eat algae inside the coral by eating the coral and grinding to release algae. The parrotfish is named its teeth, packed tightly forming a parrot-like beak.

To eat the calcium carbonate coral skeleton, parrotfish need jaws with a very powerful biting force. Parrotfish have a four-bar mechanism in their jaws to obtain significant mechanical advantage when the jaws are closing.

Bleeker's Parrotfish (Chlorurus bleeker)

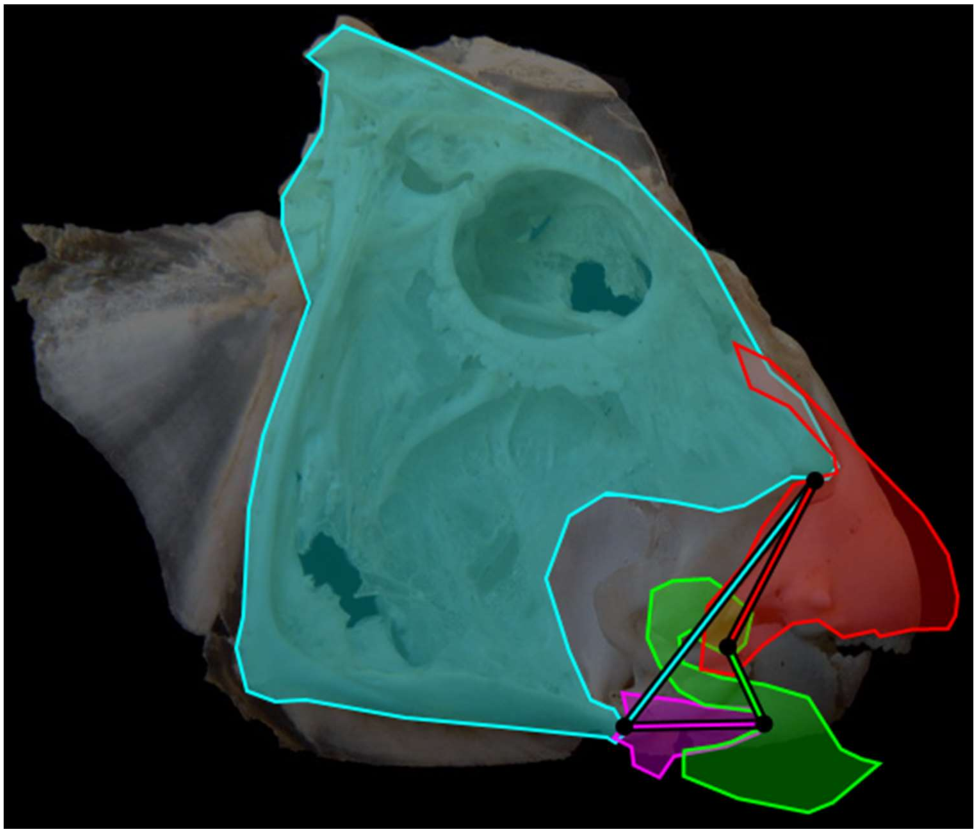

Parrotfish Jaw Four-bar Mechanism

Moray eel has second set of jaws

From the Freakin' Fascinatin' Files

or

Hollywood Imitates Nature

The **Moray Eel** (**Muraenidae**), an effective predator, has a secondary, retractable, upper and lower set of jaws and teeth. Called the **Pharyngeal Jaw**, this can be seen in the figure. This evolutionary adaptation helps grip prey as the main jaws let go to rotate the prey head-first into the eel's mouth.

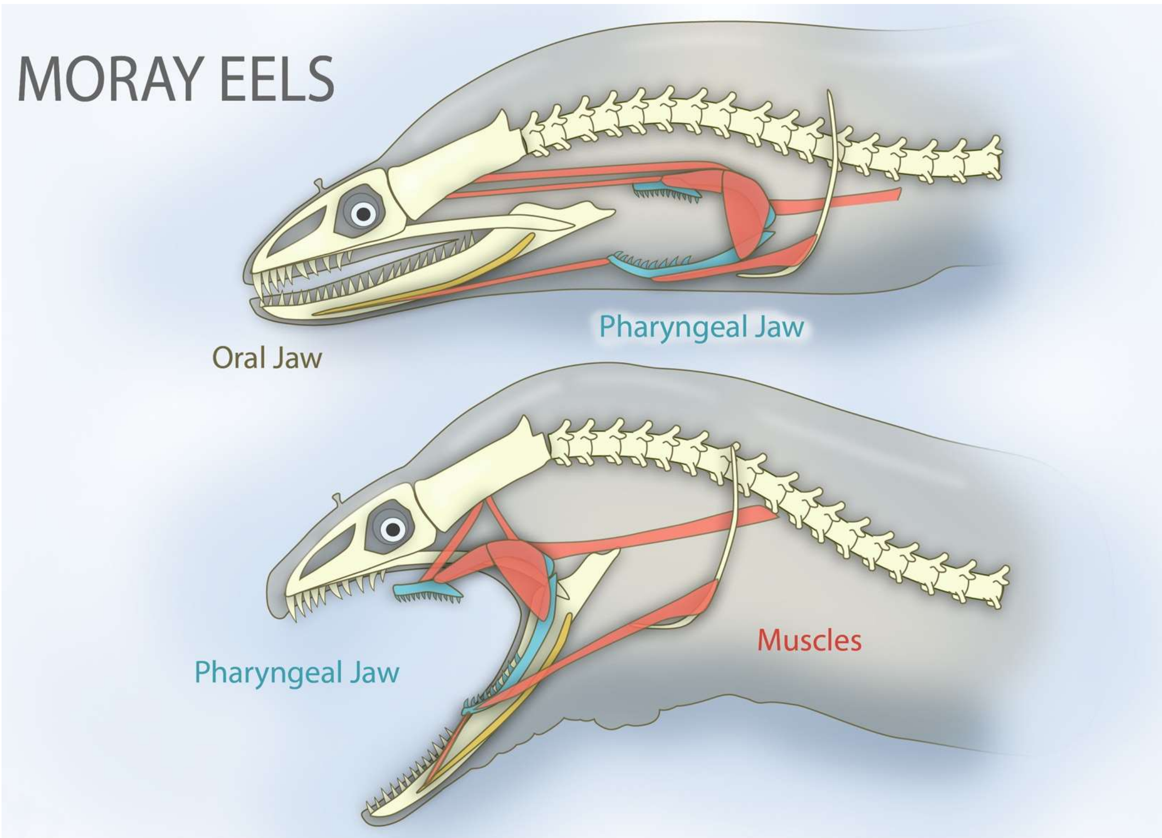

wikipedia/commons/e/e3/Pharyngeal_jaws_of_moray_eels

For a great National Geographic YouTube video on this topic see:

www.youtube.com/watch?v=VAampciNSyo#action=share

I would definitely watch the whole thing. But the **Pharyngeal Jaw** activation animation starts at 1:45.

Biology and Mathematics: Population Modeling

Mathematicians have modeled the population of a single species in a closed ecosystem with the following equation[3]:

$$P_{k+1} = \gamma P_k (1 - P_k)$$

Where the normalized population P is a maximum of 1 for 100% population in this equation, P_{k+1} is the normalized population at the next time step $k + 1$, P_k is the normalized population at the current time step k (the time step units are counts, which can be associated with real-time in seconds, days, years, etc.), and γ is a normalized population propagation constant:

$0 < \gamma < 1$	results in extinction (zero population)
$1 < \gamma < 3$	results in smooth population change
$3 < \gamma < 3.57$	results in stable population oscillations
$3.57 < \gamma < \infty$	results in chaotic population oscillations

For the simulation shown in the graphs below, and initial normalized population of $P_k = 0.3$ is assumed.

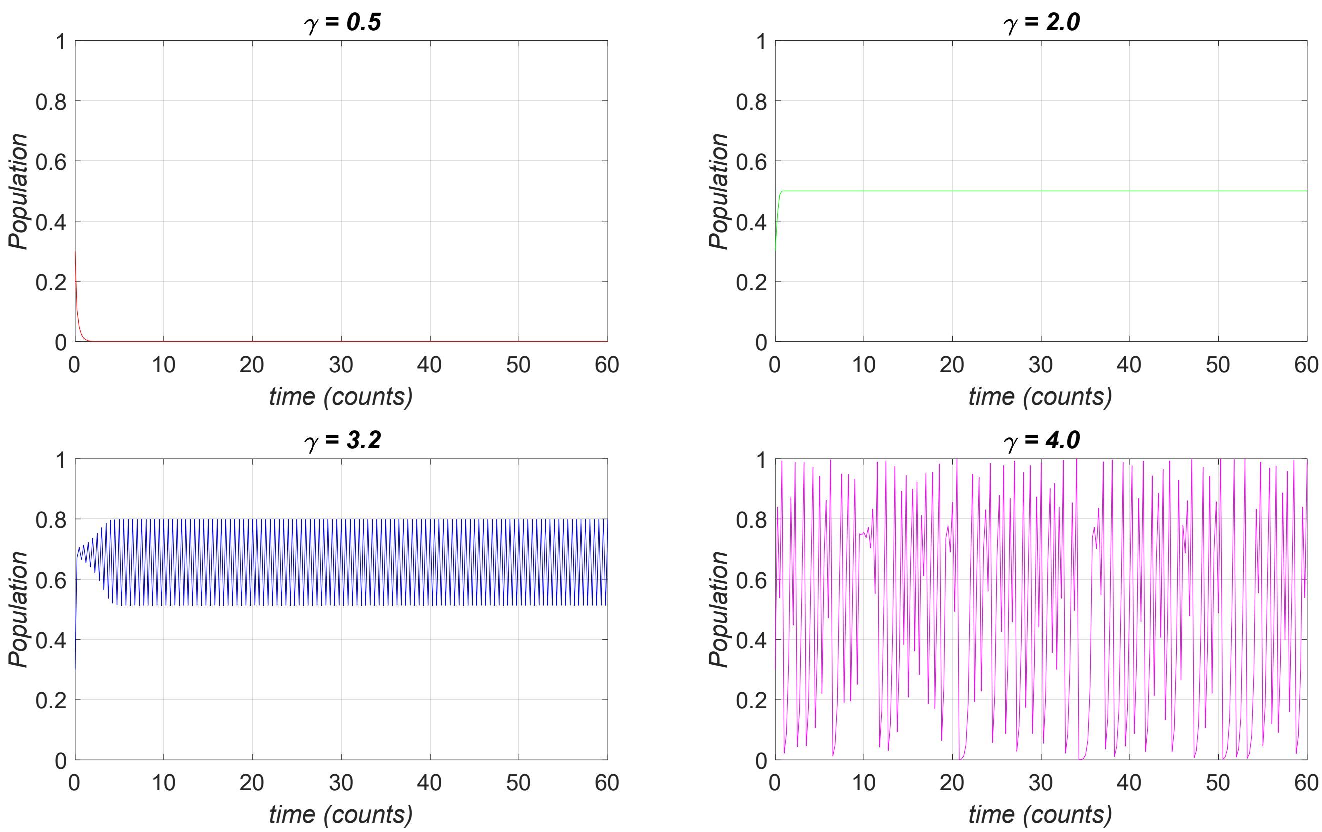

[3] The Strange Case of the Dog in the Nighttime, Mark Haddon, 2003.

Human vs. Chimpanzee DNA

The Chimpanzee (Pan troglodytes) is the closest evolutionary relative of Human Beings (Homo sapiens).

Our DNA is 98.8% IDENTICAL to the Chimp!

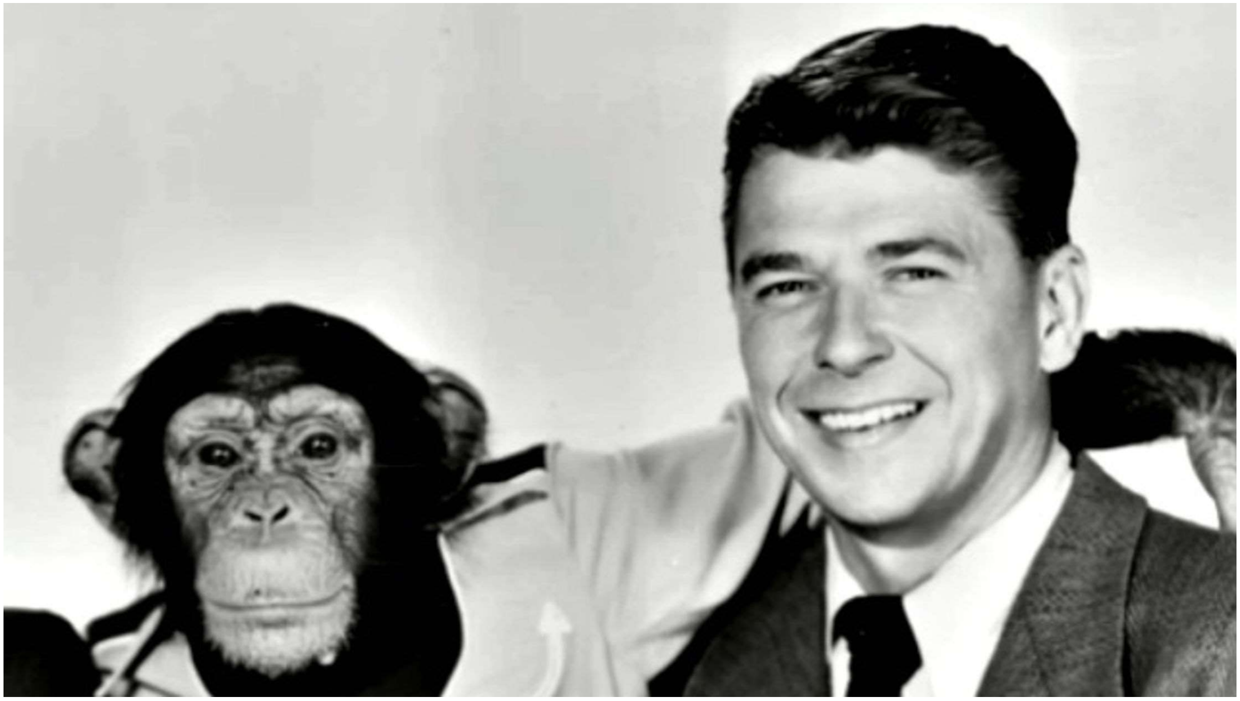

chimp_primary.jpg (2220×1248) (minutemediacdn.com)

Human, chimps, and bonobos (Pan paniscus) descended from a common ancestor 7 million years ago. If our DNA is so common, how are there such differences between the species? Each human cell contains 3 billion base pairs; 1.2% of that is 36 million differences (some big, others smaller).

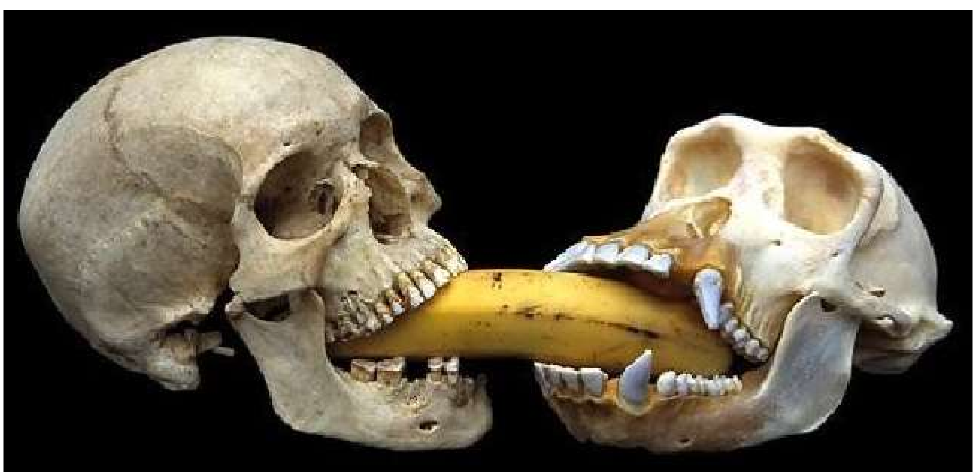

evolution-and-the-98-chimpanzee-10-728.jpg (728×546) (slidesharecdn.com)

Did that freak you out?!? Well, our DNA is also 60% IDENTICAL to the Banana!! (Musa paradisiaca)

2. Human Skeletal Anatomy and Physiology

Anatomy comes from the Greek (literally, 'to cut apart'); **Dissection** comes from the Latin, meaning the same. This shows the importance of cadaver dissections in learning anatomy.

2.1 Human Skeletal Anatomy

Useless Human Tiny Knee Bone making a Comeback

The **Fabella** (Latin: little bean) is a small bone in the human knee, connected only via one tendon. It is a vestigial bone, inherited evolutionarily from great apes, for whom the fabella allowed more force from leg muscles.

This bone essentially disappeared in modern humans, but is now making a comeback! The likely reason is that modern humans are getting heavier. Anatomists are calling the fabella the 'appendix of the skeleton', due to its vestigial nature. There is no agreement about its current use, but ideas include redirecting muscle force or reducing tendon friction. However, it is known that the fabella is not beneficial to osteoarthritis sufferers, increasing knee pain compared to patients without the fabella present.

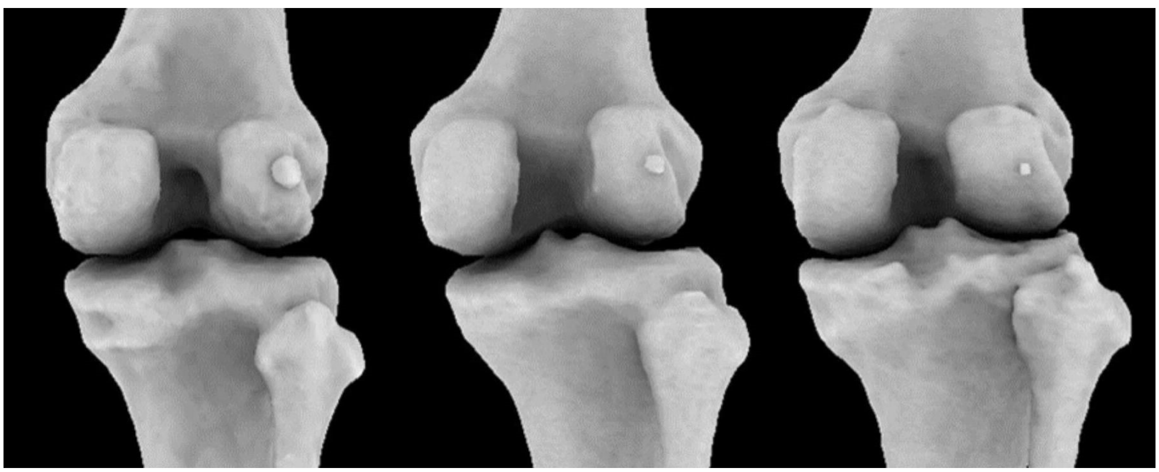

Various-Sized Tiny Fabella Bones in Human Knees

www.the-scientist.com/news-opinion/tiny-knee-bone--once-lost-in-humans--is-making-a-comeback

Fabella Bone in a Human Knee

https://en.wikipedia.org/wiki/Fabella

The next two pages present some of the major human body **Bony Landmarks**, both anterior and posterior. These are generally accessible by palpation from the human body surface. They are used for various reasons by physicians and nurses, chiropractors, physical therapists, massage therapists, anatomists, physiologists, biomechanicists, both researchers and clinicians in each category, to orient skeletal anatomy for individuals.

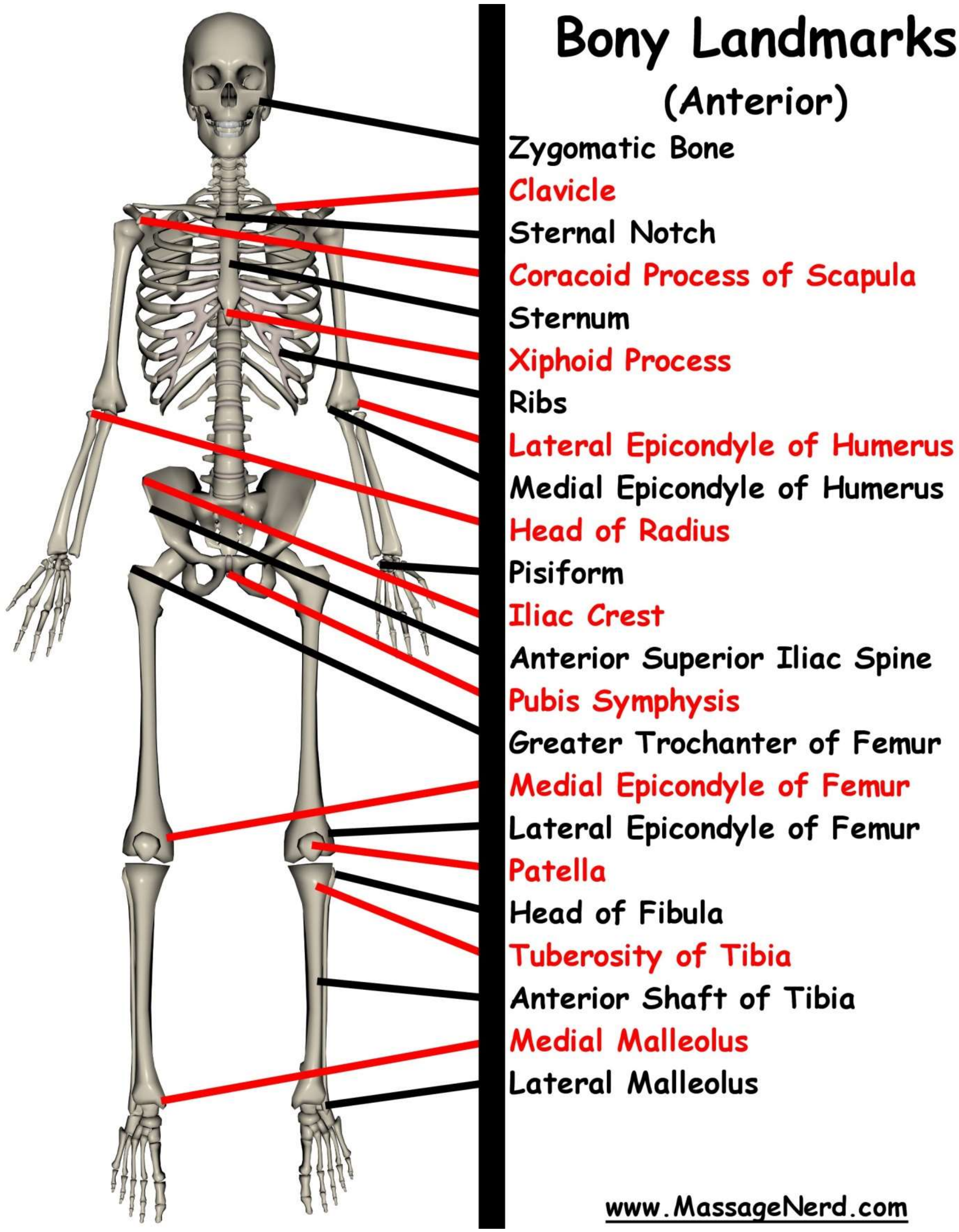

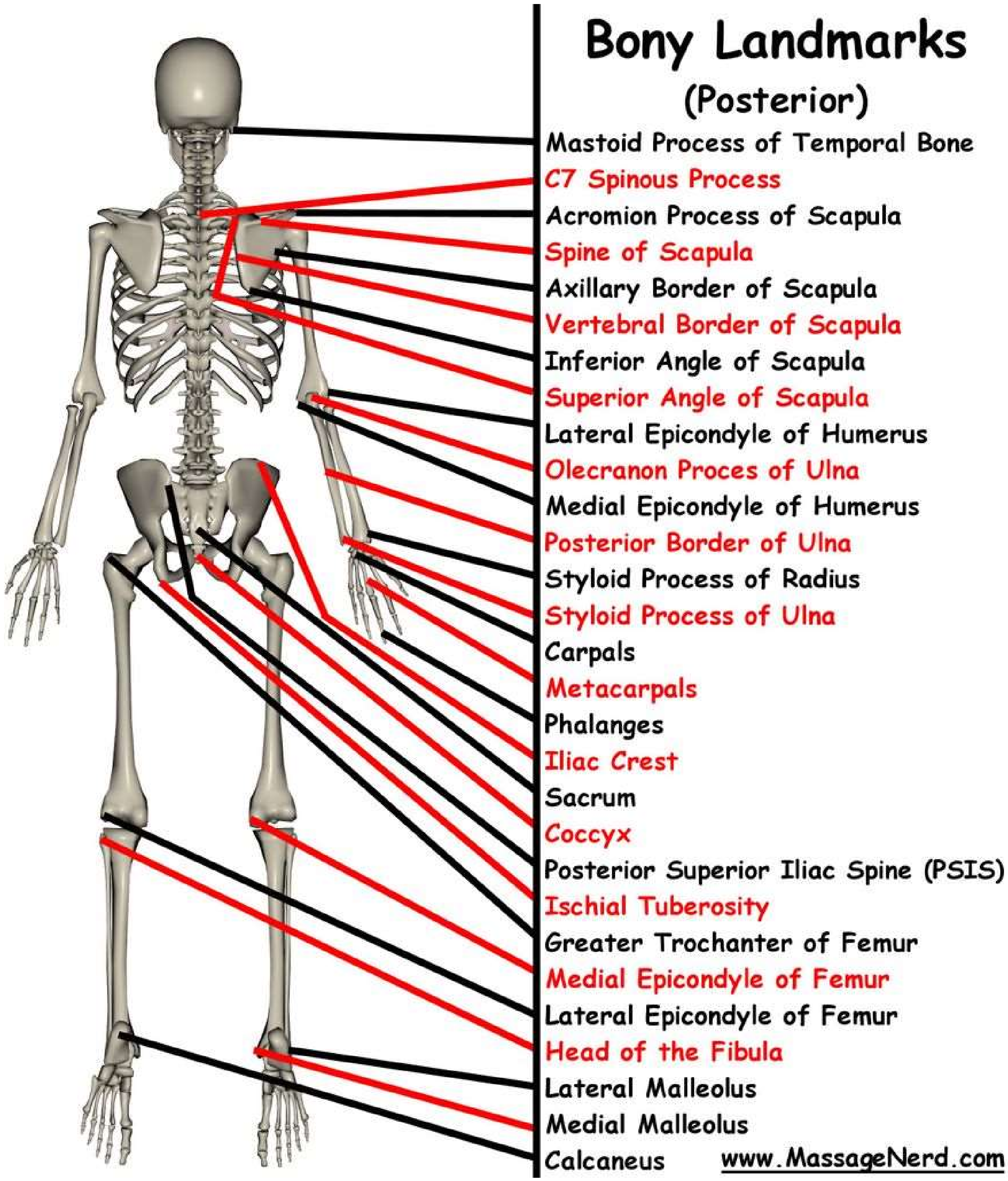
Bony Landmarks
(Posterior)
Mastoid Process of Temporal Bone
C7 Spinous Process
Acromion Process of Scapula
Spine of Scapula
Axillary Border of Scapula
Vertebral Border of Scapula
Inferior Angle of Scapula
Superior Angle of Scapula
Lateral Epicondyle of Humerus
Olecranon Proces of Ulna
Medial Epicondyle of Humerus
Posterior Border of Ulna
Styloid Process of Radius
Styloid Process of Ulna
Carpals
Metacarpals
Phalanges
Iliac Crest
Sacrum
Coccyx
Posterior Superior Iliac Spine (PSIS)
Ischial Tuberosity
Greater Trochanter of Femur
Medial Epicondyle of Femur
Lateral Epicondyle of Femur
Head of the Fibula
Lateral Malleolus
Medial Malleolus
Calcaneus
www.MassageNerd.com

Hero Shrew Skeletal Anatomy

Hero Shrew has Unique Super-Strong Spine. Almost all mammals, from rats to cats to humans to camels, have the same basic spine design, similar to the normal African Giant Shrew shown on the left below. Characteristic of this normalcy is two spinus processes on each vertebra.

In 1910, in the Congo, the Hero Shrew was discovered – a normal-looking though large shrew (the size of a small rat). Natives demonstrated that an adult human could stand on the Hero Shrew's back for 5 minutes and then the animal scurried away afterwards. The anatomy of the Hero Shrew vertebrae are radically different – the overall spine looks more like a Triscuit cracker than a spine, and individual vertebra have up to 20 interlocking spinus processes instead of just two!

Scientists have been long-puzzled by the reason for this unique adaptation. The latest theory is that the Hero Shrew uses its spine to lever logs for hunting insects.

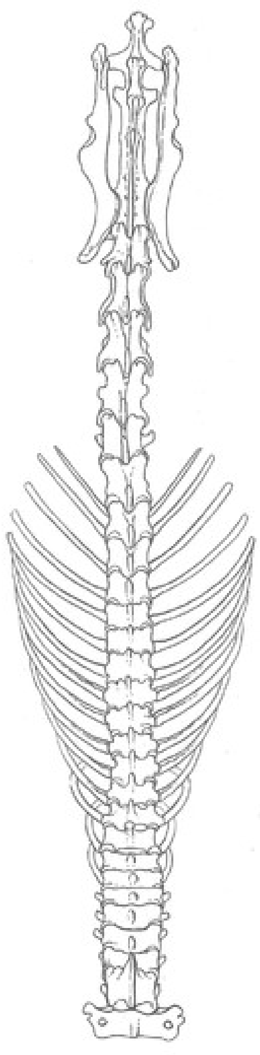

African Giant Shrew

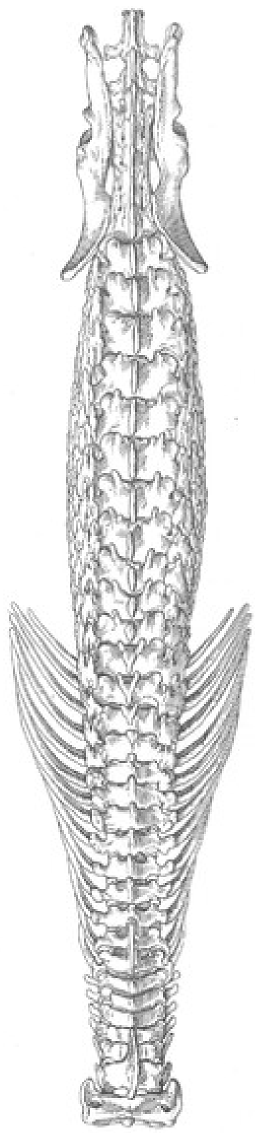

Hero Shrew

wikipedia.org

More Bone Pathologies

Metastatic Calcification is deposition of calcium in tissues that don't normally have calcium.


Tumblr: Image

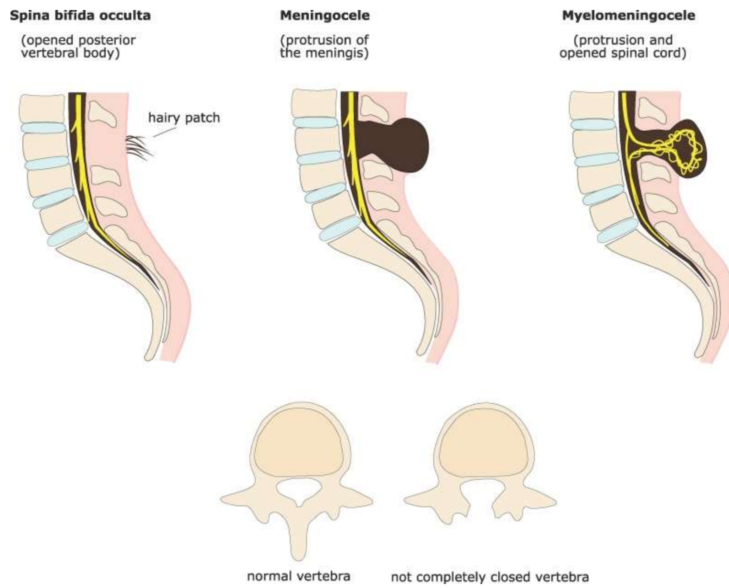

spina-bifida_shutterstock_318856385 copy.jpg (spineuniverse.com)

Spina Bifida. Posterior portions of the vertebrae fail to form a complete bony arch around the spinal cord. This is a birth defect normally occurring in the lumbar and sacral regions.

Osteomyelitis is a bacterium or fungal infection of the periosteum, marrow, and bone tissue.

04_19_2018_Orthotices_for_Osteomelitis.jpg (shopify.com)

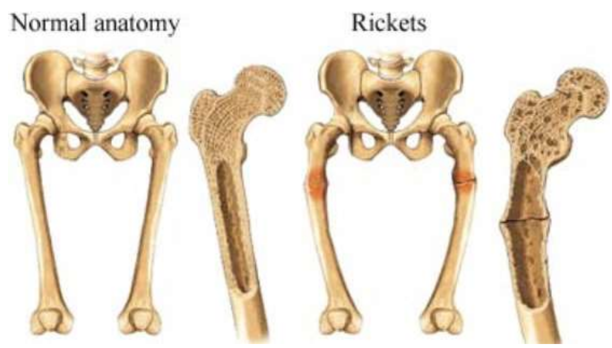

rickets.jpg (570×324) (kauveryhospital.com)

Rickets and Osteomalacia involve demineralization and softening of bone, due to deficiencies in calcium, phosphorus, vitamin D and/or sunlight.

Neoplasms of Bone are benign and malignant tumors.

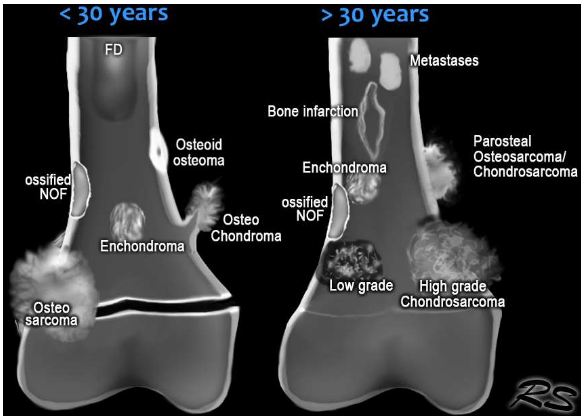

a5278ab702cee1_TEK-BOT-scler.jpg (desk.nl)

Tallest-man-shortest-man-410143.jpg (dailystar.co.uk)

Abnormal Growth Patterns result from excessive or deficient growth hormone (GH) from the anterior pituitary gland. Too much GH can cause abnormally increased growth patterns. In adults this is called **acromegaly** and in children it is called **gigantism**. Too little growth hormone can cause a slow or flat rate of growth in children. In adults, it can sometimes cause changes in energy, muscle mass, cholesterol levels, and bone strength.

Tuberculosis (TB) of the Bone is referred to as **Potts' Disease** (see photo and X-ray below). **TB** is a bacterium infection of bone carried from the lungs or lymph nodes.

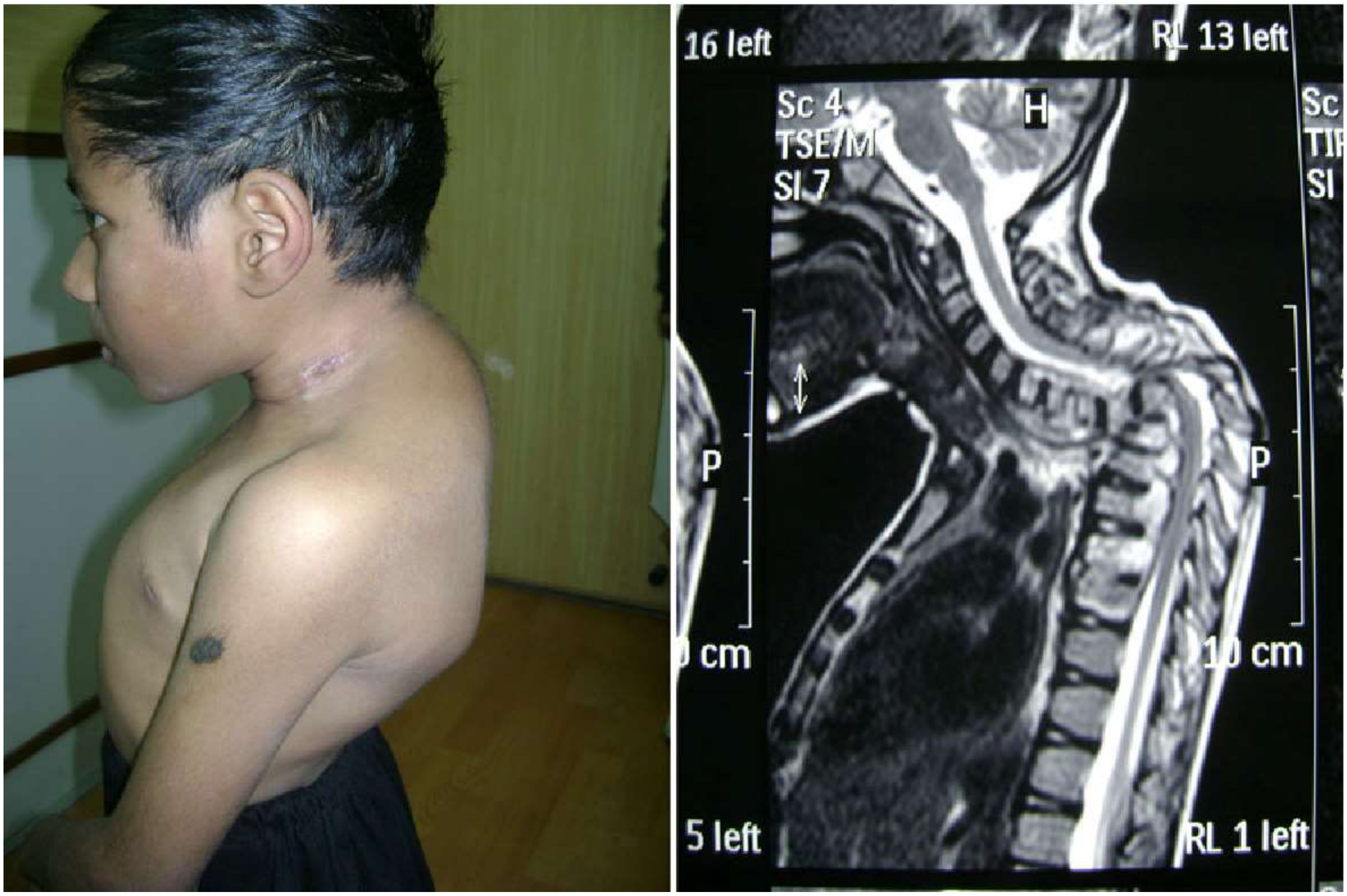

Tuberculosis of the Bone

Tuberculosis of the Lymph Nodes is known as Scrofula or the King's Evil (since it was believed the touch of a monarch could cure the associated lesions).

Fibrodysplasia Ossificans Progressiva (**Münchmeyer Disease**) is an extremely rare and insidious connective tissue disease in which muscle is replaced by bone, until the affected individual can no longer move. Death often occurs by age 40. There is no known cure or treatment. This is the only known disease in which one human tissue replaces another.

Fibrodysplasia Ossificans Progressiva

fibrodysplasia_ossificans_progressiva_by_atirum-d74wcd4.png (752×1063) (wixmp.com)

2.2 Human Skeletal Physiology

<u>Fryette's Laws for Physiologic Motion of the Spine</u>

The three major principles of physiologic motion of the spine from osteopathy are:

I. When the thoracic and lumbar spine is in a neutral position, the coupled motions of sidebending and rotation for a group of vertebrae are such that sidebending and rotation occur in opposite directions (with rotation occurring toward the convexity). See the Type I motion figure.

II. When the thoracic and lumbar spine is sufficiently forward or backward bent (non-neutral), the coupled motions of sidebending and rotation in a single vertebral unit occur in the same direction. See the Type II motion figure.

III. Initiating motion of a vertebral segment in any plane of motion will modify the movement of that segment in other planes of motion.

Principles I and II of thoracic and lumbar spinal motion described by H.H. Fryette, DO, in 1918. Principle III was described by C.R. Nelson, DO, in 1948.

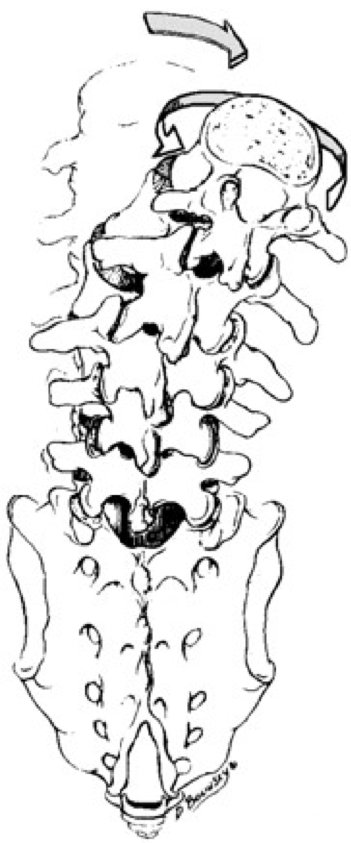

Type I Motion

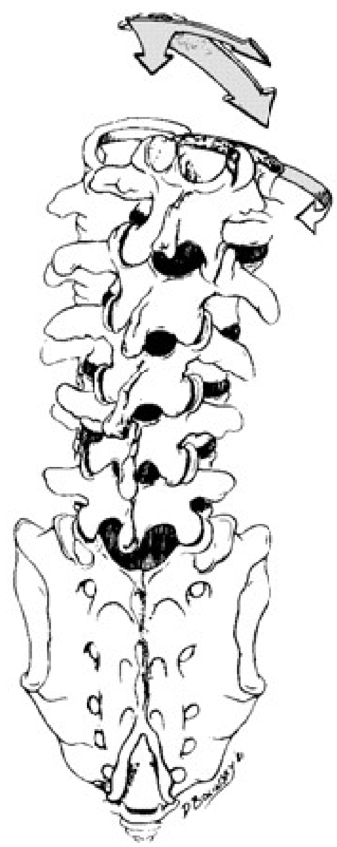

Type II Motion

interlinea.org

Tensegrity. The osteopathic physicians say the human body is all connected. Come to think of it, that old song says the same ('the head bone connected to the neck bone . . .'). In engineering a **tensegrity structure** (see left figure below) is one whose elements and members are loaded only in tension forces (i.e. no compression, shear or moments). Though the spine is primarily in compression, a **tensegrity structure** may be a good model for the overall human spine and musculoskeletal system (see the second two figures below).

S.M. Levin, The Tensegrity-Truss as a Model for Spine Mechanics: Biotensegrity, Journal of Mechanics in Medicine and Biology, 2(3,4): 375-388.

Tensegrity Model for the Human Musculoskeletal System

Lordosis (**swayback**, **saddle back**, or **hyper-lordosis**) is a medical term used to describe an inward curvature of a portion of the vertebral column. Two segments of the vertebral column, namely cervical and lumbar, are *normally* lordotic, that is, they are set in a curve that has its convexity anteriorly (the front) and concavity posteriorly (behind), in the context of human anatomy. Curvature in the opposite direction, apex posteriorly, is termed kyphosis. Some animals (notably horses) have naturally concave, lordotic backs.

en.wikipedia.org

Kyphosis (from the Greek *kyphos* meaning a hump), also called **hunchback**, is a common condition of a curvature of the upper spine. It can be either the result of degenerative diseases such as arthritis, developmental problems, osteoporosis with compression fractures of the vertebrae, and/or trauma. In the sense of a deformity, it is the pathological curving of the spine, where parts of the spinal column lose some or all of their lordotic profile. This causes a bowing of the back, seen as a slouching back and breathing difficulties. Severe cases can cause great discomfort and even lead to death.

en.wikipedia.org

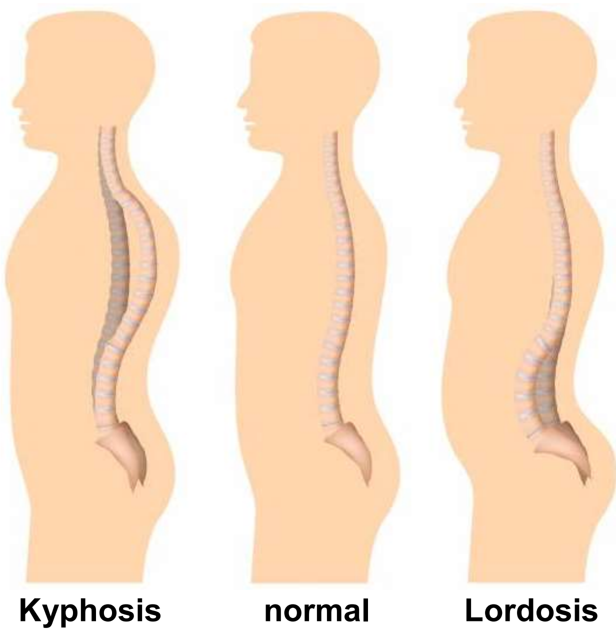

breakingmuscle.com

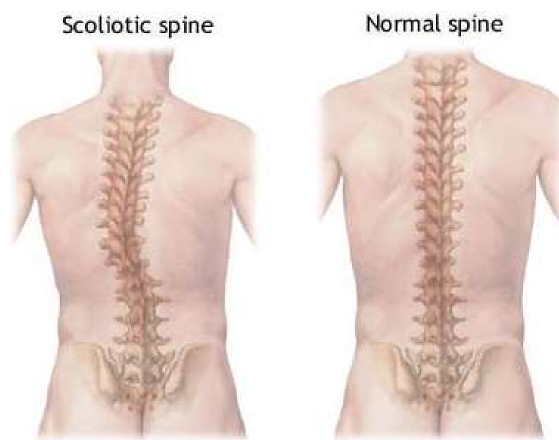

graphics8.nytimes.com

Scoliosis (from the Greek *skoliōsis* meaning crooked condition) is a medical condition in which a person's spine is curved from side to side. Although it is a complex three-dimensional deformity, on an x-ray, viewed from the rear, the spine of an individual with a typical scoliosis may look more like an "S" or a "C" than a straight line. It is typically classified as either congenital (caused by vertebral anomalies present at birth), idiopathic (cause unknown, sub-classified as infantile, juvenile, adolescent, or adult according to when onset occurred) or neuromuscular (having developed as a secondary symptom of another condition, such as spina bifida, cerebral palsy, spinal muscular atrophy or physical trauma). This condition affects approximately 7 million people in the United States.

en.wikipedia.org

Child with Externally-Visible Scoliosis

Scoliosis X-Rays

Scoliosis can also result from normal growth spurts in childhood. A scoliotic patient has less room for the heart and lungs to function efficiently.

Short-Leg Syndrome is a common condition in which one leg is functionally shorter than the other. This mechanical problem, referred to as a 'short man disease' by my brother Tim Williams (5'7"), can cause sacral base unleveling, vertebral side bending and rotation, innominate rotation, and potentially severe low-back pain. This can easily be treated by a partial-length-discrepancy heel lift and osteopathic manipulative medicine (OMM).

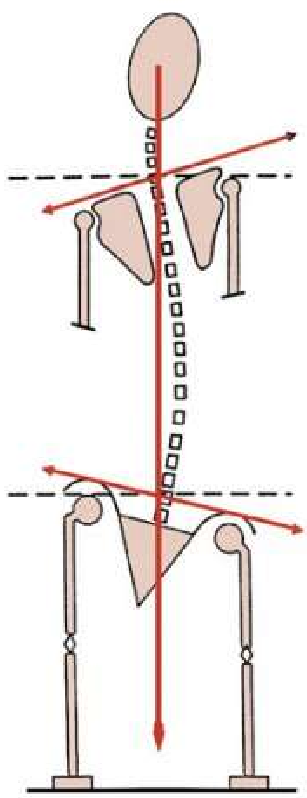

Short-Leg Syndrome

Varus and Valgus Knee

As seen in the image below, **Varus Knee** is associated with bowleggedness, and **Valgus Knee** with knock-knee.

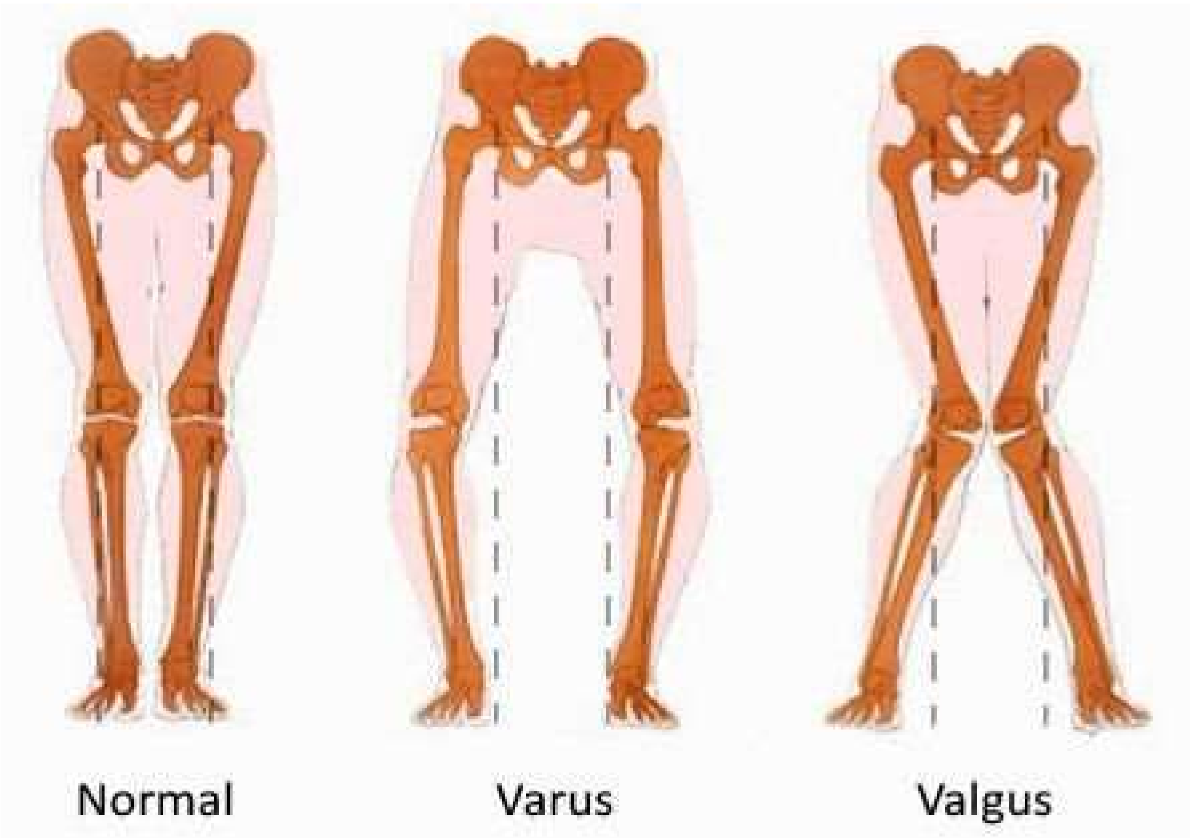

Varus vs. Valgus Knee

2489f8354caf1d6902eccf3fea3d4ba5.jpg (450×316) (pinimg.com)

Osteoarthritis

Arthritis is a disorder of the joints with inflammation causing pain. **Rheumatoid Arthritis** is a chronic autoimmune inflammatory disease of the joints.

Osteoarthritis is very common (> 3M patients per year in the U.S.) and occurs when protective cartilage in joints wears down over time, due to aging, disease, or injury. There is no known cure, though treatments can manage the condition. **Osteoarthritis** most commonly affects the joints in hands, knees, hips, and spine.

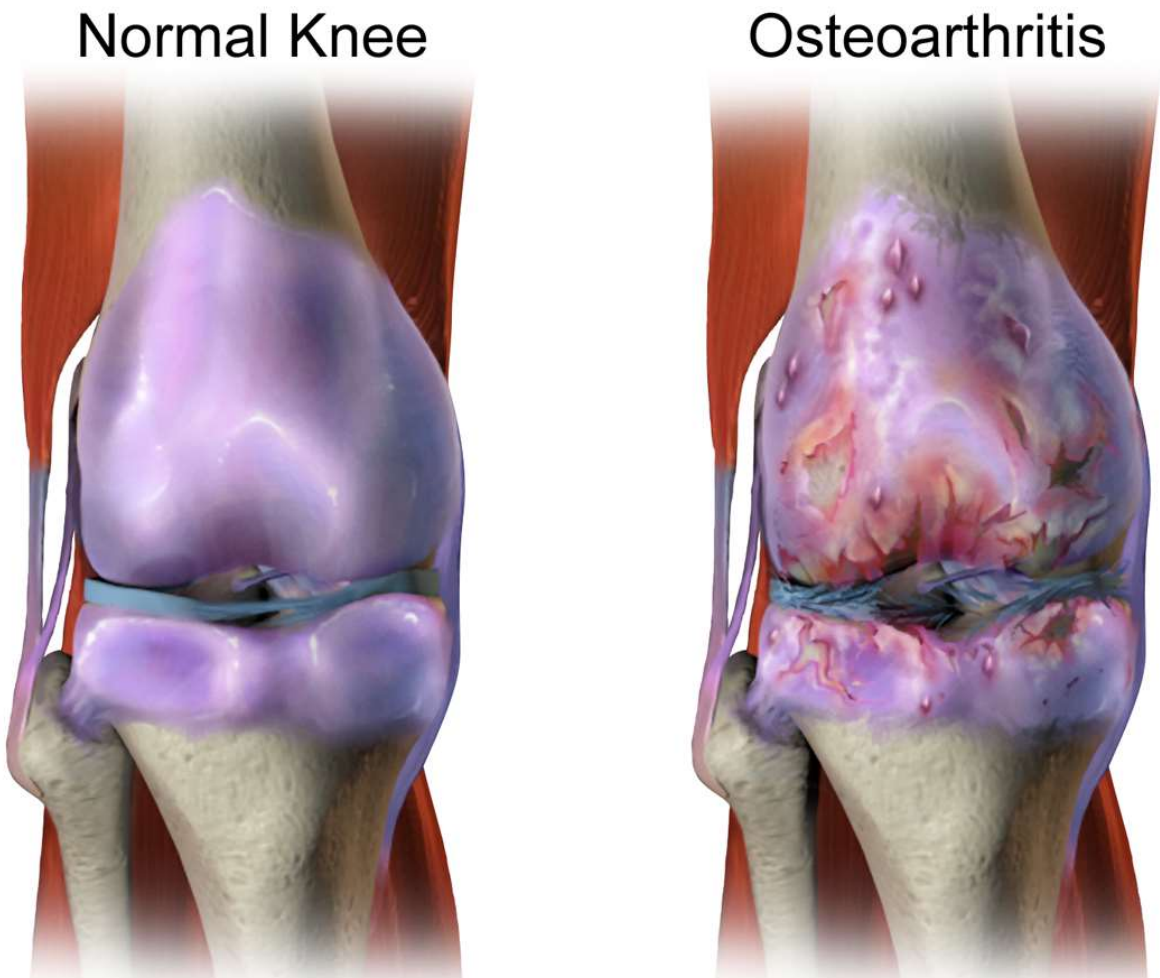

Joint Replacements

Many patients have benefitted from shoulder and/or hip replacements. Many surgeons focus on nothing else. These surgeries replace the biological joints with artificial, engineered joints. The reason would be to alleviate arthritis pain and improve mobility in the case of joint degeneration due to aging or disease.

Shown below is an engineered shoulder joint that is inverted (right image, **Reverse**). In this case the normal (left image, original, and middle image, standard shoulder replacement) ball-and-socket joint is reversed, as shown. The reversed situation allows a more stable joint with a fixed fulcrum. It is used in situations in which the conventional surgery (**Anatomical**) would lead to poor outcomes and high failure rates. It would also appear that the reversed shoulder leads to a great range of motion.

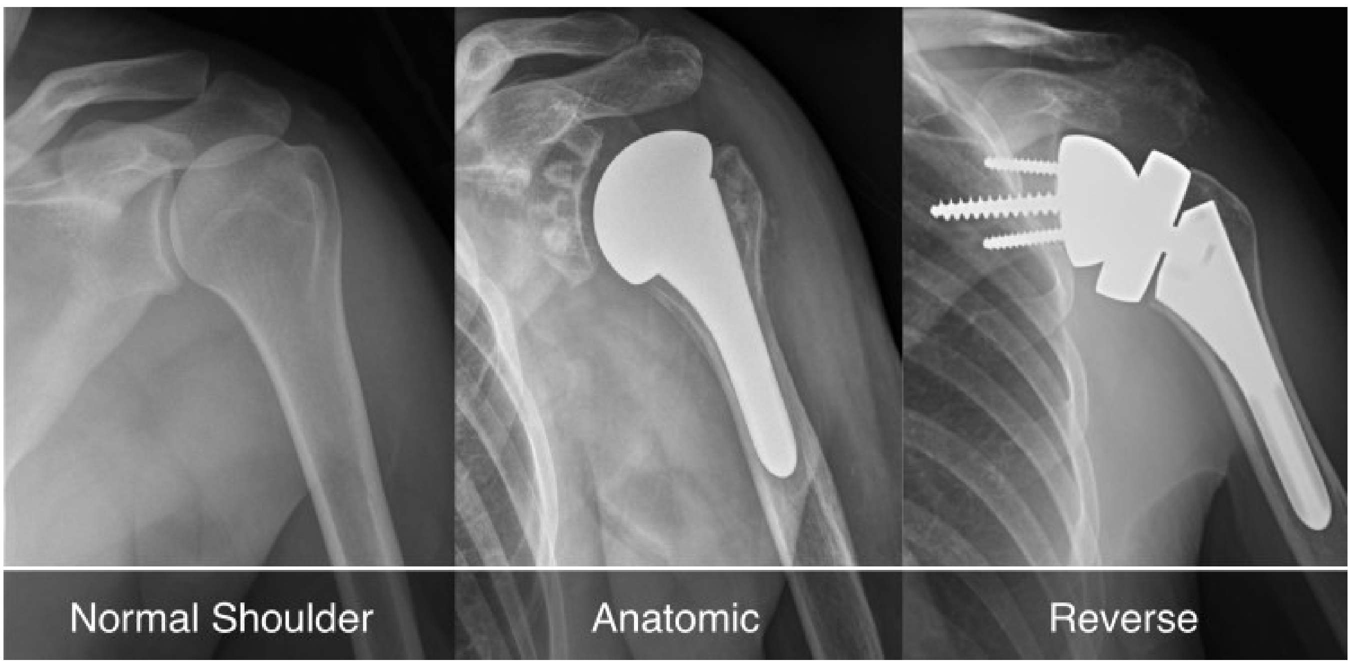

Shoulder Surgery, Conventional (Anatomic) and Inversed (Reverse)

The **Anatomic** shoulder joint replacement is a better load-bearing option since the ball and shaft are joined into the bone. Patients who normally require the **Reverse** shoulder joint replacement have a non-reparable torn rotator cuff.

3. Human Muscular Anatomy and Physiology

Dr. Bob with Michelangelo's David in Florence Italy, Spring Break 2023

Cheetah vs. the Click Beetle

The cheetah is the fastest land animal on Earth, capable of 70 – 75 mph in short bursts of **speed**. The cheetah's **acceleration** is about 15 m / sec^2. Compare that to the lowly click beetle, that can accelerate in jumping up to 400*g*, i.e. 3924 m / sec^2! This is 10x the amount of acceleration a human can tolerate! In this way they can jump 20x higher than their length.

Fastest Land Animal
cheetah-speed.jpg (pictures-of-cats.org)

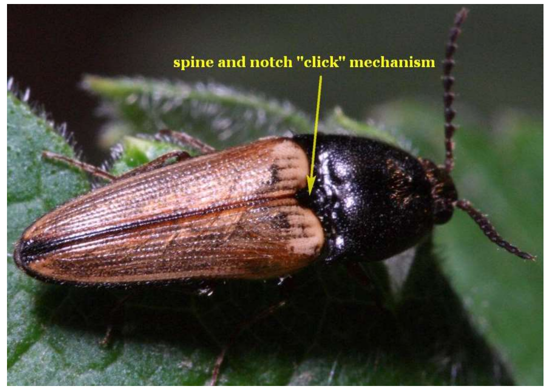

Click Beetle
click-beetle-mechanism.jpg (cirrusimage.com)

At small scales, such as in insects, muscles suffer from force-velocity tradeoffs, limiting their maximum power. This limitation is due to the intrinsic maximal contraction speed of a sarcomere, which is very consistent over all animals (from insects to mice to elephants, including humans). To overcome this limitation, click beetles use stored spring energy, suddenly released by a latch, to achieve great acceleration for locomotion, hunting, or escaping predators. This leaping energy is loaded slowly using muscles and released by the latch in a very short time (milliseconds), leading to power amplification (compared to pure muscle potential). The spring-and-latch mechanism is on the underside of their exoskeleton.

An analogy of this power amplification is found in a human archer. The human muscles slowly load the bow and string with elastic energy. The hand acts as the latch, releasing the same energy but in a very short time frame.

Human Archer
the-hunger-games-katniss-archer.jpg

3.1 Human Muscular Anatomy

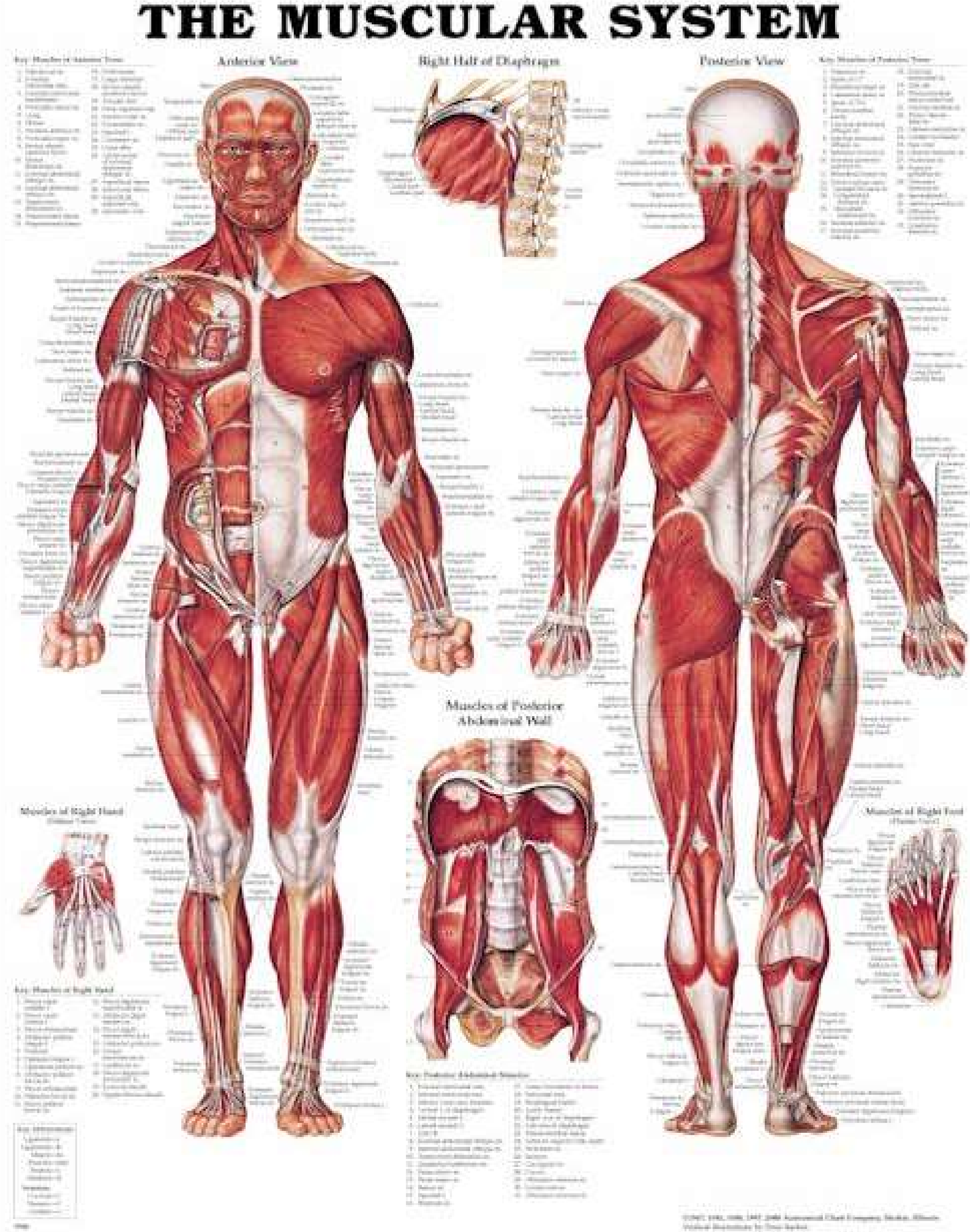

Peter Bachin

Anterior and posterior adult male muscular system plus right half of diaphragm, muscles of the posterior abdominal wall, and muscles of the right hand and foot

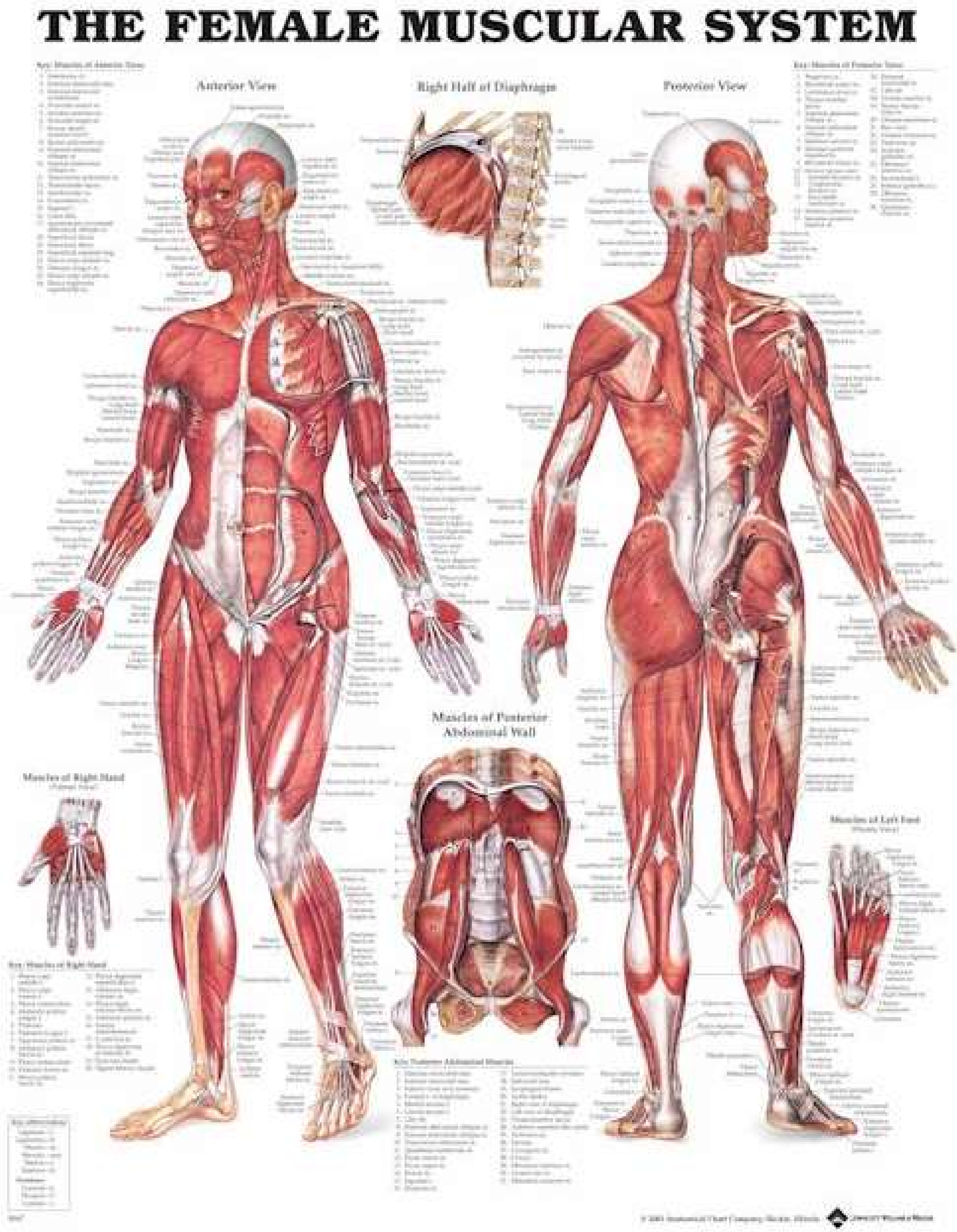

Peter Bachin

Anterior and posterior adult female muscular system plus right half of diaphragm, muscles of the posterior abdominal wall, and muscles of the right hand and foot

Sarcomere Details

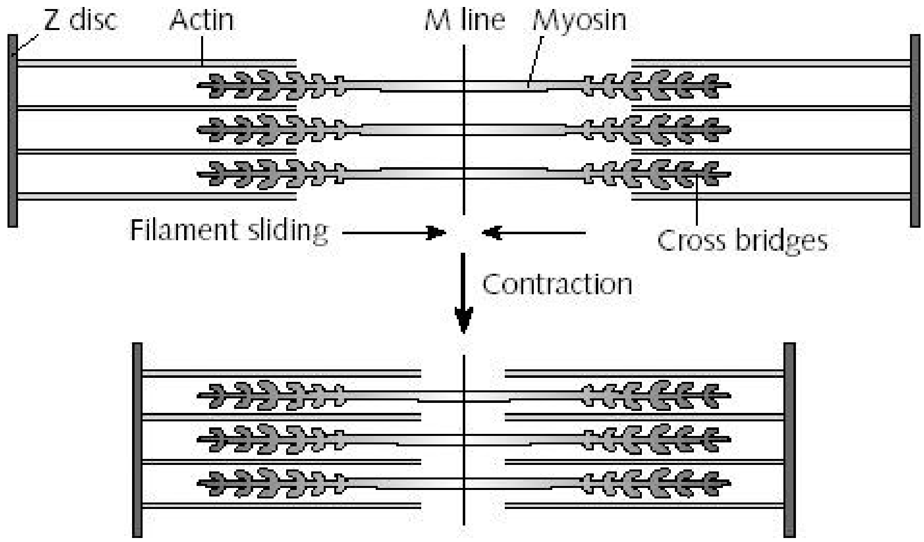

Sarcomere Relaxed (above) and Contracted (below)

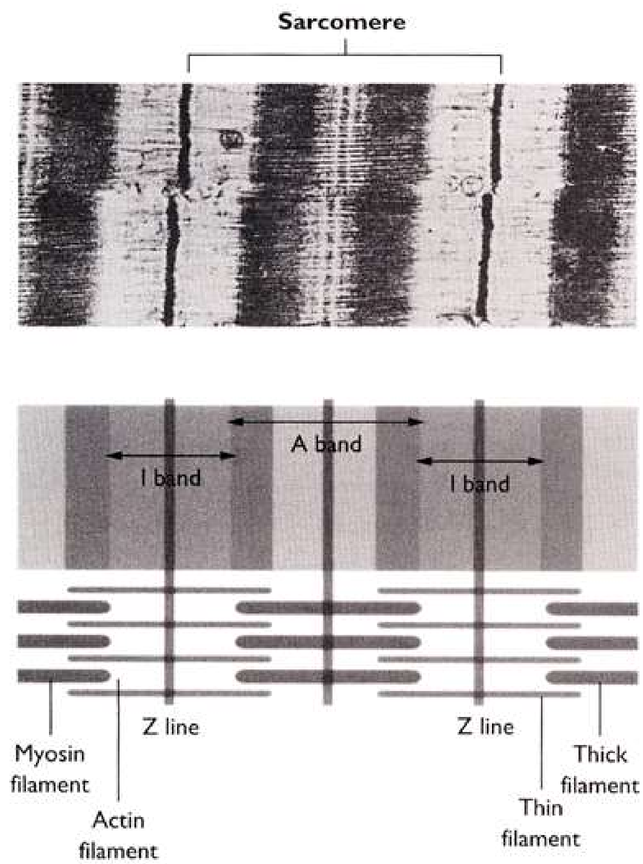

Sarcomere Image and Detail

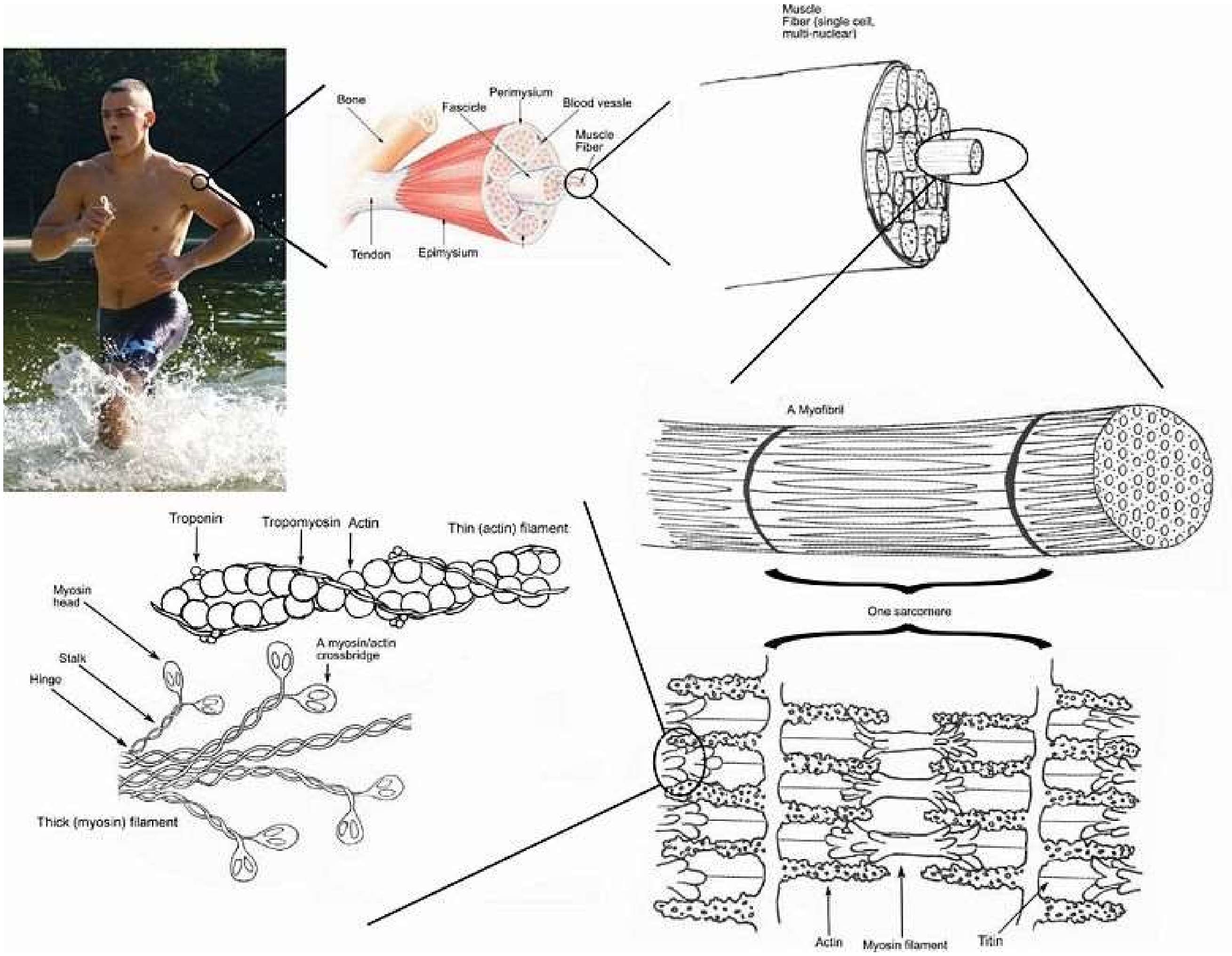

Striated Muscle Structure Yet Again

3.2 Human Muscular Physiology

Energy Sources for Muscle Contraction

- **Oxidative metabolism** provides **adenosine triphosphate** (**ATP**) in an **aerobic** process.

- The nucleotide **ATP** is the molecular currency of intracellular energy transfer in biochemistry because **ATP** is able to store and transport chemical energy within cells. ATP also participates in nucleic acids synthesis.

- **ATP** and **lactic acid** are produced during intense activity by **nonoxidative** (**anaerobic**) **metabolism**.

- **Creatine phosphate** (**CP**) is the reserve energy source

Immediately following initiation of muscle contraction, normal metabolism may not be able to produce enough **ATP** for muscle energy. Here is the **CP** reserve energy chemical reaction, where **ADP** is **adenosine diphosphate** and **C** is creatine.

$$\mathrm{CP + ADP} \rightleftharpoons \mathrm{ATP + C}$$

During activity, this reaction is from left to right. During rest the reaction reverses to replenish **CP**.

CP formula	$C_4H_{10}N_3O_5P$	**ADP** formula	$C_{10}H_{15}N_5O_{10}P_2$
ATP formula	$C_{10}H_{16}N_5O_{13}P_3$	**C** formula	$C_4H_9N_3O_2$

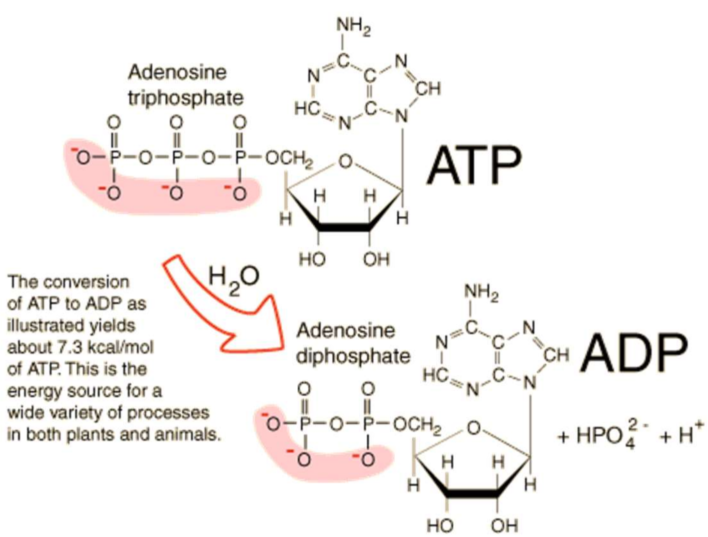

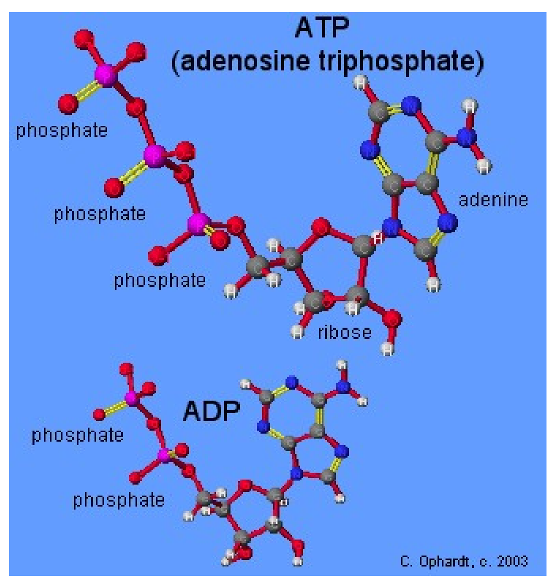

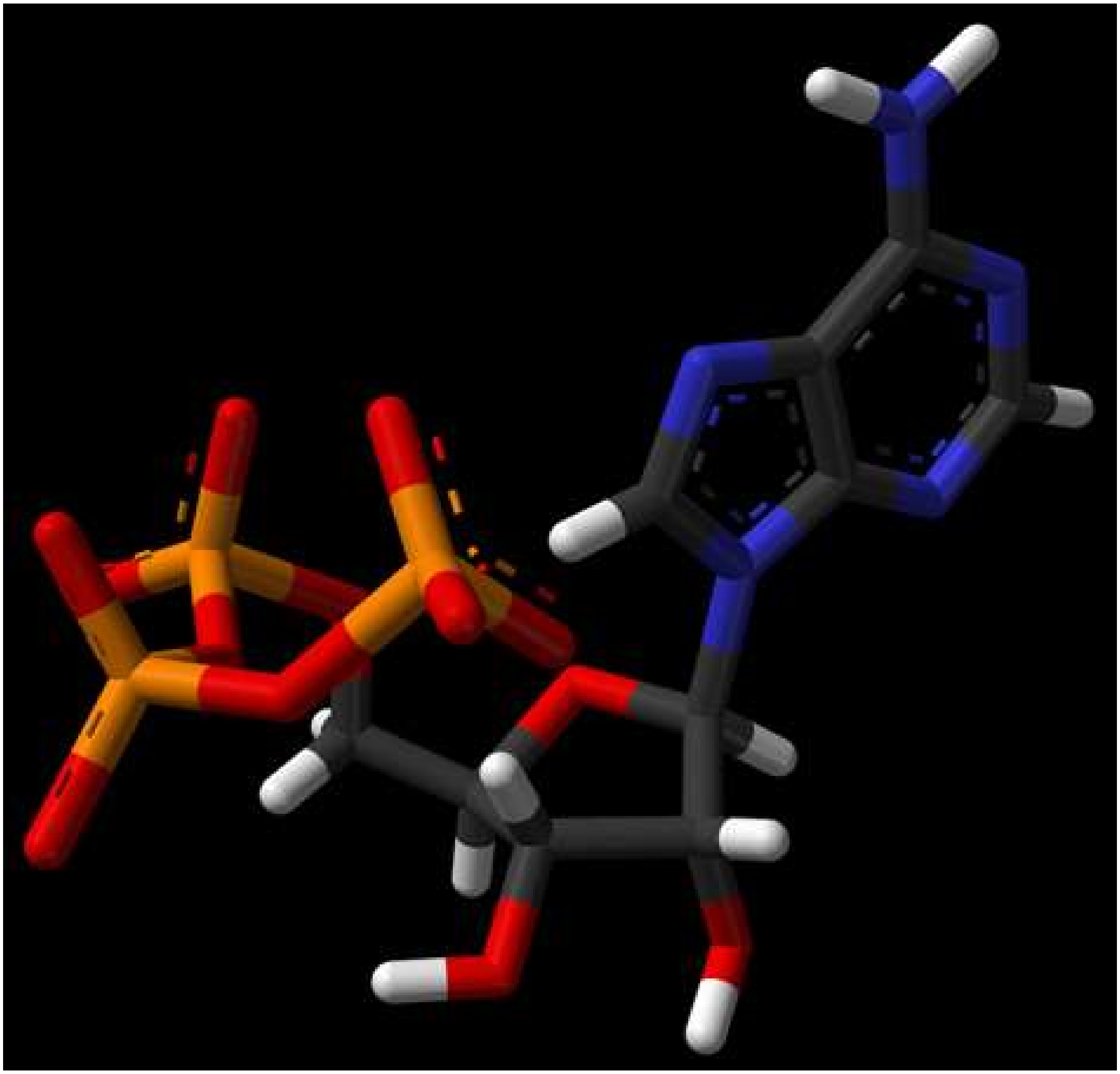

ATP Molecule CAD/VR Model

Virtual Reality (VR) with haptics (force and touch feedback via special computer interfaces) has been implemented for complex molecules synthesis where there are multiple solutions and the expert microbiologist finds appropriate solutions via touch, fitting molecules together via feel for minimum energy of the chemical bonds.

Muscle contraction requires energy to drive the crossbridges through their cyclic interactions with actin (thin filaments): in each cycle the myosin (thick filaments; connected to actin via elastic proteins) molecule does work in moving the thin filament. Each crossbridge generates about 5×10^{-12} N (5 picoN) of force in a ratchet-like action. Also, energy is used for the process of calcium pumping by the SR.

- Energy consumption is highest when muscles are used to do external work like climbing stairs, when the body weight is lifted. Energy is also used when a weight is held up without doing work on it (isometric contraction). The least energy is used when muscles are used to lower weight, as when descending stairs, since gravity assists in this case.

- The energy for muscle contraction comes from the splitting of adenosine triphosphate (ATP) to adenosine diphosphate (ADP) and phosphate. The muscle contains enough ATP to power it at maximum output for only a couple of seconds. ATP can be regenerated in muscle rapidly from phosphocreatine (PCr), and there is enough of this substance in the muscle to last perhaps 10 to 20 seconds of maximum activity.

- The fact that we can sustain strenuous activity beyond 10 seconds is due to the utilization of carbohydrate in the muscles, where it is stored as glycogen. This can be used to regenerate the ATP supply in two ways.
    - If oxygen is available, glucose can be oxidized to water and carbon dioxide, with two-thirds of the energy released used to rebuild the ATP supply.
    - If oxygen is not available, the process stops with glucose converted to lactic acid and only about 6% of the energy used for building ATP.

- The lactic acid leaves the muscle cells and can accumulate in the blood. In addition to carbohydrate, muscles use fat, in the form of fatty acids taken up from the blood, as a substrate for oxidation; this is important for prolonged activity, since the body's energy stored as fat is much greater than that stored as carbohydrate.

- The availability of oxygen depends on its delivery by the blood; when muscle becomes active, the products of its metabolism cause the vessels to dilate, and this enables a rapid increase in the blood flow.

see SDSU Biology 590 video sci.sdsu.edu/movies/actin_myosin_gif.html

Autonomic Nervous System (ANS)

This class focuses on voluntary control of the musculoskeletal system. For completeness, here we summarize the autonomic nervous system (ANS), responsible for autonomous functions in the human body:

1. Secretion of glands.
2. Actions of many smooth muscles.
3. Extrinsic control of the heart.
4. A variety of metabolic processes including release of catecholamines, glucagon, insulin, and others.

The **sympathetic nervous system** (**SNS**) is a branch of the autonomic nervous system along with the enteric nervous system and parasympathetic nervous system. It is always active at a basal level (called sympathetic tone) and becomes more active during times of stress. Its actions during the stress response comprise the fight-or-flight response.

The sympathetic nervous system is responsible for up- and down-regulating many homeostatic mechanisms in living organisms. Fibers from the SNS innervate tissues in almost every organ system, providing at least some regulatory function to things as diverse as pupil diameter, gut motility, and urinary output. It is perhaps best known for mediating the neuronal and hormonal stress response commonly known as the fight-or-flight response. This response is also known as sympatho-adrenal response of the body, as the preganglionic sympathetic fibers that end in the adrenal medulla (but also all other sympathetic fibers) secrete acetylcholine, which activates the secretion of adrenaline (epinephrine) and to a lesser extent noradrenaline (norepinephrine) from it. Therefore, this response that acts primarily on the cardiovascular system is mediated directly via impulses transmitted through the sympathetic nervous system and indirectly via catecholamines secreted from the adrenal medulla.

Science typically looks at the SNS as an automatic regulation system, that is, one that operates without the intervention of conscious thought. Some evolutionary theorists suggest that the sympathetic nervous system operated in early organisms to maintain survival as the sympathetic nervous system is responsible for priming the body for action. One example of this priming is in the moments before waking, in which sympathetic outflow spontaneously increases in preparation for action.

The **parasympathetic nervous system** (**PSNS**) is a division of the autonomic nervous system (ANS), along with the sympathetic nervous system (SNS) and enteric nervous system (ENS or ‘bowels NS’). The ANS is a subdivision of the peripheral nervous system (PNS). ANS sends fibers to three tissues: cardiac muscle, smooth muscle, or glandular tissue. This stimulation, sympathetic or parasympathetic, is to control smooth muscle contraction, regulate cardiac muscle, or stimulate or inhibit glandular secretion.

Relation to sympathetic nervous system

Sympathetic and **parasympathetic** divisions typically function in opposition to each other. But this opposition is better termed complementary in nature rather than antagonistic. For an analogy, one may think of the sympathetic division as the accelerator and the parasympathetic division as the brake. The sympathetic division typically functions in actions requiring quick responses. The parasympathetic division functions with actions that do not require immediate reaction. The main actions of the parasympathetic nervous system are summarized by the phrase "rest and repose" or "rest and digest" (in contrast to the "fight-or-flight" of the sympathetic nervous system). A rarely used (but useful) acronym used to summarize the functions of the parasympathetic nervous system is SLUDD (salivation, lacrimation, urination, digestion and defecation).

en.wikipedia.org

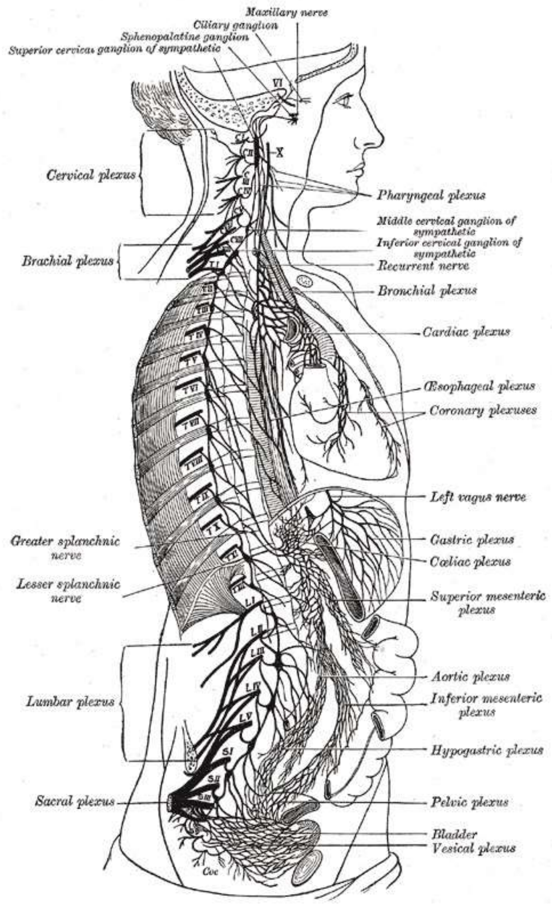

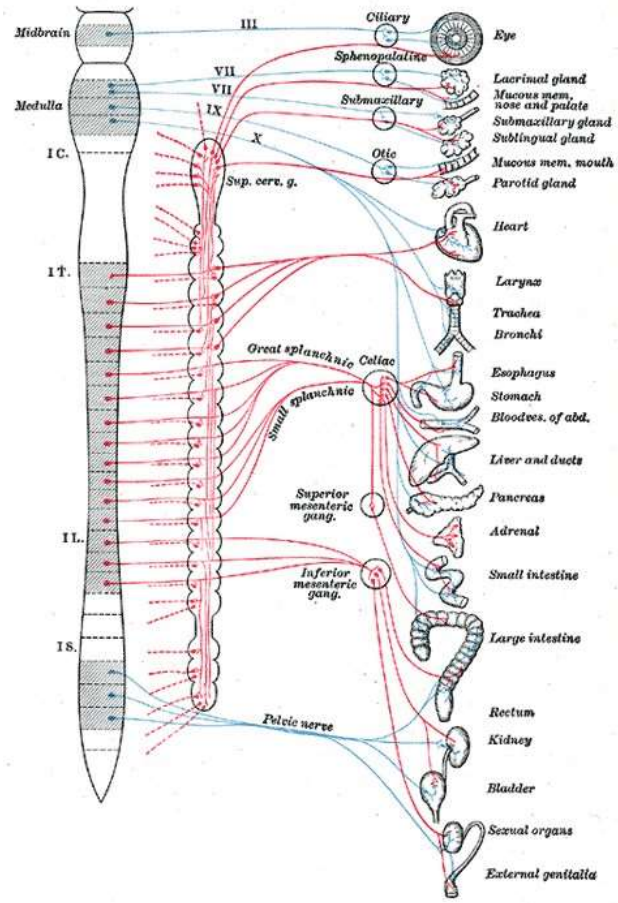

The **sympathetic nervous system** extends from the thoracic to lumbar vertebrae and has connections with the thoracic, abdominal, and pelvic plexuses.	Autonomic nervous system innervation, showing the **sympathetic** and **parasympathetic** (craniosacral) systems, in red and blue, respectively.

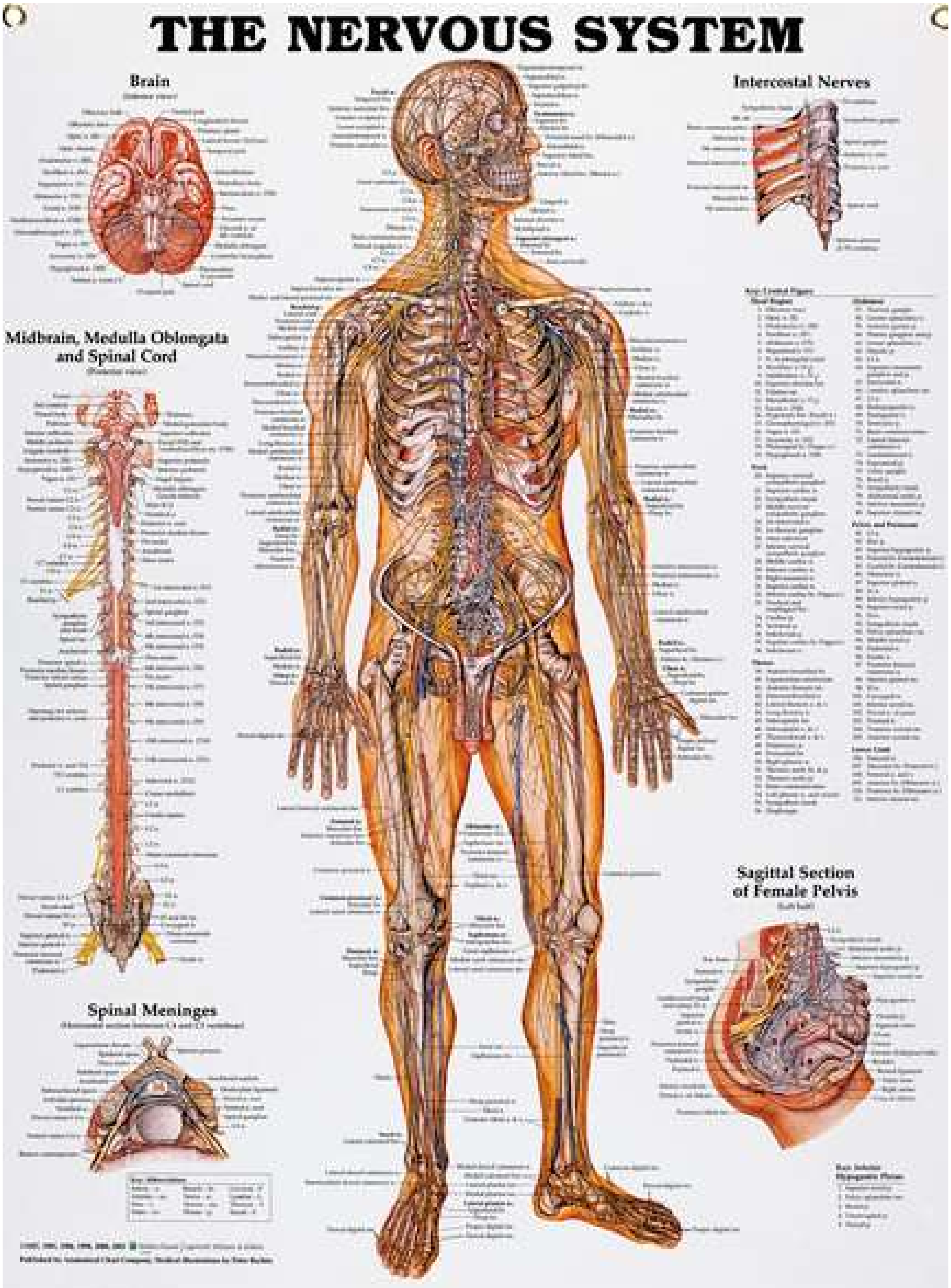

Peter Bachin

3.3 Muscle Mathematical Model

This section presents a common single skeletal muscle dynamics model, including the figure, equations, state-space form, and simulations. This is a vibrational model, included for completeness, to show one type of engineering mechanics modeling for muscles. In this class we will generally treat the effect of muscles more simply, i.e. as simple cables in tension with no mass, spring constants, or dynamics of their own.

The model in this section was suggested by Dr. Scott Hooper (OU Biological Sciences) and the equations were derived and the simulations performed by Elvedin Kljuno (OU Fulbright Scholar from Bosnia). Dr. Hooper uses this model to study neural muscular control in the stomachs of lobsters, but he says it can be scaled to adequately model skeletal muscle in many animals, including humans.

The skeletal muscle vibrational dynamics model is shown below. The lumped mass m represents the load the muscle is lifting vs. gravity g. The muscle itself is represented by linear elastic spring stiffness k_1, in parallel with linear elastic spring stiffness k_2 that is in series with linear dissipative dashpot b. The absolute displacement of the dashpot end and the muscle end are measured by coordinates x and y, respectively. Lengths L_{1R} and L_{2R} (not shown) are the resting lengths (not stretched by gravity) of springs 1 and 2, respectively. In vibrations it is more common to measure change in displacements relative to the gravity-stretched position, but biologists need to include the absolute spring lengths as well. The actuator F_A represents the contractile element of the muscle and F_m is the force generated by the muscle. Note: this derivation assumes zero pennation angle, i.e. zero angle α between the muscle fibers and the tendons.

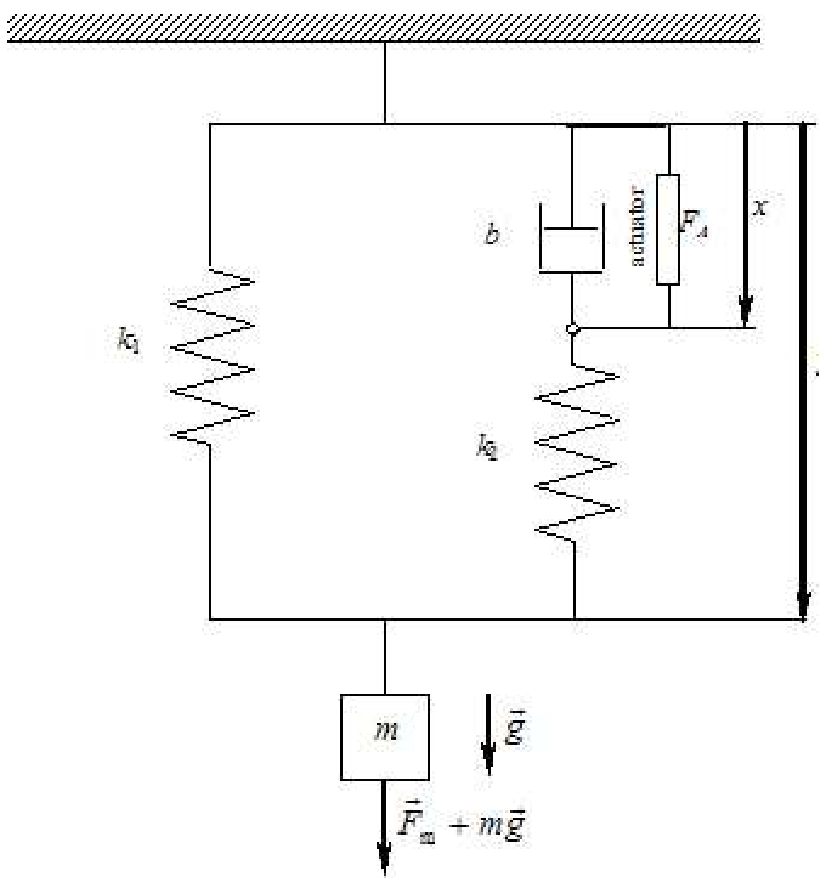

Dynamic Skeletal Muscle Diagram

The **parallel elastic component** k_1, provided by the muscle membranes, gives spring resistance when passively stretched. The **series elastic component** k_2 represents the tendons, storing elastic energy when a muscle is stretched. The tension-generating **contractile** effect of the sarcomeres, modeled by actuator force F_A, is in parallel with the membranes and in series with the tendons.

From the left figure below, the equation for the left spring is

$$k_1(y - L_{1R}) = F_1 \tag{1}$$

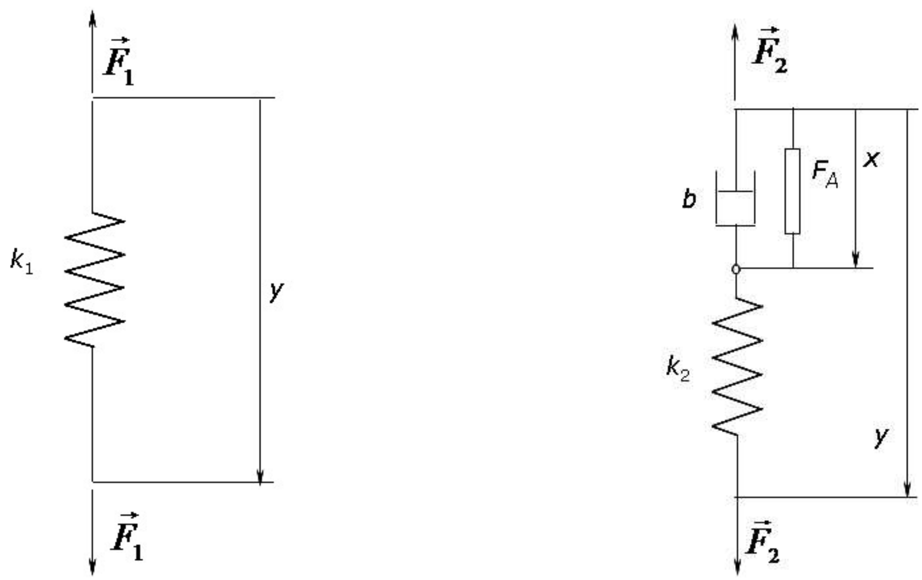

From the right figure above, the equations for the right spring and dashpot are:

$$\begin{aligned} k_2(y - x - L_{2R}) &= F_2 \\ b\dot{x} &= F_2 + F_A \end{aligned} \tag{2, 3}$$

From the FBD below, the dynamics equation for the mass is obtained using Newton's Second law.

$$\begin{aligned} \sum F_{vert} &= m a_{vert} \\ -F_1 - F_2 + F_m + mg &= m\ddot{y} \end{aligned} \tag{4}$$

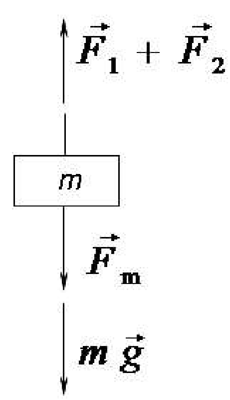

Substituting (1) and (2) into (4), and also substituting (2) into (3) yields the following coupled second- and first-order linear vibrational dynamics model for skeletal muscle:

$$\begin{aligned} m\ddot{y} + k_1(y - L_{1\mathrm{R}}) + k_2(y - x - L_{2\mathrm{R}}) &= mg + F_{\mathrm{m}} \\ b\dot{x} - k_2(y - x - L_{2\mathrm{R}}) &= F_{\mathrm{A}} \end{aligned} \tag{5, 6}$$

Equations (5, 6) can be written in the following form:

$$\begin{aligned} \ddot{y} + \frac{1}{m}(k_1 + k_2)y - \frac{k_2}{m}x &= \frac{1}{m}(k_1 L_{1\mathrm{R}} + k_2 L_{2\mathrm{R}}) + g + \frac{F_{\mathrm{m}}}{m} \\ \dot{x} + \frac{k_2}{b}x - \frac{k_2}{b}y &= \frac{F_{\mathrm{A}}}{b} - \frac{k_2}{b}L_{2\mathrm{R}} \end{aligned} \tag{7, 8}$$

As mentioned above, (7, 8) can be simplified by choosing more adequate coordinates that will measure the deviation from the static position only. The form shown above is formed intentionally for biological systems, using absolute coordinates and initial spring lengths.

The system of differential equations (7, 8) can be solved for coordinates x and y as functions of time given time functions for F_A and F_{m}. In the case of a simple form of F_A and F_{m} the solution could be found using reduction and decoupling by a formation of a single third-order linear ordinary differential equation.

$$\dddot{y}(t) + \frac{k_2}{b}\ddot{y}(t) + \frac{(k_1 + k_2)}{m}\dot{y}(t) + \frac{k_1 k_2}{mb}y(t) \quad = \quad \frac{\dot{F}_m(t)}{m} + \frac{k_2}{mb}(F_A(t) + F_m(t) + mg + k_1 L_{1R}) \tag{9}$$

Equation (9) can be solved for $y(t)$ which is then substituted into (8) to directly solve for $x(t)$.

As an alternative approach, the system of differential equations (7, 8) can be transformed into a state-space system of coupled first-order ODEs.

$$\begin{bmatrix} \dot{x}_1(t) \\ \dot{x}_2(t) \\ \dot{x}_3(t) \end{bmatrix} = \begin{bmatrix} -\frac{k_2}{b} & \frac{k_2}{b} & 0 \\ 0 & 0 & 1 \\ \frac{k_2}{m} & -\frac{1}{m}(k_1 + k_2) & 0 \end{bmatrix} \begin{bmatrix} x_1(t) \\ x_2(t) \\ x_3(t) \end{bmatrix} + \begin{bmatrix} \frac{1}{b} & 0 \\ 0 & 0 \\ 0 & \frac{1}{m} \end{bmatrix} \begin{bmatrix} F_{A1}(t) \\ F_M(t) \end{bmatrix} \tag{10}$$

where

$$\begin{bmatrix} F_{A1}(t) \\ F_M(t) \end{bmatrix} = \begin{bmatrix} F_A(t) - k_2 L_{2\mathrm{R}} \\ F_{\mathrm{m}}(t) + mg + k_1 L_{1\mathrm{R}} + k_2 L_{2\mathrm{R}} \end{bmatrix}$$

are the modified system inputs, and

$$x_1(t) = x(t)$$
$$x_2(t) = y(t)$$
$$x_3(t) = \dot{x}_2(t) = \dot{y}(t)$$

are the state variable definitions.

The system (10) can be rearranged in a form such that the constant terms within the inputs are moved to the state variables x_1, x_2 and x_3, which would not affect the time derivatives.

Simulation Results

The state-space coupled first-order differential equations (10) can be solved (simulated) using a numerical simulation method such as MATLAB's Simulink or MATLAB's SimMechanics.

We now simulate this single skeletal muscle model using the following dummy parameters (not from any biological system, just for demonstration purposes): m = 1 kg, k_1 = 1 N/m, k_2 = 1 N/m, b = 1 N-s/m, L_{1R} = 1 m, and L_{2R} = 1 m.

Dr. Hooper's lab measures experimental values for the stiffness and damping parameters *in vitro* in the laboratory for crustacean stomach muscles. This is far more difficult for human tissue and so the literature should be consulted for appropriate values for human skeletal muscles.

In this simulation, we calculate the model output response given zero inputs, $F_A = 0$ and $F_m = 0$. The only active force is the weight; the system is held at the rest spring lengths and then released to the effects of gravity.

The MATLAB/Simulink simulation results are shown in the two figures on the next page, giving the absolute coordinates $y(t)$ and $x(t)$, respectively, vs. time. As a check of the simulation model for the zero force inputs, one can expect that the steady-state values:

$$y_{ss} - x_{ss} = L_{2R}$$
$$10.8 - 9.8 = 1.0$$

The simulation results shown below confirm this result.

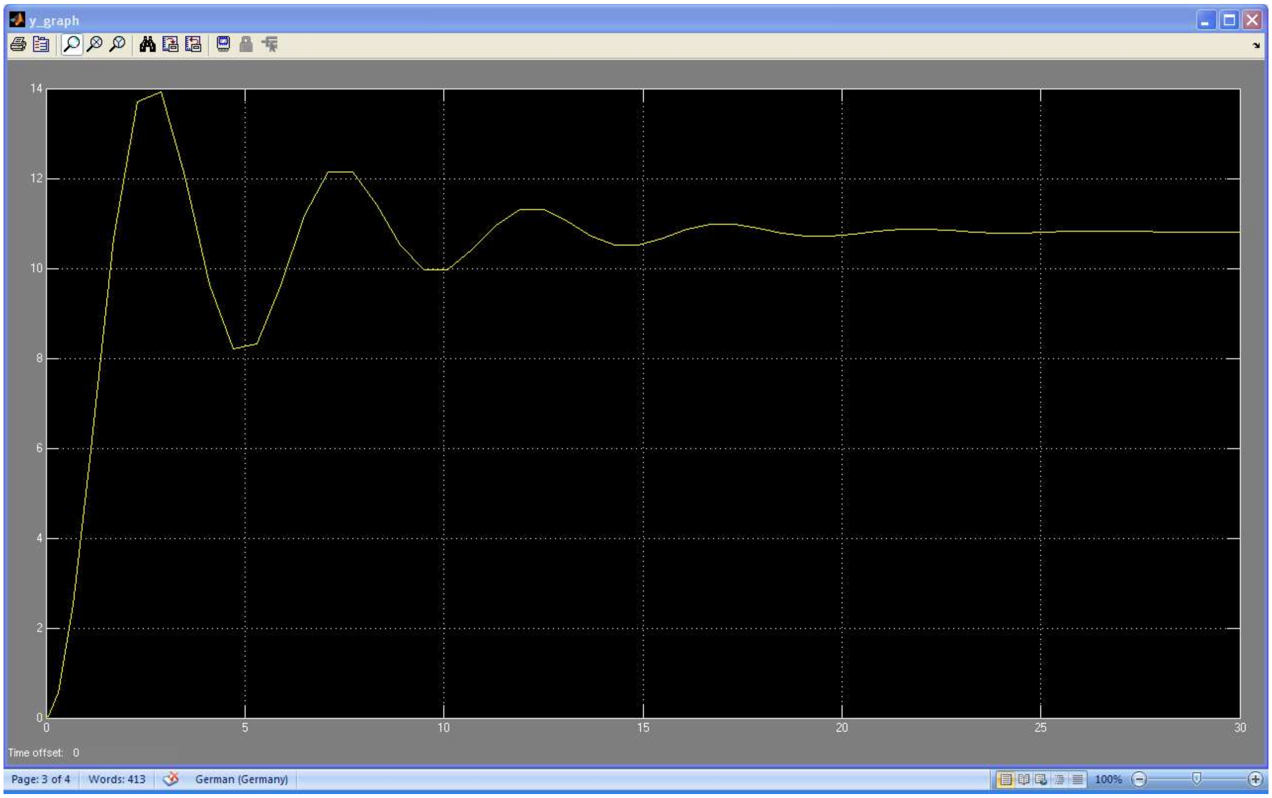

***y*(*t*) Coordinate Simulation Output**

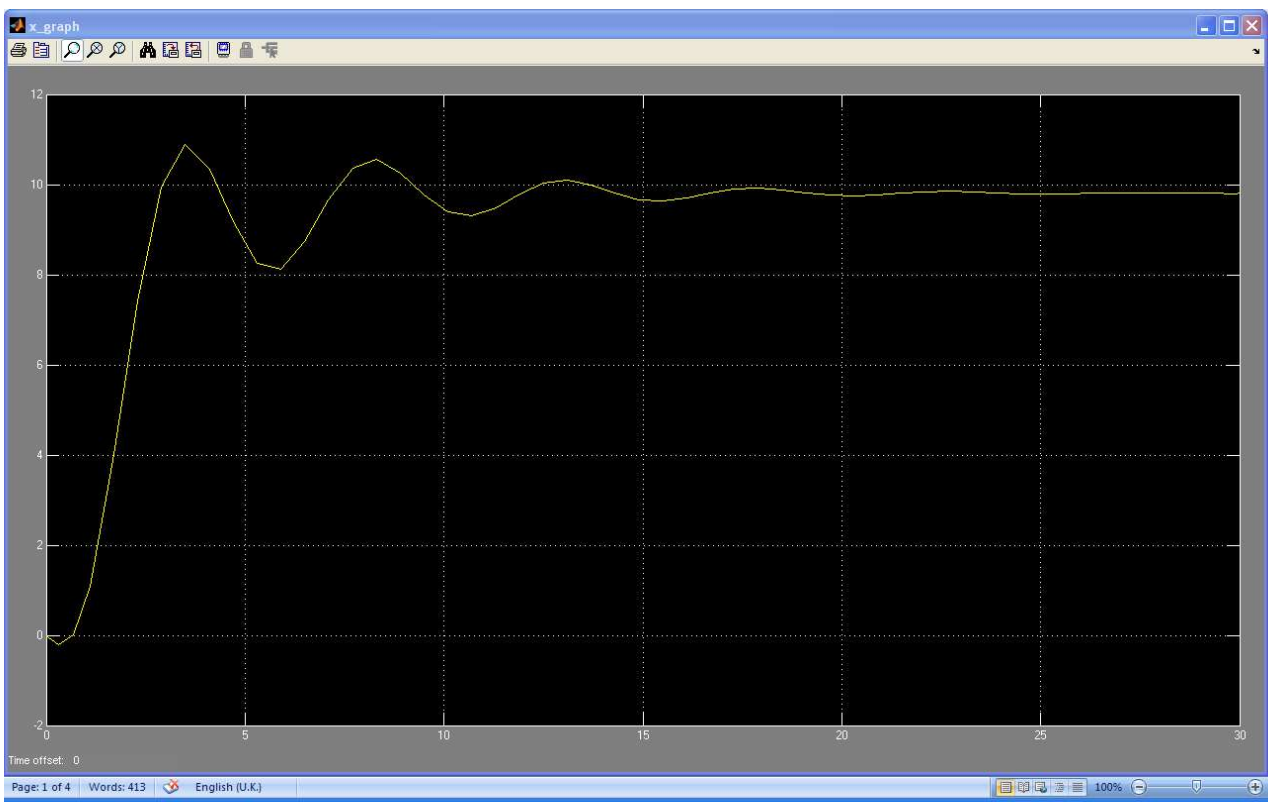

***x*(*t*) Coordinate Simulation Output**

The figure below shows the Simulink model used for this simulation. The model parameters m, k_1, k_2, b, L_{1R}, and L_{2R} can be changed within the model block diagram and the simulation results can be viewed on the scopes for x and y. The numerical results are displayed at each time step as the simulation proceeds.

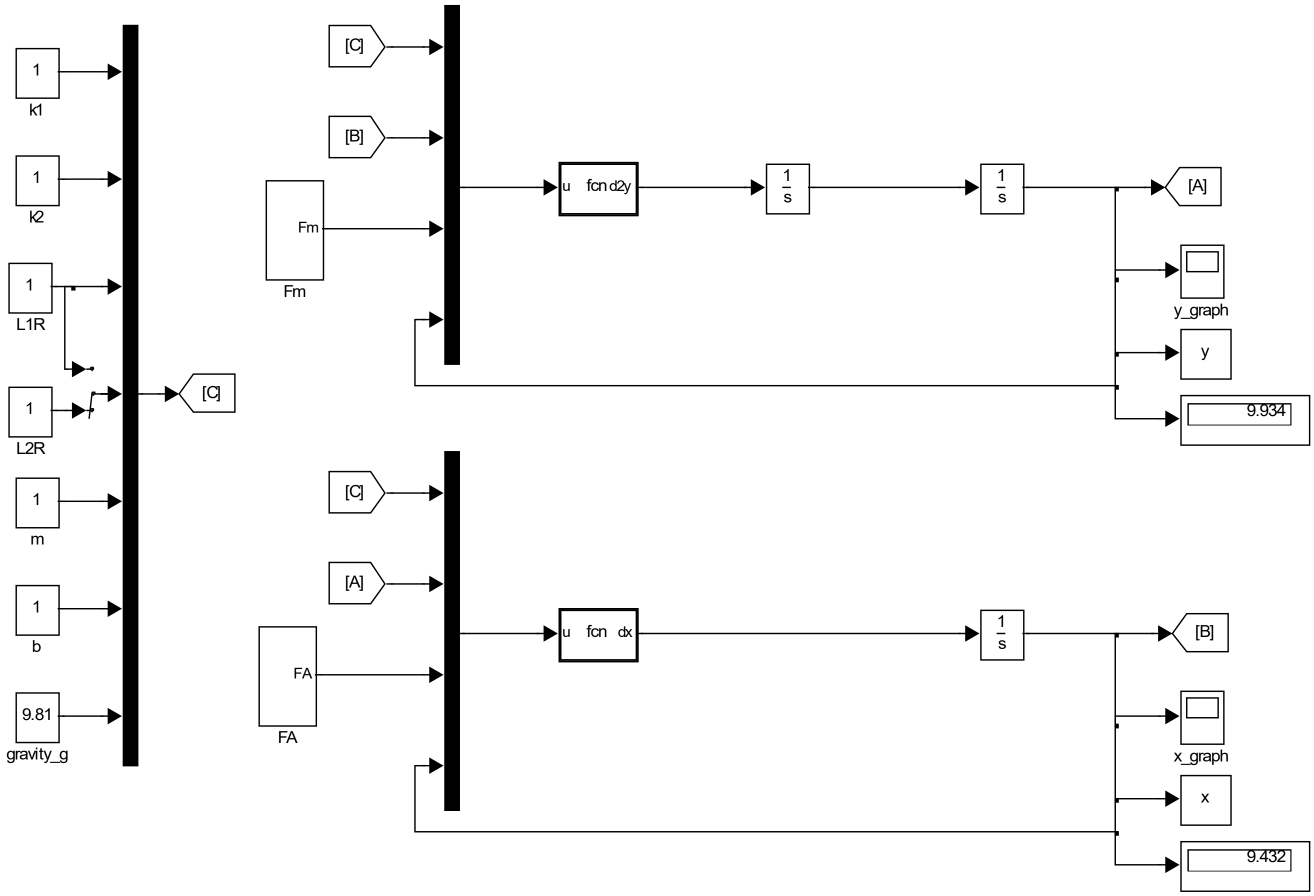

Simulink Muscle Model Block Diagram

Damped Pendulum Model

Dr. Hooper also suggested the following damped pendulum model as a simple representation of any limb actuated by agonist / antagonist muscles.

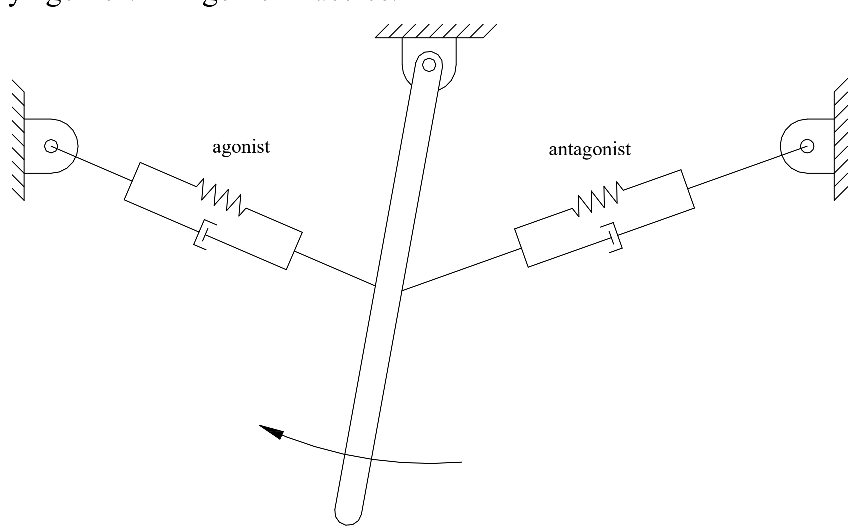

4. Human Body Engineering Mechanics: Kinematics

4.2 Human Arm Kinematics

Human Arm Velocity Kinematics

The human arm velocity equations come from the first time derivative of the FPK expressions (expressed in {0} coordinates):

$$
\begin{aligned}
x_H &= L_1 c_1 + L_2 c_{12} + L_3 c_{123} \\
y_H &= L_1 s_1 + L_2 s_{12} + L_3 s_{123} \\
\phi &= \theta_1 + \theta_2 + \theta_3
\end{aligned}
$$

$$
\begin{aligned}
c_1 &= \cos\theta_1 & c_{12} &= \cos(\theta_1 + \theta_2) & c_{123} &= \cos(\theta_1 + \theta_2 + \theta_3) \\
s_1 &= \sin\theta_1 & s_{12} &= \sin(\theta_1 + \theta_2) & s_{123} &= \sin(\theta_1 + \theta_2 + \theta_3)
\end{aligned}
$$

$$
\begin{aligned}
\dot{x}_H &= -L_1\dot{\theta}_1 s_1 - L_2(\dot{\theta}_1 + \dot{\theta}_2)s_{12} - L_3(\dot{\theta}_1 + \dot{\theta}_2 + \dot{\theta}_3)s_{123} \\
\dot{y}_H &= \quad L_1\dot{\theta}_1 c_1 + L_2(\dot{\theta}_1 + \dot{\theta}_2)c_{12} + L_3(\dot{\theta}_1 + \dot{\theta}_2 + \dot{\theta}_3)c_{123} \\
\dot{\phi} &= \quad \dot{\theta}_1 + \dot{\theta}_2 + \dot{\theta}_3
\end{aligned}
$$

Matrix-vector form

$$
{}^{\mathbf{0}}\dot{\mathbf{X}}_{\mathbf{H}} = {}^{\mathbf{0}}\mathbf{J}\dot{\mathbf{\Theta}}
$$

$$
\begin{Bmatrix} \dot{x}_H \\ \dot{y}_H \\ \dot{\phi} \end{Bmatrix} = \begin{bmatrix} -L_1 s_1 - L_2 s_{12} - L_3 s_{123} & -L_2 s_{12} - L_3 s_{123} & -L_3 s_{123} \\ L_1 c_1 + L_2 c_{12} + L_3 c_{123} & L_2 c_{12} + L_3 c_{123} & L_3 c_{123} \\ 1 & 1 & 1 \end{bmatrix} \begin{Bmatrix} \dot{\theta}_1 \\ \dot{\theta}_2 \\ \dot{\theta}_3 \end{Bmatrix}
$$

where ${}^{\mathbf{0}}\dot{\mathbf{X}}_{\mathbf{H}} = \{\dot{x}_H \quad \dot{y}_H \quad \dot{\phi}\}^T$ are the absolute Cartesian velocities of the hand relative to the base {0}, $\dot{\mathbf{\Theta}} = \{\dot{\theta}_1 \quad \dot{\theta}_2 \quad \dot{\theta}_3\}^T$ are the relative joint velocities, and

$$
{}^{\mathbf{0}}\mathbf{J} = \begin{bmatrix} -L_1 s_1 - L_2 s_{12} - L_3 s_{123} & -L_2 s_{12} - L_3 s_{123} & -L_3 s_{123} \\ L_1 c_1 + L_2 c_{12} + L_3 c_{123} & L_2 c_{12} + L_3 c_{123} & L_3 c_{123} \\ 1 & 1 & 1 \end{bmatrix}
$$

is the Jacobian matrix expressed in {0}.

Human Arm Acceleration Kinematics

The human arm acceleration equations come from the first time derivative of the velocity equations (expressed in {0} coordinates):

$$\begin{aligned}
\dot{x}_H &= -L_1\dot{\theta}_1 s_1 - L_2(\dot{\theta}_1+\dot{\theta}_2)s_{12} - L_3(\dot{\theta}_1+\dot{\theta}_2+\dot{\theta}_3)s_{123} \\
\dot{y}_H &= \ \ L_1\dot{\theta}_1 c_1 + L_2(\dot{\theta}_1+\dot{\theta}_2)c_{12} + L_3(\dot{\theta}_1+\dot{\theta}_2+\dot{\theta}_3)c_{123} \\
\dot{\phi} &= \ \ \dot{\theta}_1+\dot{\theta}_2+\dot{\theta}_3
\end{aligned}$$

$$\begin{aligned}
c_1 &= \cos\theta_1 & c_{12} &= \cos(\theta_1+\theta_2) & c_{123} &= \cos(\theta_1+\theta_2+\theta_3) \\
s_1 &= \sin\theta_1 & s_{12} &= \sin(\theta_1+\theta_2) & s_{123} &= \sin(\theta_1+\theta_2+\theta_3)
\end{aligned}$$

$$\begin{aligned}
\ddot{x}_H &= -L_1\ddot{\theta}_1 s_1 - L_1\dot{\theta}_1^2 c_1 - L_2(\ddot{\theta}_1+\ddot{\theta}_2)s_{12} - L_2(\dot{\theta}_1+\dot{\theta}_2)^2 c_{12} - L_3(\ddot{\theta}_1+\ddot{\theta}_2+\ddot{\theta}_3)s_{123} - L_3(\dot{\theta}_1+\dot{\theta}_2+\dot{\theta}_3)^2 c_{123} \\
\ddot{y}_H &= \ \ L_1\ddot{\theta}_1 c_1 - L_1\dot{\theta}_1^2 s_1 + L_2(\ddot{\theta}_1+\ddot{\theta}_2)c_{12} - L_2(\dot{\theta}_1+\dot{\theta}_2)^2 s_{12} + L_3(\ddot{\theta}_1+\ddot{\theta}_2+\ddot{\theta}_3)c_{123} - L_3(\dot{\theta}_1+\dot{\theta}_2+\dot{\theta}_3)^2 s_{123} \\
\ddot{\phi} &= \ \ \ddot{\theta}_1+\ddot{\theta}_2+\ddot{\theta}_3
\end{aligned}$$

$$\begin{Bmatrix} \ddot{x}_H \\ \ddot{y}_H \\ \ddot{\phi} \end{Bmatrix} = \begin{bmatrix} -L_1s_1-L_2s_{12}-L_3s_{123} & -L_2s_{12}-L_3s_{123} & -L_3s_{123} \\ L_1c_1+L_2c_{12}+L_3c_{123} & L_2c_{12}+L_3c_{123} & L_3c_{123} \\ 1 & 1 & 1 \end{bmatrix} \begin{Bmatrix} \ddot{\theta}_1 \\ \ddot{\theta}_2 \\ \ddot{\theta}_3 \end{Bmatrix} + \begin{bmatrix} -L_1c_1 & -L_2c_{12} & -L_3c_{123} \\ -L_1s_1 & -L_2s_{12} & -L_3s_{123} \\ 1 & 1 & 1 \end{bmatrix} \begin{Bmatrix} \dot{\theta}_1^2 \\ \dot{\theta}_{12}^2 \\ \dot{\theta}_{123}^2 \end{Bmatrix}$$

Matrix-vector form

$$ {}^{\mathbf{0}}\ddot{\mathbf{X}}_{\mathbf{H}} = {}^{\mathbf{0}}\mathbf{J}\ddot{\boldsymbol{\Theta}} + {}^{\mathbf{0}}\dot{\mathbf{J}}\dot{\boldsymbol{\Theta}}$$

$$\begin{Bmatrix} \ddot{x}_H \\ \ddot{y}_H \\ \ddot{\phi} \end{Bmatrix} = \begin{bmatrix} -L_1s_1-L_2s_{12}-L_3s_{123} & -L_2s_{12}-L_3s_{123} & -L_3s_{123} \\ L_1c_1+L_2c_{12}+L_3c_{123} & L_2c_{12}+L_3c_{123} & L_3c_{123} \\ 1 & 1 & 1 \end{bmatrix} \begin{Bmatrix} \ddot{\theta}_1 \\ \ddot{\theta}_2 \\ \ddot{\theta}_3 \end{Bmatrix} +$$

$$\begin{bmatrix} -L_1c_1\dot{\theta}_1-L_2c_{12}\dot{\theta}_{12}-L_3c_{123}\dot{\theta}_{123} & -L_2c_{12}\dot{\theta}_{12}-L_3c_{123}\dot{\theta}_{123} & -L_3c_{123}\dot{\theta}_{123} \\ -L_1s_1\dot{\theta}_1-L_2s_{12}\dot{\theta}_{12}-L_3s_{123}\dot{\theta}_{123} & -L_2s_{12}\dot{\theta}_{12}-L_3s_{123}\dot{\theta}_{123} & -L_3s_{123}\dot{\theta}_{123} \\ 1 & 1 & 1 \end{bmatrix} \begin{Bmatrix} \dot{\theta}_1 \\ \dot{\theta}_2 \\ \dot{\theta}_3 \end{Bmatrix}$$

where ${}^{\mathbf{0}}\ddot{\mathbf{X}}_{\mathbf{H}} = \{\ddot{x}_H \quad \ddot{y}_H \quad \ddot{\phi}\}^T$ are the absolute Cartesian accelerations of the hand relative to the base {0}, $\ddot{\boldsymbol{\Theta}} = \{\ddot{\theta}_1 \quad \ddot{\theta}_2 \quad \ddot{\theta}_3\}^T$ are the relative joint accelerations, $\dot{\theta}_{12} = \dot{\theta}_1 + \dot{\theta}_2$ and $\dot{\theta}_{123} = \dot{\theta}_1 + \dot{\theta}_2 + \dot{\theta}_3$.

5. Human Body Engineering Mechanics: Statics

5.1 Additional Human Body Statics Examples

Example 8

2-D Static Analysis of Shoulder Abduction

Question Slow shoulder abduction in the frontal plane with a weight in the hand is a common exercise to strengthen the deltoids. What are the forces required to sustain a weight held in the hand at an abduction angle of 90 degrees (Figure 2.3a)?

Solution We will treat the model as planar, so we can use a 2-D analysis. We now must decide what details to include in our analysis. Since we are interested in only the forces at the shoulder, we can leave the entire arm plus the weight as a single segment. The specified external forces are the weight of each anatomic segment—upper arm, forearm, and hand—plus the free weight. We will assume in this problem that the entire arm weighs 30 N and its center of mass is 30 cm from the center of the scapulo-humeral joint along a line from the center of the shoulder joint to the center of the of the wrist. We will also assume that the free weight is 60 N and is along the same line at a distance of 50 cm from the scapulo-humeral joint.

We begin by isolating the segment from the shoulder and drawing a free-body diagram of the arm plus weight (Figure 2.3b). The full free-body diagram would include a number of force-carrying elements across the shoulder joint. In fact, it would be necessary to decide the extent of the shoulder joint—does it include only the scapulo-humeral joint? If we assume that it does, then we would "cut" the following muscles across the joint: the deltoid, the pectoralis major, the supraspinatus, the infraspinatus, the teres minor, the teres major, the subscapularis, the latissimus dorsi, the biceps brachii, and the triceps brachii.

If we regard each of these muscles as single vectors, each represents two unknown scalar quantities. We will now make another common assumption,

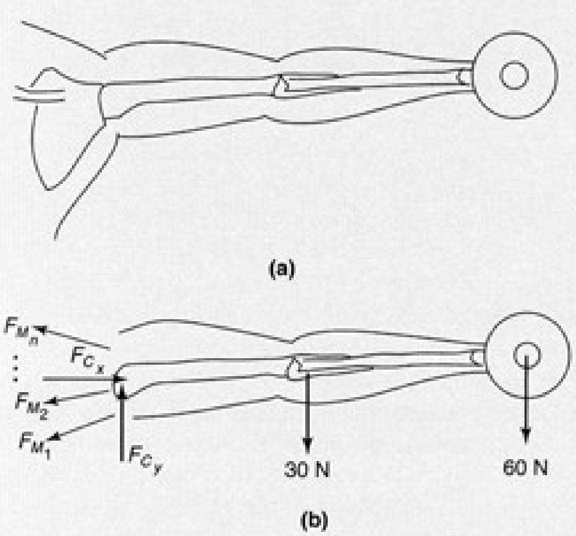

FIGURE 2.3 (a) Supporting a weight with the arm horizontal. (b) Free-body diagram of the arm and weight as a single segment.

namely, that we know the line of action of each muscle force from knowledge of the anatomy. We thereby reduce each muscle force to a single unknown magnitude. We can also assume that the joint contact force acts through a known point, the center humeral head. We cannot assume anything about the direction of the contact force, so it represents two unknowns in this problem. In addition, there are ligamentous and capsular forces. Another reasonable assumption might be that the shoulder is not at its limits of the range of motion, and as a result, the ligaments do not develop significant forces. Accepting all these assumptions reduces the unknowns to 10 muscle force magnitudes and 2 components of the unknown contact force. We can express the equations of equilibrium in terms of horizontal (x direction) forces, vertical (y direction) forces, and a moment equation taken about the shoulder as follows:

$$\sum_{i=1}^{10} F_{M_i}\cos(\theta_i) + F_{J_x} = 0$$

$$\sum_{i=1}^{10} F_{M_i}\sin(\theta_i) + F_{J_y} - 60 - 30 = 0$$

$$\sum_{i=1}^{10} F_{M_i}d_i - (60)(50) - (30)(30) = 0$$

Here, i refers to the muscle number, F_{M_i} refers to the muscle force magnitude, θ_i refers to the (known) angle between the x axis and the direction of the muscle force, and d_i refers to the (known) moment arm of the muscle with respect to the shoulder. Obviously, with 12 unknowns and only three equations, we cannot solve for individual muscle forces and the joint contact force. The most we can do is express their relationship to the external forces and moments; that is,

$$\sum_{i=1}^{10} F_{M_i}\cos(\theta_i) + F_{J_x} = 0$$

$$\sum_{i=1}^{10} F_{M_i}\sin(\theta_i) + F_{J_y} = 90$$

$$\sum_{i=1}^{10} F_{M_i}d_i = 3900$$

It is evident that the equations of statics alone are insufficient to determine individual muscle forces and the joint contact force, even given several major assumptions. In fact, to reduce the equations to a determinate set, we would have to limit the action to only one muscle. If, for example, we chose to consider only the deltoid to be active, the equations would become

$$F_M\cos\theta + F_{J_x} = 0$$

$$F_M\sin\theta + F_{J_y} = 90$$

$$F_M d = 3900$$

Obviously, this problem is now solvable for the deltoid muscle force and the two components of the joint contact force once we specify the geometric parameters d and θ that define the line of action of the deltoid. If, for example, the muscle acts at an angle of $\theta = 175°$ (i.e., 5° above horizontal in the medial direction) and with a moment arm $d = 3$ cm, the equations yield

$$F_M = 1300 \text{ N}$$

$$F_{Jx} = +1295 \text{ N}$$

$$F_{Jy} = -23 \text{ N}$$

Note that the results are very sensitive to uncertainties in the values of d and θ.

Bartel et al. (2006)

Example 9

How much compression acts on the hip during two-legged standing, given that the joint supports 250 N of body weight and the abductor muscles are producing 600 N of tension?

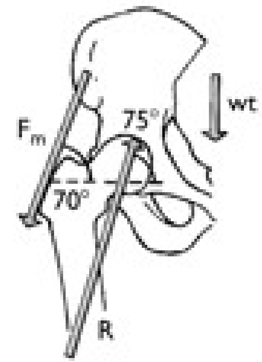

Known

$$wt = 250$$
$$F_m = 600\ N$$

Graphic Solution

Since the body is motionless, all vertical force components must sum to zero and all horizontal force components must sum to zero. Graphically, this means that all acting forces can be transposed to form a closed force polygon (in this case, a triangle). The forces from the diagram of the hip above can be reconfigured to form a triangle.

If the triangle is drawn to scale (perhaps 1 cm = 100 N), the amount of joint compression can be approximated by measuring the length of the joint reaction force (R).

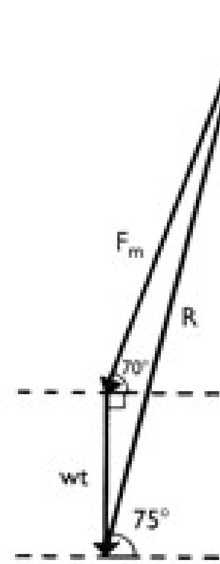

$$R \approx 750\ N$$

Mathematical Solution

The law of cosines can be used with the same triangle to calculate the length of R.

$$R^2 = F_m^{\,2} + wt^2 - 2(F_m)\,(wt)\cos 160°$$
$$R^2 = 600\ N^2 + 250\ N^2 - 2(600\ N)\,(250\ N)\cos 160°$$
$$R = 751\ N$$

Hall (2007)

Note from Dr. Bob – this example has an error; the cosine law is correct, but the conclusion was calculated incorrectly. The correct answer is R = 839.3 N. The joint reaction force can be calculated using the sine law:

$$\gamma = \sin^{-1}\left(\frac{600}{R}\sin 160^\circ\right) = 14.2^\circ$$

Since γ is the complement of the desired angle, the answer is 75.8°, close to what is shown in the figure.

Example 10

How much compression acts on the patellofemoral joint when the quadriceps exerts 300 N of tension and the angle between the quadriceps and the patellar tendon is (a) 160° and (b) 90°?

Known

$$F_m = 300 \text{ N}$$

Angle between F_m and F_t:

1. 160°
2. 90°

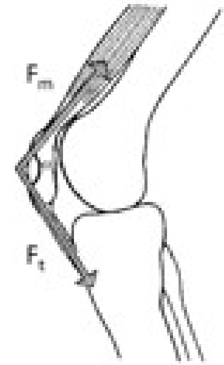

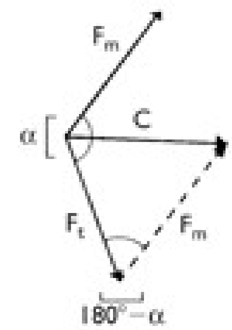

Graphic Solution

Vectors for F_m and F_t are drawn to scale (perhaps 1 cm: 100 N), with the angle between them first at 160° and then at 90°. The tip-to-tail method of vector composition is then used (see Chapter 3) to translate one of the vectors so that its tail is positioned on the tip of the other vector. The compression force is the resultant of F_m and F_t and is constructed with its tail on the tail of the original vector and its tip on the tip of the transposed vector.

The amount of joint compression can be approximated by measuring the length of vector C.

1. $C \approx 100$ N
2. $C \approx 420$ N

Mathematical Solution

The angle between F_t and transposed vector F_m is 180° minus the size of the angle between the two original vectors, or (a) 20° and (b) 90°. The law of cosines can be used to calculate the length of C.

1. $C^2 = F_m{}^2 + F_t{}^2 - 2(F_m)(F_t)\cos 20$

   $C^2 = 300 \text{ N}^2 + 300 \text{ N}^2 - 2(300 \text{ N})(300 \text{ N})\cos 20$

   $C = 104$ N

2. $C^2 = F_m{}^2 + F_t{}^2 - 2(F_m)(F_t)\cos 90$

   $C^2 = 300 \text{ N}^2 + 300 \text{ N}^2 - 2(300 \text{ N})(300 \text{ N})\cos 90$

   $C = 424$ N

Note: This problem illustrates the extent to which patellofemoral compression can increase due solely to changes in knee flexion.

Normally, there is also increased quadriceps force with increased knee flexion.

Hall (2007)

Example 11

The quadriceps tendon attaches to the tibia at a 30° angle 4 cm from the joint center at the knee. When an 80 N weight is attached to the ankle 28 cm from the knee joint, how much force is required of the quadriceps to maintain the leg in a horizontal position? What is the magnitude and direction of the reaction force exerted by the femur on the tibia? (Neglect the weight of the leg and the action of other muscles.)

$$wt = 80\ N$$
$$d_{wt} = 0.28\ \ m$$
$$d_F = 0.04\ \ m$$

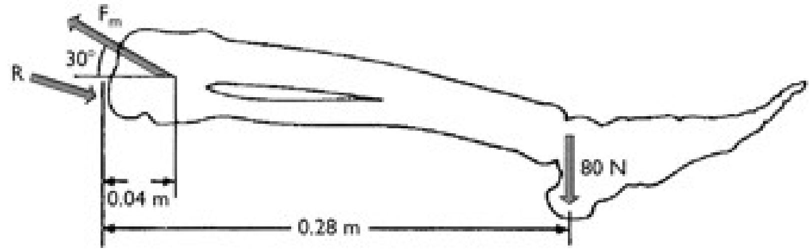

Solution

The equations of static equilibrium can be used to solve for the unknown quantities:

$$\Sigma T_k = 0$$
$$\Sigma T_k = (F_m \sin 30)\,(d_F) - (wt)\,(d_{wt})$$
$$0 = (F_m \sin 30)\,(0.04\ m) - (80\ N)\,(0.28\ m)$$
$$F_m = 1120\ N$$

The equations of static equilibrium can be used to solve for the vertical and horizontal components of the reaction force exerted by the femur on the tibia. Summation of vertical forces yields the following:

$$\Sigma F_v = 0$$
$$\Sigma F_v = R_v + (F_m \sin 30) - wt$$
$$0 = R_v + 1120 \sin 30\ N - 80\ N$$
$$R_v = -480\ N$$

Summation of horizontal forces yields the following:

$$\Sigma F_h = 0$$
$$\Sigma F_h = R_h - (F_m \cos 30)$$
$$0 = R_h - 1120 \cos 30\ N$$
$$R_h = 970\ N$$

The Pythagorean theorem can now be used to find the magnitude of the resultant reaction force:

$$R = \sqrt{(-480\ N)^2 + (970\ N)^2}$$
$$= 1082\ N$$

The tangent relationship can be used to find the angle of orientation of the resultant reaction force:

$$\tan \alpha = \frac{480\ N}{970\ N}$$
$$\alpha = 26.3$$
$$R = 1082\ N,\ \alpha = 26.3\ \text{degrees}$$

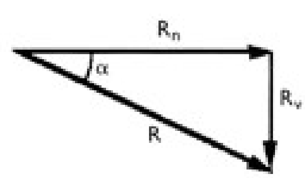

Hall (2007)

Example 12

Free-Body Diagram of the Lower Leg During Stair Climbing

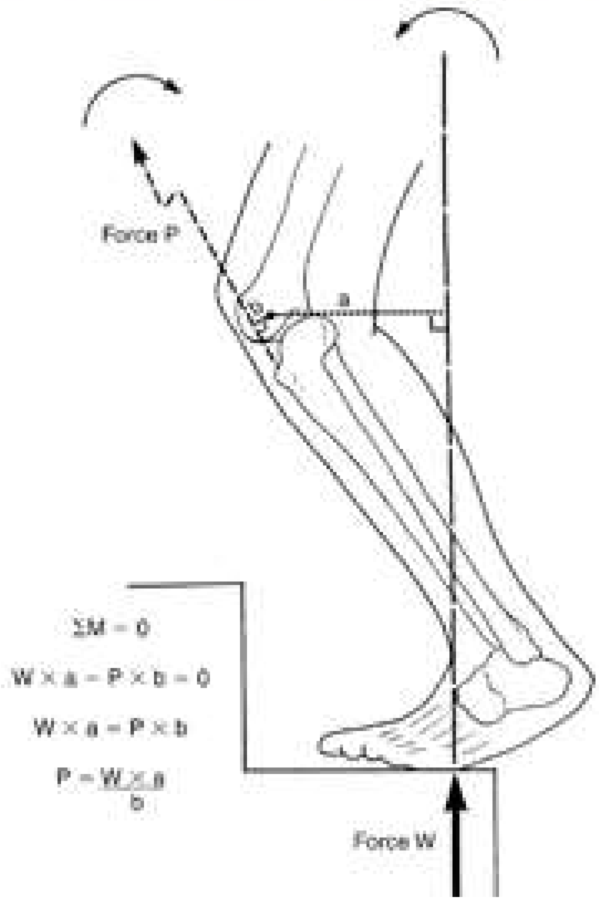

The two main moments acting around the center of motion of the tibiofemoral joint (solid dot) are designated on the free-body diagram of the lower leg during stair climbing (Calculation Box Fig. 7-2-1).

The flexing moment on the lower leg is the product of the weight of the body[1] (W, the ground reaction force) and its lever arm (a), which is the perpendicular distance of the force W to the center of motion of the tibiofemoral joint. The counterbalancing extending moment is the product of the quadriceps muscle force through the patellar tendon (P) and its lever arm (b). Because the lower leg is in equilibrium, the sum of these two moments must equal zero ($\Sigma M = 0$).

In this example, the counterclockwise moment is arbitrarily designated as positive ($W \times a - P \times b = 0$). Values for lever arms a and b can be measured from anatomical specimens or on soft tissue imaging or fluoroscopy (Kellis & Baltzopoulos, 1999; Wretenberg et al., 1996), and the magnitude of W can be determined from the body weight of the individual. The magnitude of P can then be found from the moment equilibrium equation:

$$P = \frac{W \times a}{b}$$

[1]Again the weight of the lower leg is disregarded because it is less than one tenth of body weight.

Nordin and Frankel (2001)

Example 13

Joint Reaction Forces at the Knee in Flexion

Knee flexion influences the patellofemoral joint reaction force by changing the angle between the patellar tendon and the quadriceps tendon (Calculation Box Fig. 7-3-1, *A & B*).

The angle between the patellar tendon (P) and the quadriceps tendon (Q) is 35° with the knee flexed 5° (left top) and 80° with the knee flexed 90° (left bottom). Values for the tendon angles are from Matthews and Associates (1977), who determined the angle roentgenographically after placing two metal wires along each of these tendons.

The patellofemoral joint reaction force with the knee in 5 and 90° of flexion is obtained by constructing a parallelogram of forces for each situation and using trigonometric calculations. The patellofemoral joint reaction force (J) is the resultant of the two equal force components through the patellar tendon (P) and the quadriceps tendon (Q). As the angle between these force components becomes more acute with greater knee flexion, the resultant joint reaction force (J) becomes larger. *Adapted from Wiktorin, C.v.H. & Nordin, M. (1986).* Introduction to Problem Solving in Biomechanics *(pp. 87–129). Philadelphia: Lea & Febiger.*

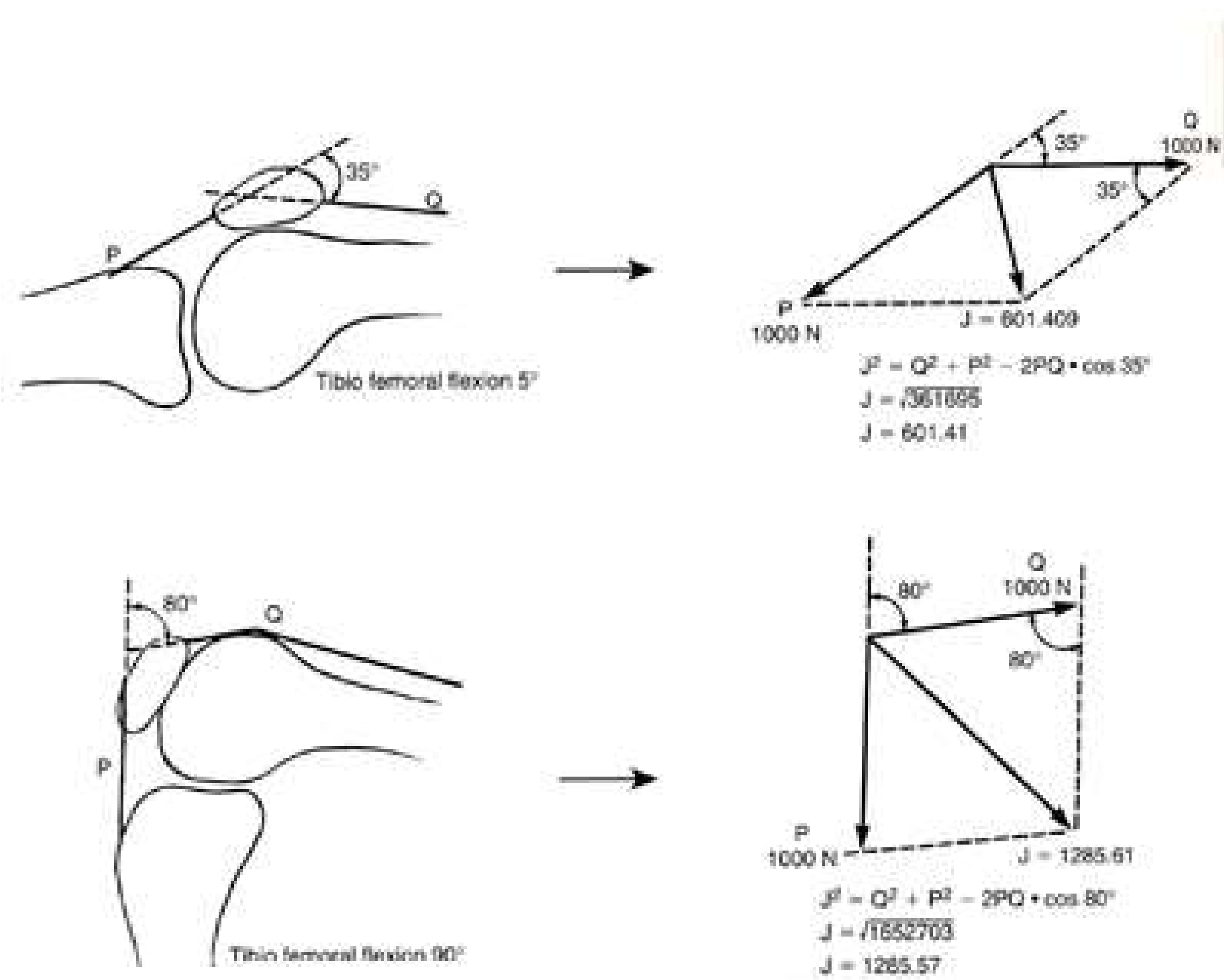

Nordin and Frankel (2001)

7. Human Body Metrology

Biomechanicists perform human motion studies for various reasons: medical, physical therapy, rehabilitation, sports, ergonomics, design, safety, injury, and the arts. Metrology is the science of measurement. This section presents some metrology technology used in human motion studies.

Whole-Body Scanning

The Computerized Anthropometric Research and Design (CARD) Laboratory at Wright-Patterson Air Force Base with industrial partners and SAE have conducted an international anthropometric survey of civilians, called the Civilian American and European Surface Anthropometry Resource, or CAESAR.

This survey uses the latest three-dimensional (3-D) surface anthropometry technology for detailed measurement of the outer surface of the human body. These technologies can capture hundreds of thousands of points in three-dimensions on the human body surface in a few seconds. It is non-contact and allows natural clothing, equipment, and postures. It can be used for fitting uniforms to specific individuals and for statistical biomechanics.

The goal of CAESAR is to represent the anthropometric variability of men and women, ages 18-65 in the United States and Europe (4,000 U.S. subjects (NATO most populous), 2,000 Netherlands subjects (tallest), and 2,000 Italy subjects (shortest). The measurement is static by nature, but anthropomorphic parameters may be extracted based on height and weight.

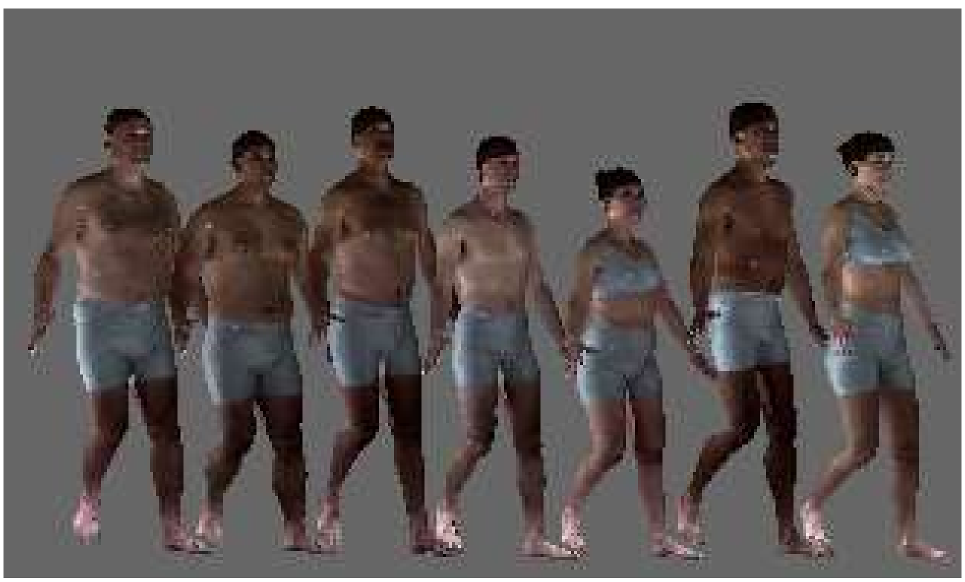

Sample CAESAR Individual Images

Muscle Electromyography (EMG)

Galvani (18th century Italian scientist) discovered that a. human skeletal muscle develops tension when electrically stimulated; and b. human skeletal muscle produces detectable current/voltage when developing tension. Recording muscle electrical activity using skin electrodes is called **electromyography** (**EMG**). EMG is used to study neuromuscular function, including which muscles are recruited for motions and nerve conduction and muscle response velocities (Hall, 2007).

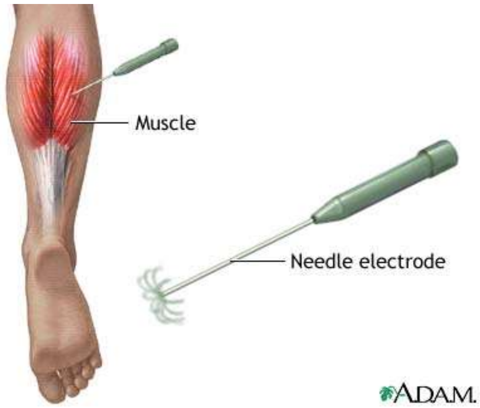

EMG Electrode
nlm.nih.gov

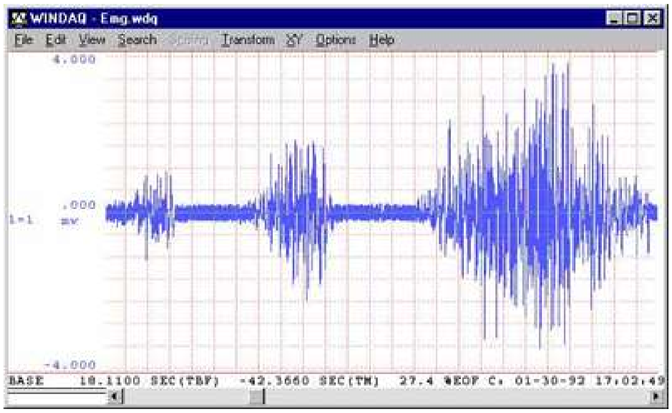

EMG Data
dataq.com

Joint Angle Measurement

Electrogoniometers convert joint angles to voltage (when worn across a joint such as the knee or elbow with an exoskeleton-like device). The voltage is sampled continuously so dynamic measurements can be made. A calibration is required to calculate relative joint angle based on voltage. There are two types of electrogoniometers, both using resistive transducers.

1. ***Potentiometers*** are variable resistors activated by changes in joint angle. The output voltage is linearly related to the input joint angle, over a large range of motion. Also used in robotics joint sensing.

2. ***Strain Gauges*** connected to a Wheatstone bridge sense strain via thin wires in certain directions – the change in the wire due to motion causes a change in resistance in the circuit.

Potentiometers
mie-uk.com/gait

Cyber Glove
immersion.com

Electrogoniometers are low-cost and easy to use; however, they are not as accurate as other sensing strategies. Also, they must be placed directly at the joint which may interfere with natural motion, with all the cabling. Finally, they only measure relative joint angles while some inverse dynamics analyses require absolute joint angles.

Electromagnetic Tracking Systems

Developed by the military and now applied widely for VR and entertainment (animation, gaming, and films). These systems can measure the absolute pose (3D, 6-dof position and orientation) of body segments mounted with a receiver. Based on Faraday's Law of magnetic induction – electrons in a conductor experience a magnetic force when moved through a magnetic field. The magnitude of the induced force is proportional to the strength of the magnetic field and the speed of the conductor. There are two types for human motion studies:

1. ***AC Magnetic Field***, such as Polhemus Incorporated's wireless Liberty system (polhemus.com).

Liberty 6-dof Tracker

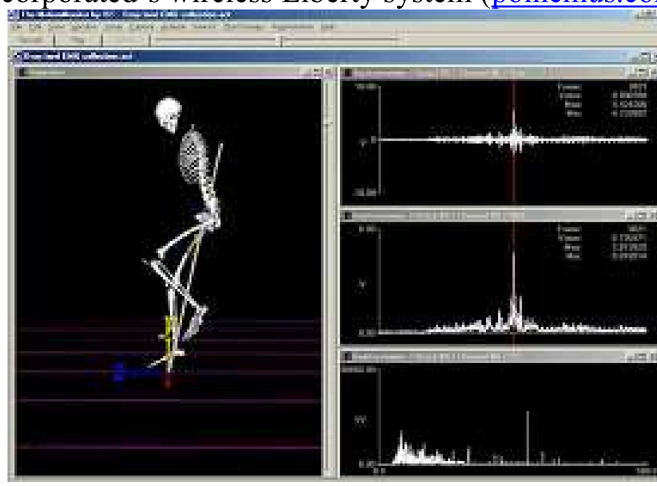

Application (innsport.com)

2. ***DC Pulsed Magnetic Field***, such as Ascension Technology Corporation's (ascension-tech.com) **Flock of Birds**.

Flock of Birds 6-dof Tracker

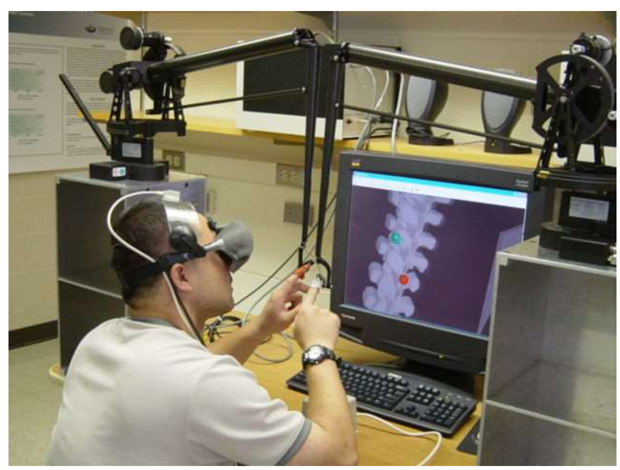

OU VHB Application

Accuracy and precision are affected by metal in the workspace and noise. Accuracy of less than 2 mm and 0.5 deg is possible. Line of sight is not necessary.

Motion Capture (MoCap) Systems

Current whole-body motion capture systems are available in two categories.

1. Wearable suit with flexible fiber optic shapetape, such as the ShapeWrap system from Measurand, Inc. (motion-capture-system.com), used in the films Lord of the Rings Series and The Polar Express.

ShapeWrap II in OU @ Lab

2. Video-camera-based optical human motion measurement systems are expensive but popular. The subject is marked with various reflective markers at points of interest and multiple cameras are used to triangulate 3D positions. Orientation may be obtained by three points on the same rigid body.

Ohio Supercomputing Center (OSC) Vicon8i **OSC Subject with Markers**

Marcel Marceau in OSC MoCap System

accad.osu.edu

Accelerometers

Accelerometers are common for measuring accelerations in the lab for engineering mechanics, using strain gauge force transducers; a variation in electrical current is measured based on pressure changes due to the inertia of the accelerometer in motion. Commonly linear accelerations are measured, which may be twice integrated (knowing initial velocities and positions) for velocity and position of the object. Accelerometers have been adapted for measuring human dynamic motions.

Force plates

Planar foot force plates measuring ground reaction forces have been developed to study human and other animal gaits, but can also be applied to starts, takeoffs, landings, swings, balance, and other dynamic motions. This is called dynamography (Hall, 2007).

Bertec Force plate in OU PT Motor Control Lab

8. Human Body Simulation Software

Human Biomechanics Software

OpenSim

OpenSim is an open-source software system that lets users develop models of musculoskeletal structures and create dynamic simulations of movement. The software provides a platform on which the biomechanics community can build a library of simulations that can be exchanged, tested, analyzed, and improved through multi-institutional collaboration. The underlying software is written in ANSI C++, and the graphical user interface (GUI) is written in Java. OpenSim technology makes it possible to develop customized controllers, analyses, contact models, and muscle models among other things. These plugins can be shared without the need to alter or compile source code. Users can analyze existing models and simulations and develop new models and simulations from within the GUI.

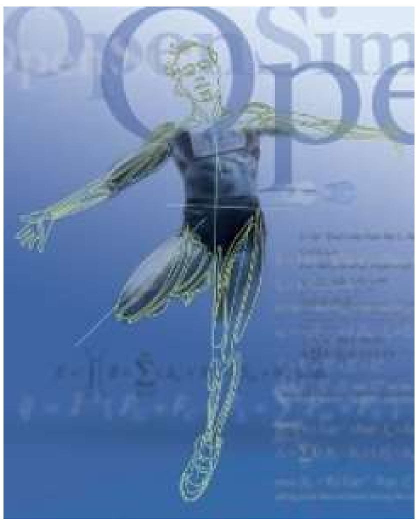

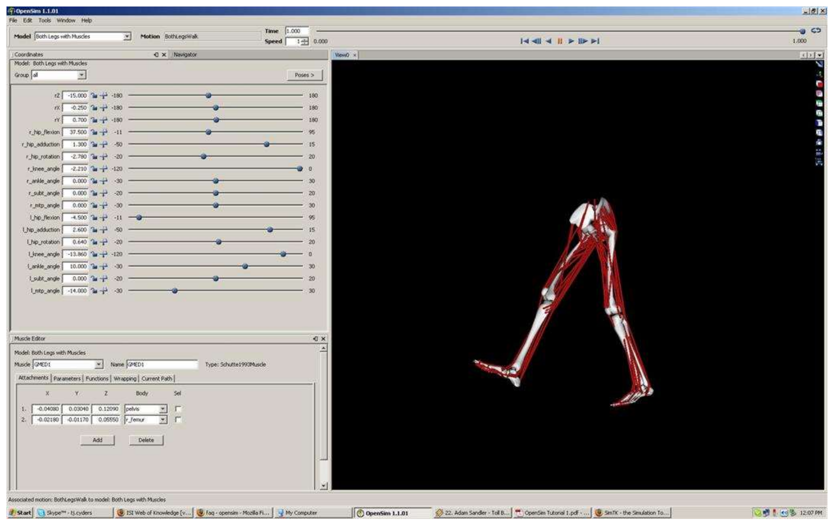

Purpose Provide easy-to-use, extensible software for modeling, simulating, controlling, and analyzing the neuromusculoskeletal system.

Audience Biomechanics scientists, clinicians, and developers who need software tools (or code) for modeling and simulating motion and forces for neuromusculoskeletal systems.

Long Term Goals and Related Uses Provide high-quality, easy-to-use, bio-simulation tools that allow for significant advances in biomechanics research.

simtk.org/home/opensim

www.dkimages.com/discover

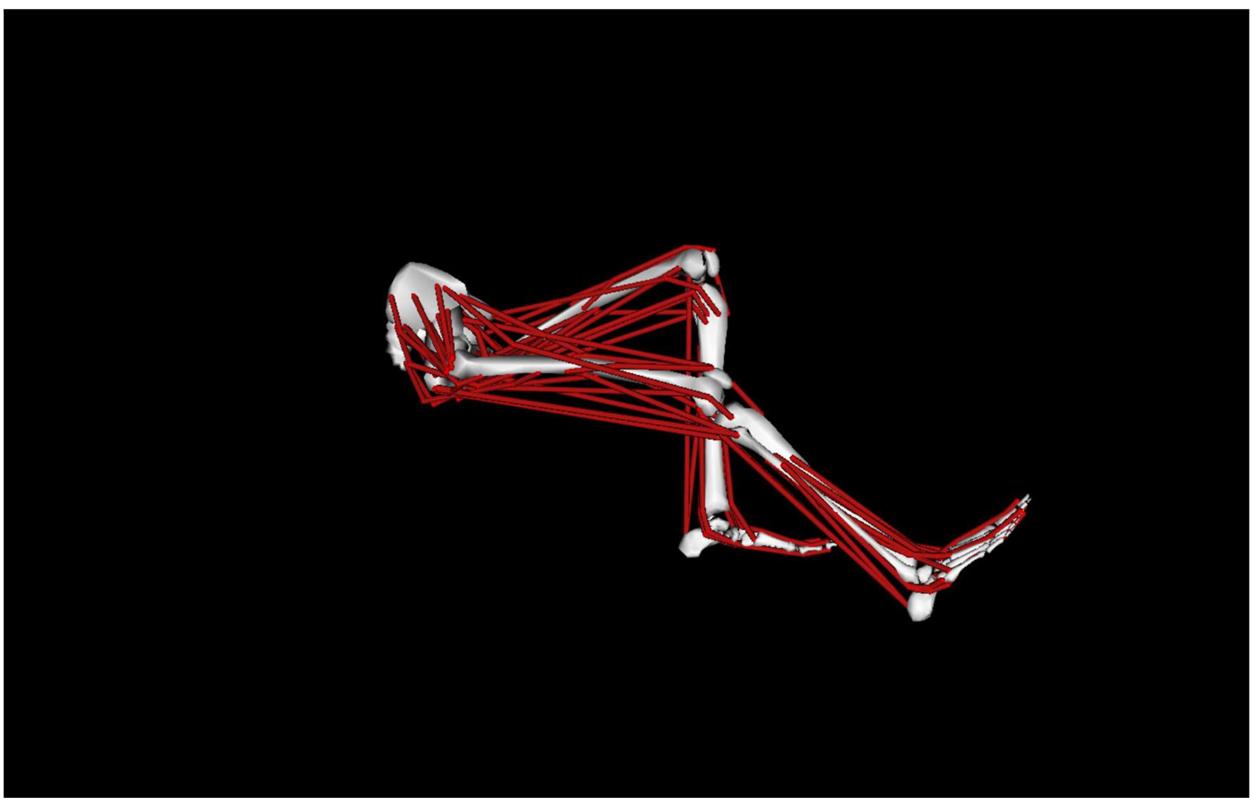

T.J. Cyders, BME 567 Project, Ohio U., Spring 2008

Recumbent Bicycle Photograph and Model

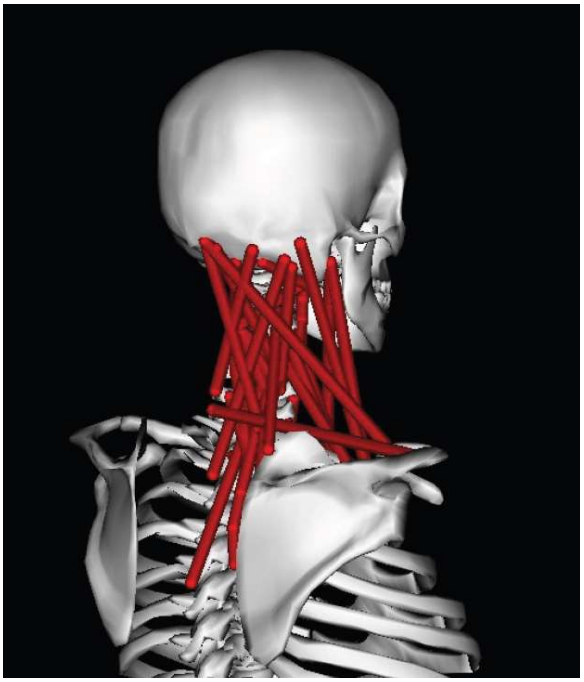

OpenSim Human Neck Model

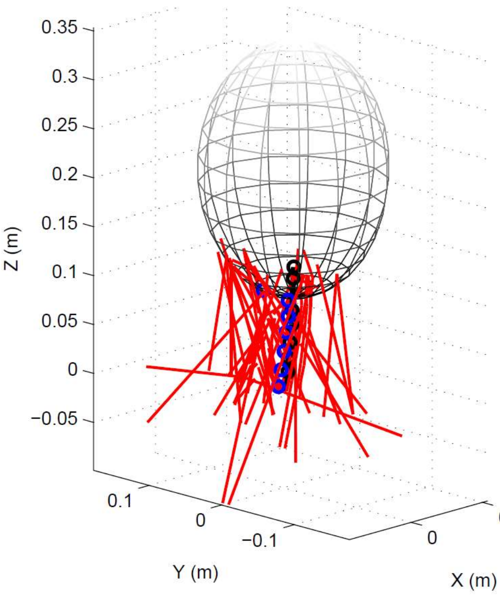

MATLAB Human Neck Model

8-link, 8S, 24-dof, 76-cable Human Neck Model

Lau, Oetomo, Halgamuge, IEEETRO 2013

Human Crash Modeling Software

Articulated Total Body (ATB, USAF) Model

The Articulated Total Body (ATB) Model is a public domain computer program used to simulate the dynamic motion of jointed systems of rigid bodies. The most common application of ATB is to model human or dummy occupant motion in vehicle crashes. The Articulated Total Body (ATB) model is a computer simulation program developed by the Air Force Research Laboratory (AFRL) for the prediction of human body dynamics during aircraft ejection, aircraft crashes, automobile accidents, and other hazardous events. The ATB model is a three-dimensional, multi body dynamics program. It is based on the Crash Victim Simulator developed by the National Highway Traffic Safety Administration (NHTSA). The AFRL has added the capability to model restraint systems, aerodynamic forces and other options, and by developing a graphics program for the display of the model's results.

atbmodel.com

ATB has been coupled with the finite element packages LS-DYNA and MSC/DYTRAN (Williams et al., 2001).

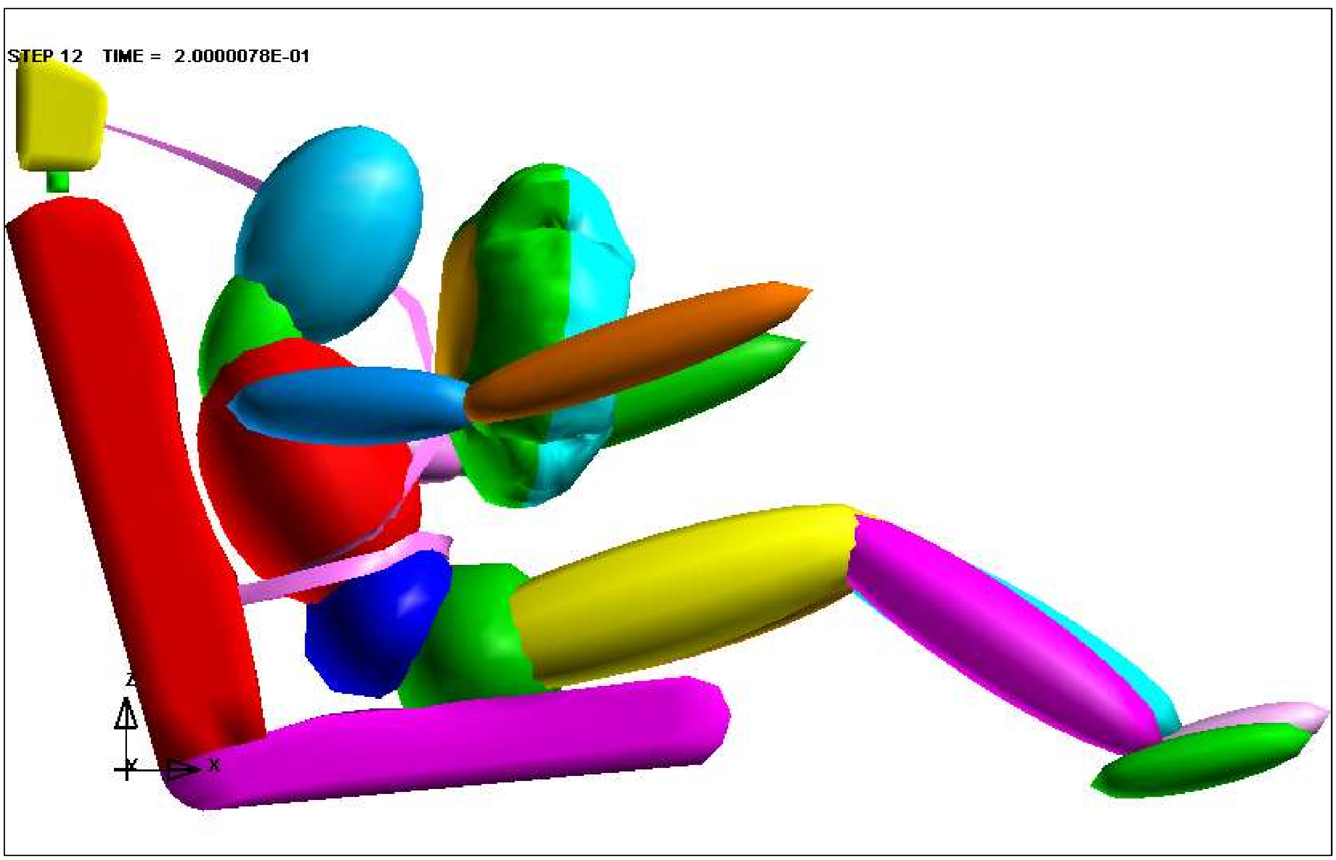

MADYMO (TNO, Netherlands)

MADYMO (**MA**thematical **DY**namic **MO**dels) is a software package that allows users to design and optimize occupant safety systems efficiently, quickly and cost-effectively. MADYMO is the worldwide standard for occupant safety analysis and simulation and it is used extensively in engineering departments, design studios, research laboratories and technical universities. It has proven itself in numerous applications, often supported by verification studies using experimental data.

With MADYMO, an occupant safety system can be thoroughly assessed and optimized early in its development cycle. Users therefore avoid the delays and costs involved in having to change a product late in its development. MADYMO also reduces the requirement for costly and time-consuming prototyping. As a result, production processes are drastically streamlined, and users can get their products to market more quickly.

tass-safe.com

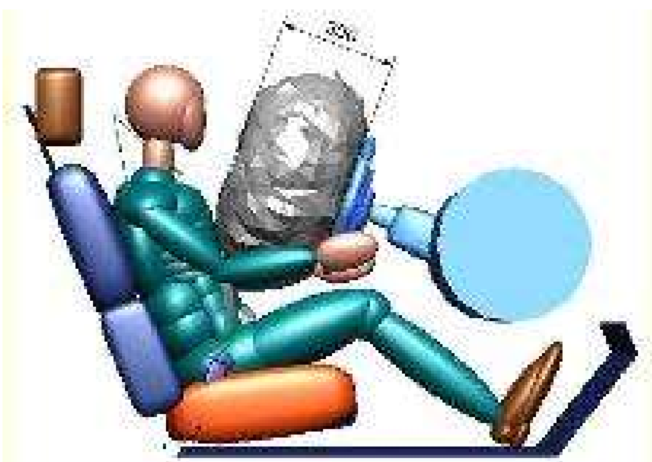

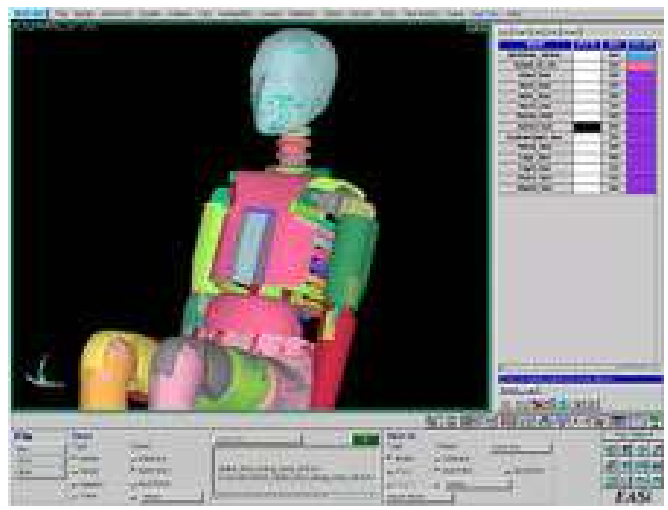

PAM-Crash/PAM-Safe 2G (ESI Group, French)

With **BioRID-II crash dummy model** (biofidelic rear impact dummy).

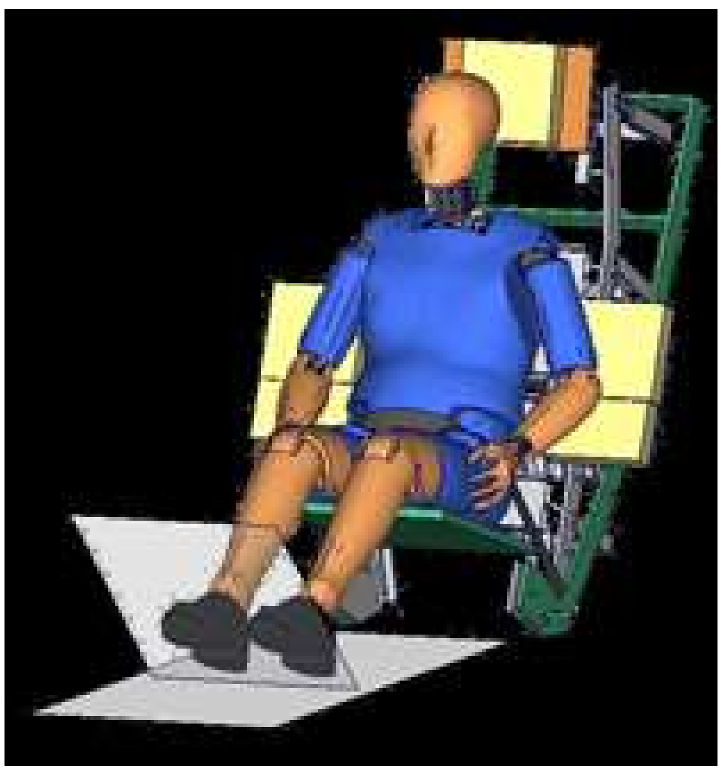

Human Motion Simulation Software

Jack

Tecnomatix' **Jack** is an ergonomics and human factors product that helps various industries to improve the ergonomics of product designs and workplace tasks. This software enables users to position biomechanically accurate digital humans of various sizes in virtual environments, assign them tasks and analyze their performance. **Jack** (and **Jill**) digital humans can tell engineers what they can see and reach, how comfortable they are, when and why they're getting hurt, when they're getting tired and other important ergonomics information. This information helps organizations design safer and more effective products faster and for less cost. Jack helps companies bring factories on-line faster and optimize productivity while improving worker safety.

plm.automation.siemens.com

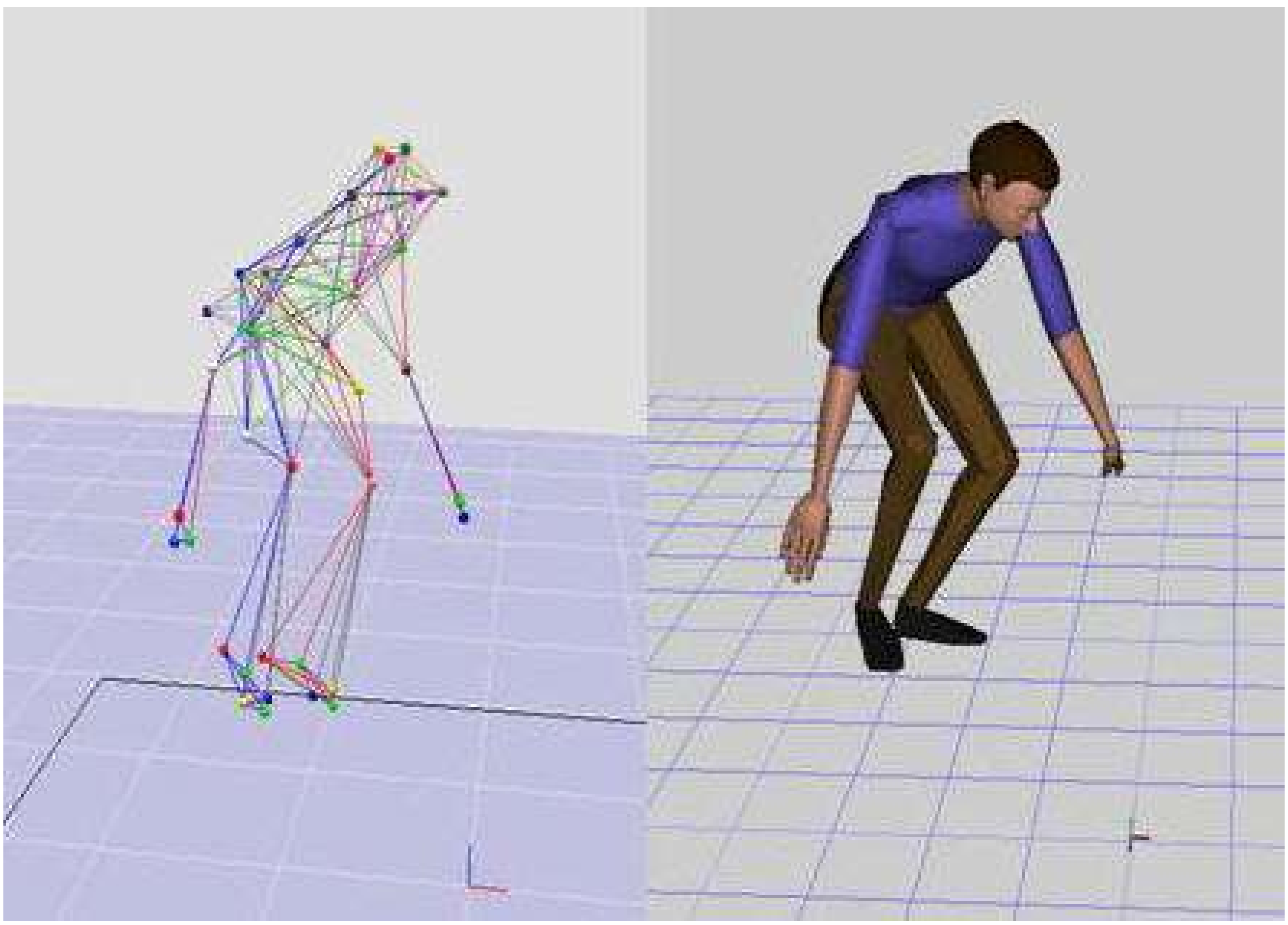

The Ohio University Virtual Haptic Back (VHB)

The **Virtual Haptic Back** (**VHB**) is intended for students of osteopathic and allopathic medicine, physical and massage therapy, and chiropractic trainees. The VHB augments traditional training in the difficult art of palpatory diagnosis (identifying medical problems via touch). Via two PHANToM® 3.0 haptic interfaces, the student can explore a realistic virtual human back with accurate graphical and haptic (force and touch feedback) representations. This product can be used for student practice and as a repeatable, objective evaluation tool to track student progress. This is the only product in existence for training and assessing students in palpatory diagnosis.

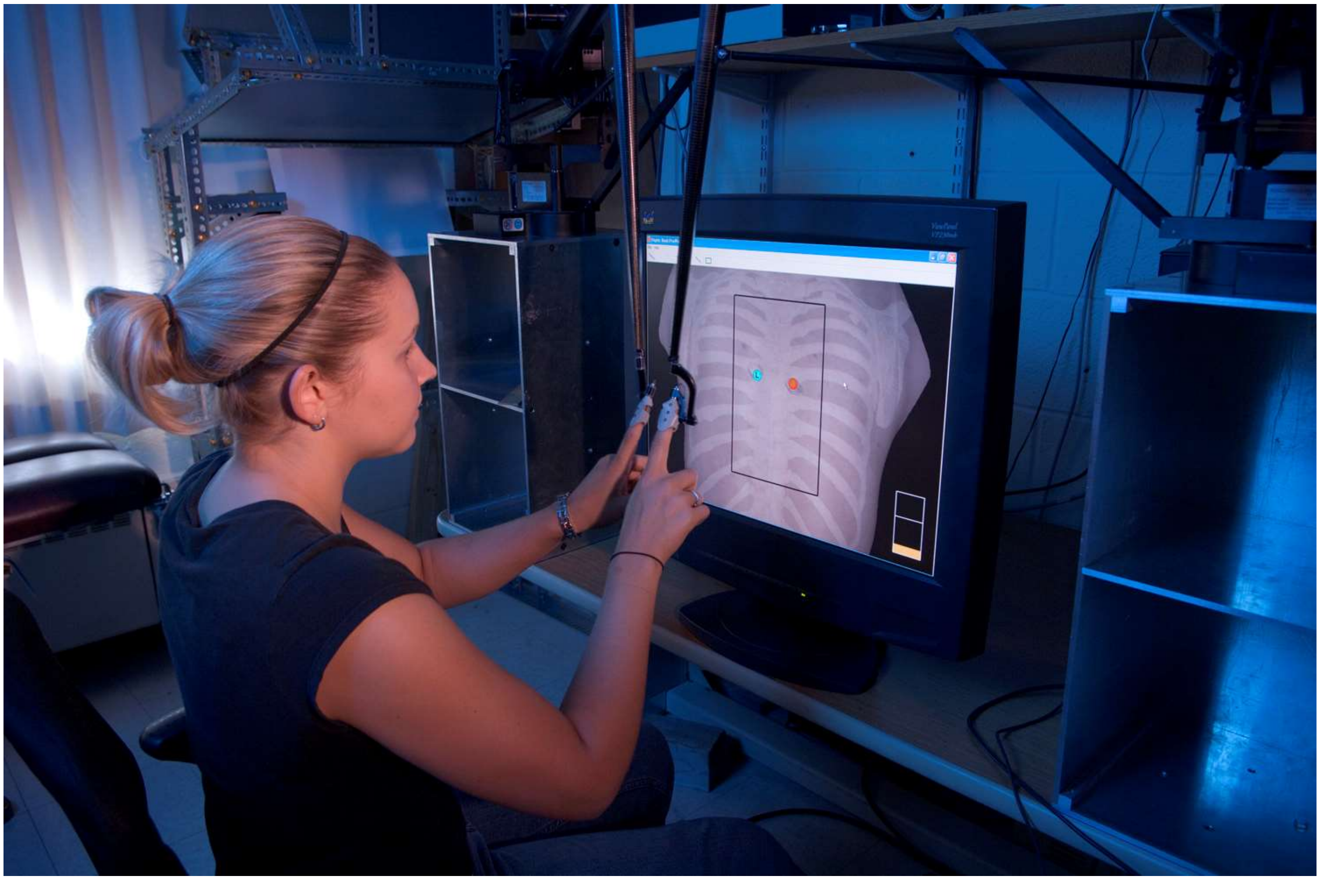

Medical Student Practicing with the Virtual Haptic Back

www.ohio.edu/people/williar4/html/VHB/VHB.html

The art of palpatory diagnosis is difficult to teach, learn, and assess. The medical student above is practicing on the VHB what she learns in osteopathic manipulative medicine laboratory. The VHB adds an objective and repeatable component of science to the art of palpatory diagnosis. Realistic somatic dysfunctions of different difficulty levels are programmed in random locations for the student to find by touch. According to our intensive evaluations with medical students and faculty, the VHB has great potential for improving and assessing manual detection skills.

The VHB started with a static back where the students can feel different simulated tissue compliances. Gross motion from the sacrum through the spine, shoulders, and arms is now enabled as shown below (the **Virtual Haptic Human Upper Body**, **VHHUB**).

VHHUB Setup

As seen below, the dysfunctional areas are highlighted as red rectangles. This is hidden from the student during practice and appears in the case of a wrong response, providing immediate feedback for the student to explore their mistakes haptically and graphically and thus learn more deeply, in a fun manner.

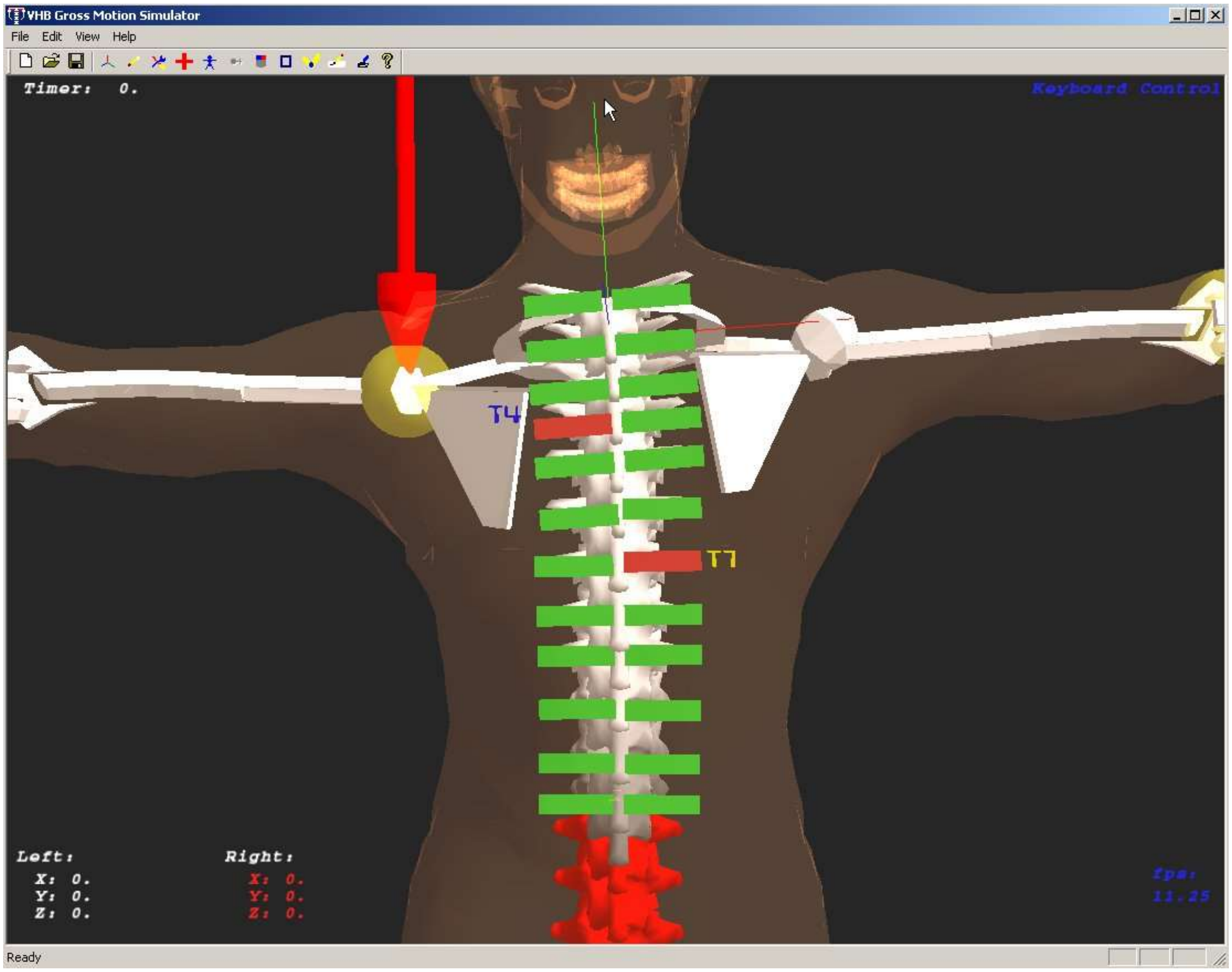

VHHUB Model (medium-build adult male)

The VHHUB allows both passive (i.e. user-applied) and active (i.e. patient-applied) gross motions. In the proposed project we will focus only on the passive mode. The gross motions allowed for motion testing are side bending (both directions) and rotation, plus compound motions, imparted by the user via the left-handed haptic interface.

Three virtual patient postures are programmed into VHHUB as shown in below for the petite adult female model. All three postures are in common use in osteopathic clinical practice.

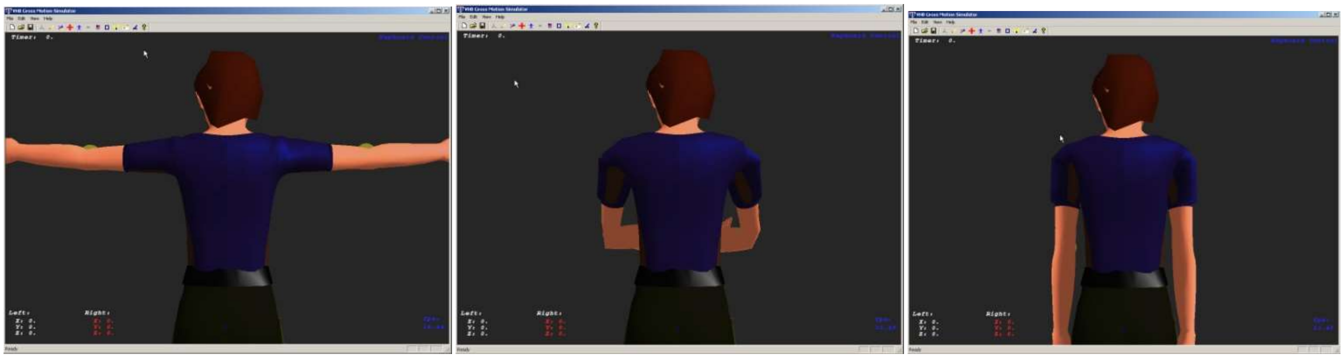

Three VHHUB postures

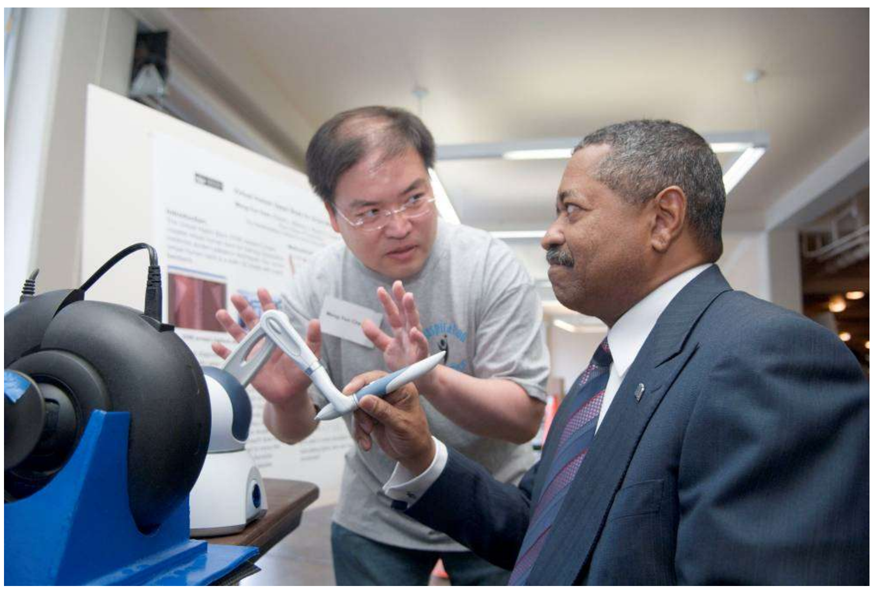

Meng-Yun Chen demonstrating the VHHUB to Ohio University President McDavis at the 2007 research fair

The University of Iowa Virtual Soldier

Santos is an intelligent avatar with realistic biomechanical abilities that functions in a human simulation environment. Santos conducts safety analysis and human factors studies in design relevant to training, production, or performance needs of real-world realistic systems. Using the Santos environment, one can examine biomechanics, gait, motion prediction, and related issues. Santos acts autonomously and predicts human motion.

digital-humans.org

HUMOSIM (Human Motion Simulation, University of Michigan)

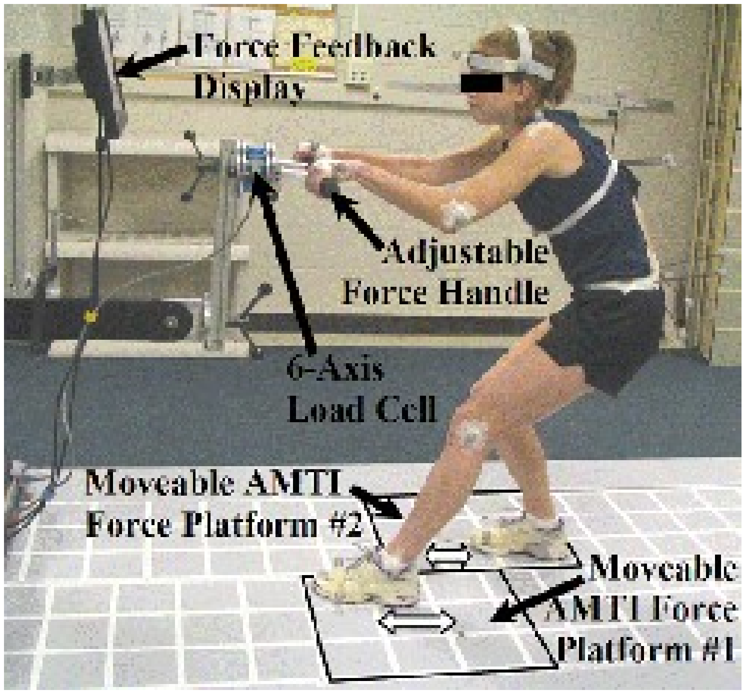

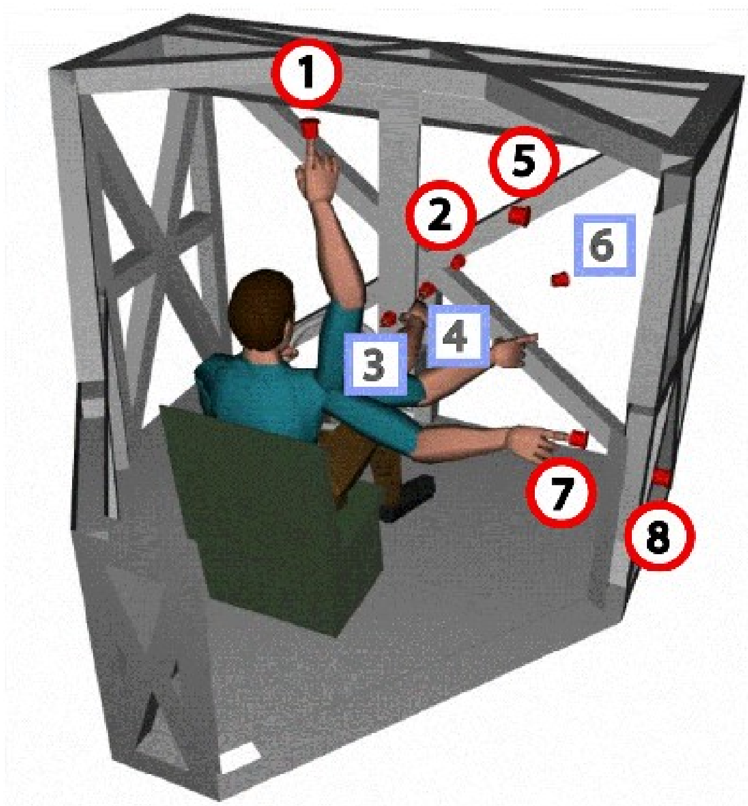

engin.umich.edu/dept/ioe/HUMOSIM

DI-Guy Real-Time Human Simulation Software

bostondynamics.com

Ellipsoid Mathematics

Some human simulation software uses ellipsoids for representing human body segments. Therefore, this section presents some ellipsoid mathematics

An ellipsoid is a three dimensional ellipse formed by putting a line through the longest part of the ellipse and rotating it. An ellipsoid is a three-dimensional figure all planar cross-sections of which are either ellipses or circles.

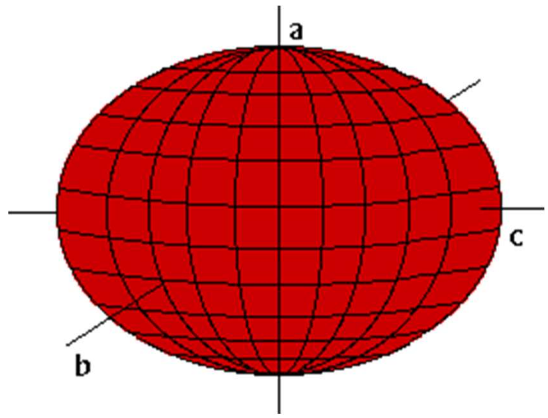

Ellipsoid

A surface defined by an algebraic equation of degree two is called a **quadric**. Spheres, circular cylinders, circular cones, hyperboloids, paraboloids, and ellipsoids are all quadrics. The equation for the points on the surface of an ellipsoid is:

$$\frac{(x-x_c)^2}{a^2}+\frac{(y-y_c)^2}{b^2}+\frac{(z-z_c)^2}{c^2}=1$$

where the center is (x_c, y_c, z_c), and $a,b,c \neq 0$ are the semi-axis lengths along the principal *xyz* directions. The volume of an ellipsoid is:

$$V=\frac{4}{3}\pi abc$$

For an ellipsoid of regular geometry and homogeneous material, the CG is the geometric center (x_c, y_c, z_c) and the mass moment of inertia tensor at the CG, along the principal directions is:

$$I_{CG}=\begin{bmatrix} \frac{m}{5}\left(b^2+c^2\right) & 0 & 0 \\ 0 & \frac{m}{5}\left(a^2+c^2\right) & 0 \\ 0 & 0 & \frac{m}{5}\left(a^2+b^2\right) \end{bmatrix}$$

where *m* is the ellipsoid mass.

For the special ellipsoid with two equal semiaxes $b = c$, we call it a prolate spheroid when $a > b$ (an ellipse rotated about its major axis) and an oblate spheroid when $a < b$ (an ellipse rotated about its minor axis).

Now, we see in Appendix D that the CGs and I_{CG} of each human body segment do not follow that of a simple ellipsoid. Therefore, one approach is to use good anthropometric data from Appendix D or other valid source for dynamics calculations and just represent the human body graphically with ellipsoids.

The MATLAB function for automatically generating ellipsoids is give below. One can use an orthonormal rotation matrix to orient the ellipsoid to any general Cartesian coordinate frame.

Ellipsoid sources:

mathforum.org

mathworld.wolfram.com

MATLAB function `ellipsoid`

ELLIPSOID Generate ellipsoid.

[X,Y,Z]=ELLIPSOID(XC,YC,ZC,XR,YR,ZR,N) generates three (N+1)-by-(N+1) matrices so that SURF(X,Y,Z) produces an ellipsoid with center (XC,YC,ZC) and radii XR, YR, ZR.

[X,Y,Z]=ELLIPSOID(XC,YC,ZC,XR,YR,ZR) uses N = 20.

ELLIPSOID(...) and ELLIPSOID(...,N) with no output arguments graph the ellipsoid as a SURFACE and do not return anything.

ELLIPSOID(AX,...) plots into AX instead of GCA.

The ellipsoidal data is generated using the equation:

```
 (X-XC)^2      (Y-YC)^2      (Z-ZC)^2
--------   +  --------   +  --------   =  1
  XR^2          YR^2          ZR^2
```

See also sphere, cylinder.

from **`help ellipsoid`** in MATLAB

9. Humanoid Robots

History

- Leonardo da Vinci created many human-inspired, robot-like sketches, designs, and models in the 1500s.

Leonardo Robot with Internal Mechanisms

- The word ‘robot’ first appeared in print in the 1920 play R.U.R. (Rossum’s Universal Robots) by Karl Kapek, a Czechoslovakian playwright. Robota is Czechoslovakian for “worker” or “serf” (peasant).

Rossum’s Universal Robots (R.U.R.)

- Isaac Asimov popularized the term *robotics* through many science-fiction novels and short stories. Asimov is a visionary who envisioned in the 1930s the "positronic brain" for controlling robots; this pre-dated digital computers. His robots were literally indistinguishable from humans. Asimov invented the three laws of robotics.

  1. A robot may not harm a human or, through inaction, allow a human to come to harm.

  2. A robot must obey the orders given by human beings, except when such orders conflict with the First Law.

  3. A robot must protect its own existence as long as it does not conflict with the First or Second Laws.

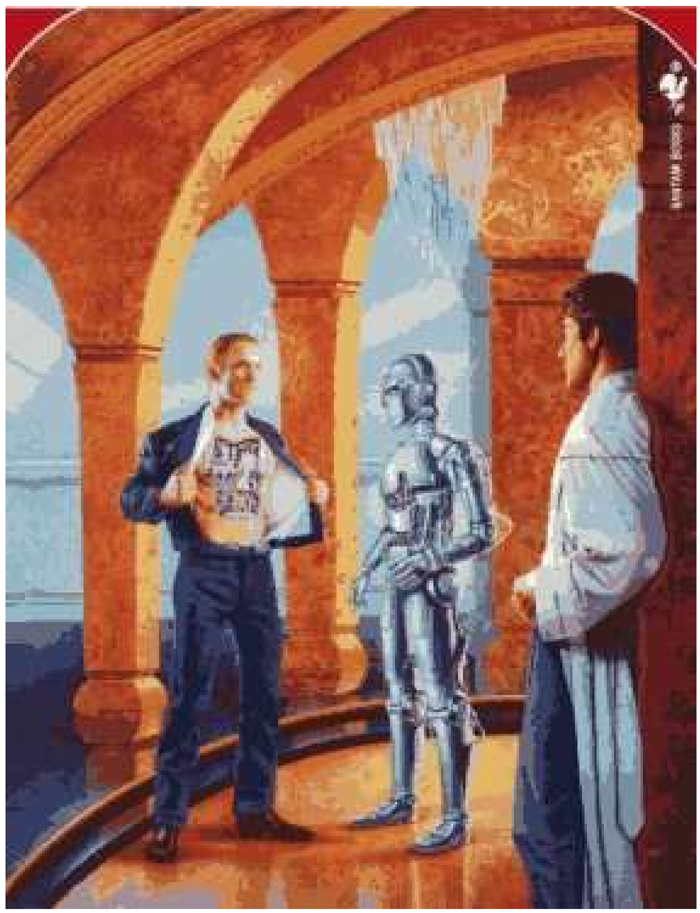

Asimov Humanoid Robots

> "The division between human and robot is perhaps not as significant as that between intelligence and non-intelligence."
>
> –R. Daneel Olivaw, The Caves of Steel, Isaac Asimov

- Joseph Engleberger and George Devoe were the fathers of industrial robots. Their company, Unimation, built the first industrial robot, the PUMA (Programmable Universal Manipulator Arm), in 1961, inspired by the human arm.

PUMA Industrial Robot

Space Humanoid Robots

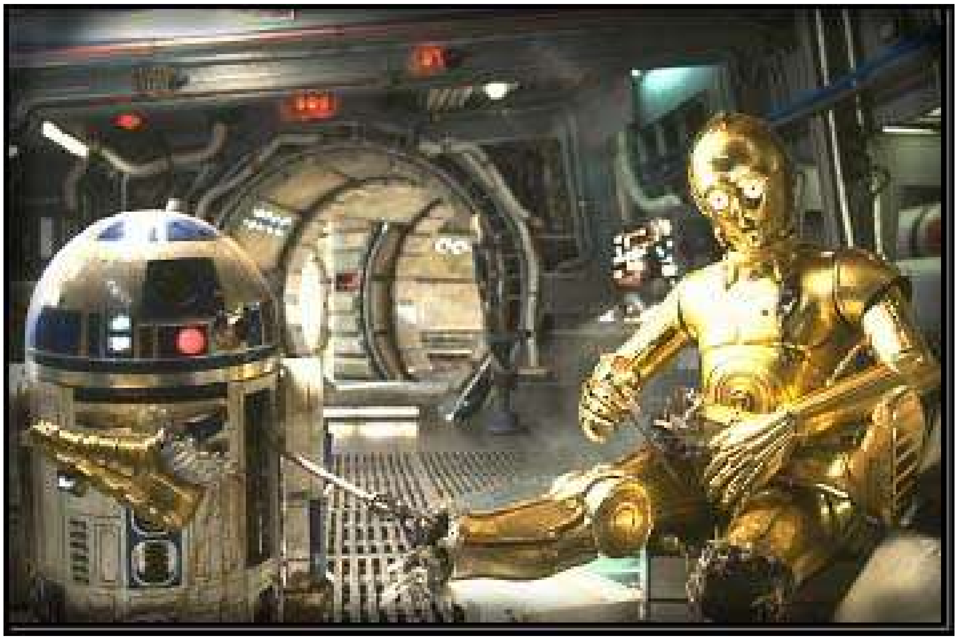

R2-D2 and C3PO (humanoid) from Star Wars

Early ISS Concept with Astronauts and Robots

Canadian Special Purpose Dexterous Manipulator (SPDM)

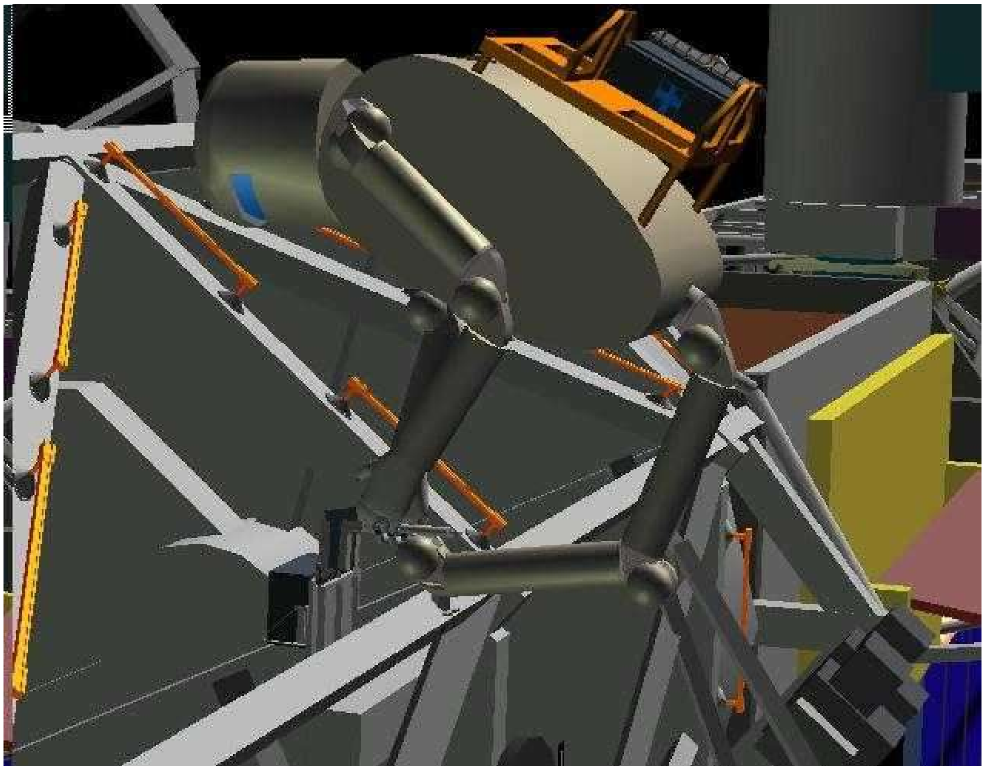

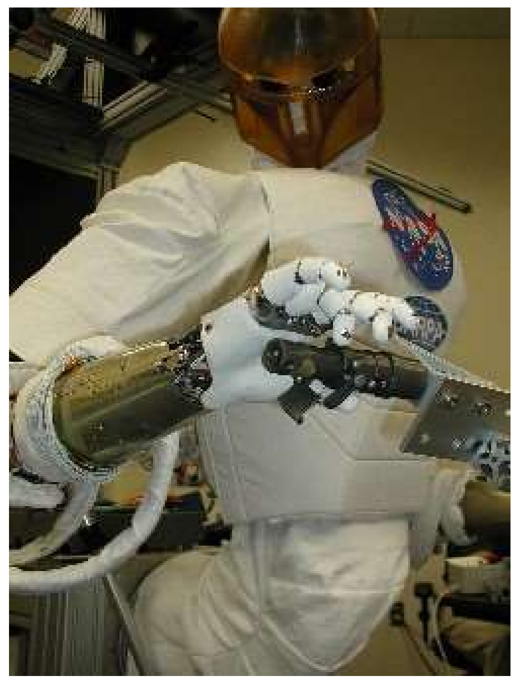

NASA JSC Robonaut

robonaut.jsc.nasa.gov

DARwIn-OP 20R 20-dof Humanoid Mobile Walking Robot

Height:	**455 mm**	**(about 18 inches)**
Mass:	**2.8 kg**	**(about 6 pounds)**

The Ohio University Robotics/Haptics/Biomechanics Laboratory received two DARwIn Humanoid robots for free from Virginia Tech in 2011 (street value: $24,000).

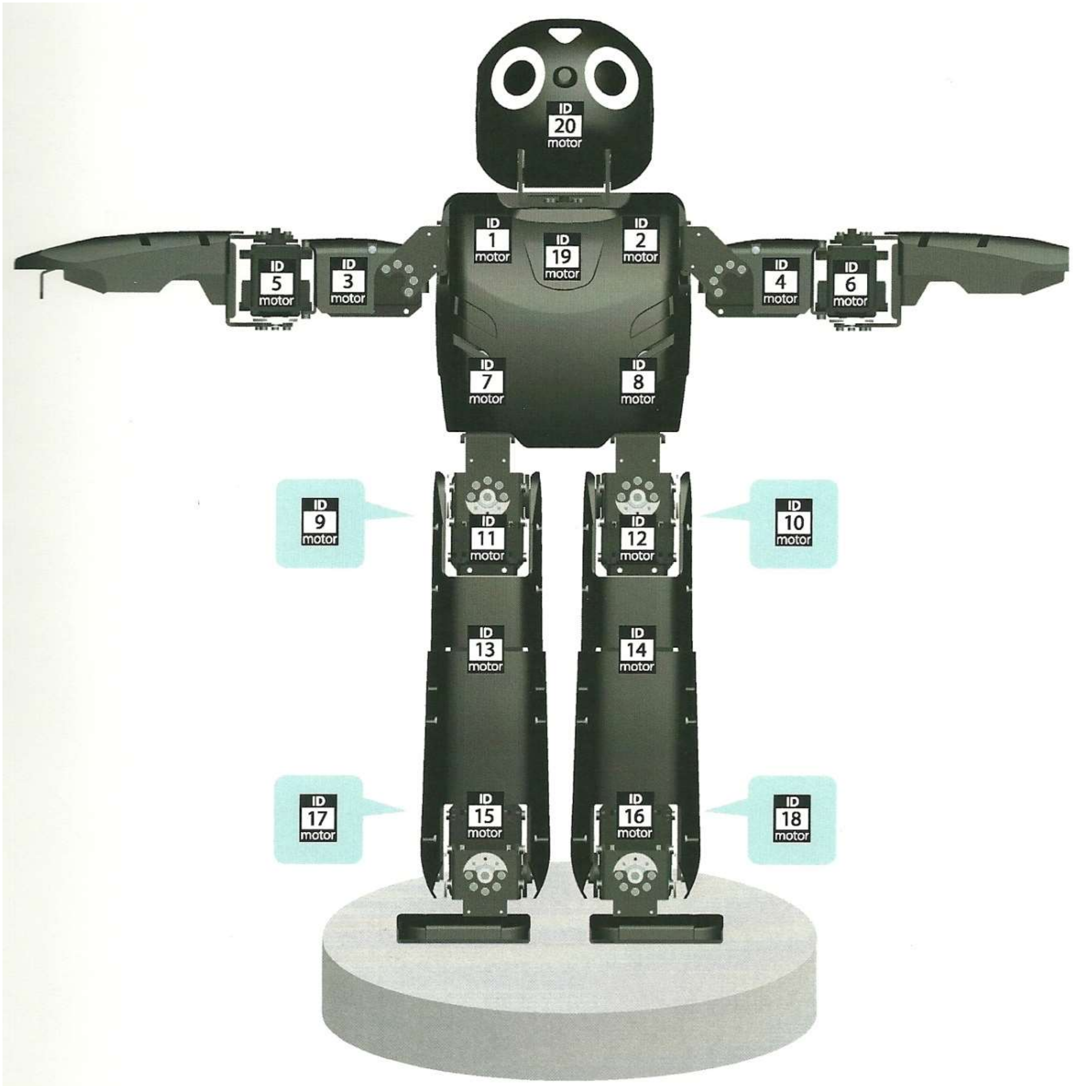

In the hardware shown above, each arm has three single-dof revolute (R) joints, each leg has six single-dof R joints, and the pan/tilt head has two single-dof R joints. Therefore, this overall robot has 20 dof. Each arm has a 2-dof (offset-U-joint) shoulder joint and a 1-dof elbow joint, for a total of 3-dof per arm. Each leg has a 3-dof (S-joint with 3 intersecting R joints) hip joint, a 1-dof knee joint, and a 2-dof (U-joint) ankle joint for a total of 6-dof per leg. The last hip joint, the knee joint, and the first ankle joint are all about parallel *Z* axes. The 2-dof head (U-joint) enables pan and tilt for the two cameras at the eye locations via an azimuth R-joint and an elevation R joint.

Each DARwIn-OP robot joint is driven by a Dynamixel MX-28 servomotor controlled by an internal CM-730 Robotis servo-controller. The DARwIn-OP sensors include an HD digital video camera, tri-axis gyroscope and accelerometer, and two microphones. The DARwIn-OP on-board computer is a 1.6 GHz Intel Atom Z530 FitPC2i with 4 GB SSD and the Ubuntu Linux operating system. DARwIn is programmed in C++ and is able to operate both tethered and battery-powered. The LiPO 3CELL 11.1v 1000mAh battery provides up to 30 operation minutes (Merlin Robotics, 2012).

R.L. Williams II, 2012, "DARwIn-OP Humanoid Robot Kinematics", Proceedings of the ASME IDETC/CIE, Chicago IL, August 12-15, 2012, DETC2012-70265.

RoboCup Humanoid League

humanoidsoccer.org

Other Humanoid Robots

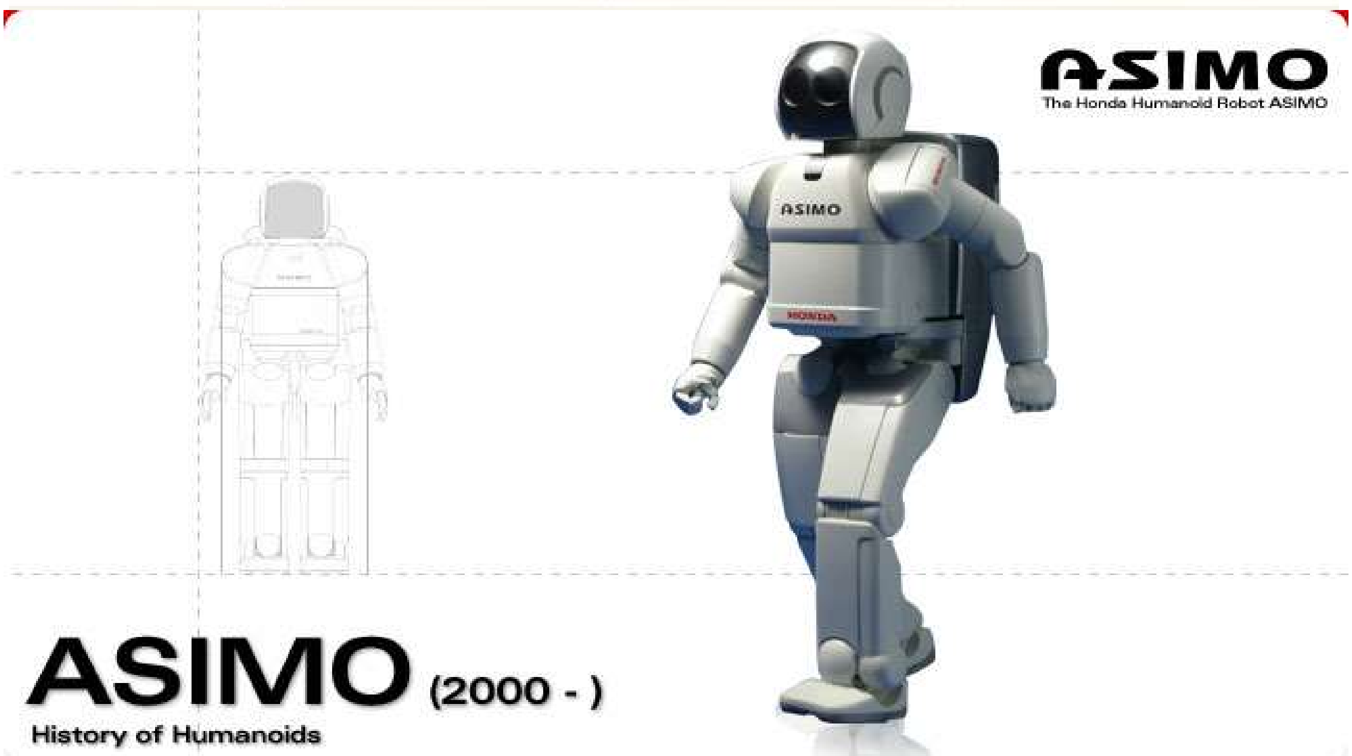

Honda ASIMO Humanoid Robot
(Advanced Step in Innovative MObility)

world.honda.com/ASIMO

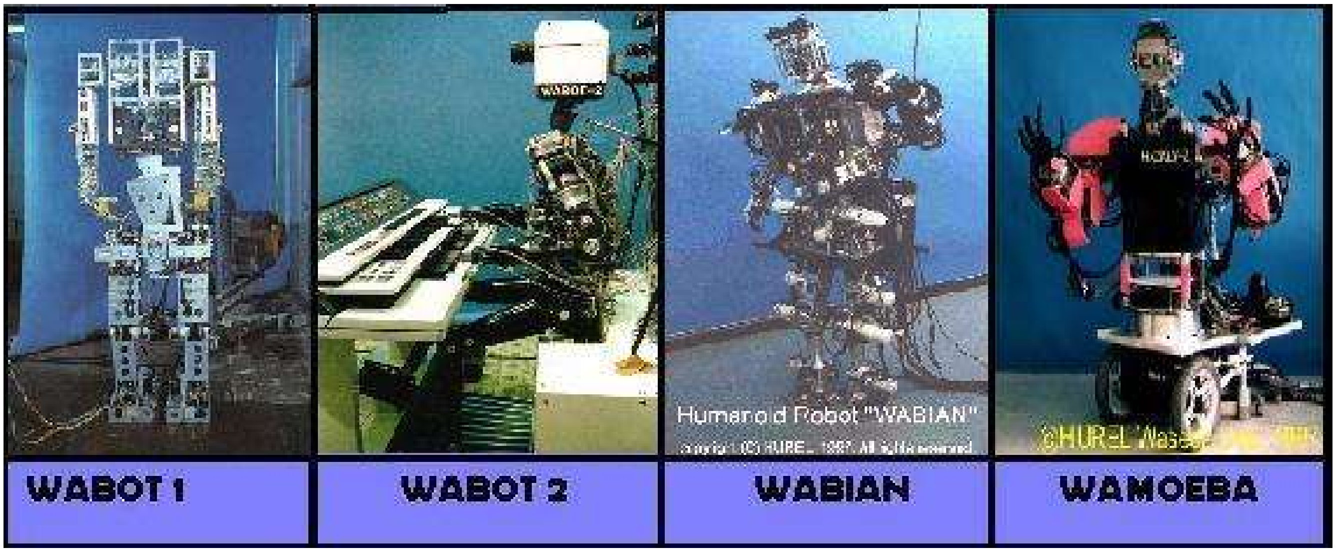

Humanoid Robots from Waseda University

humanoid.rise.waseda.ac.jp

Sony's QRIO

sony.net

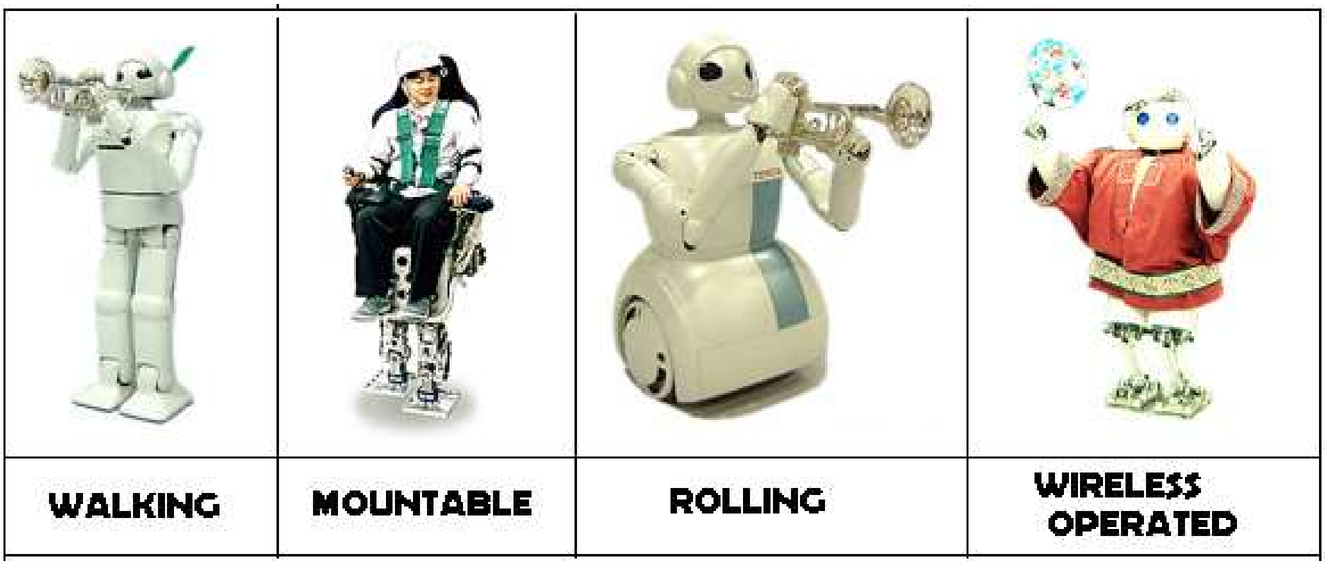

Toyota Partner Robots

toyota.co.jp

MIT Humanoid Robots

ai.mit.edu/projects/leglab

University of Queensland GuRoo

itee.uq.edu.au

Kawada Industries HRP-2

kawada.co.jp

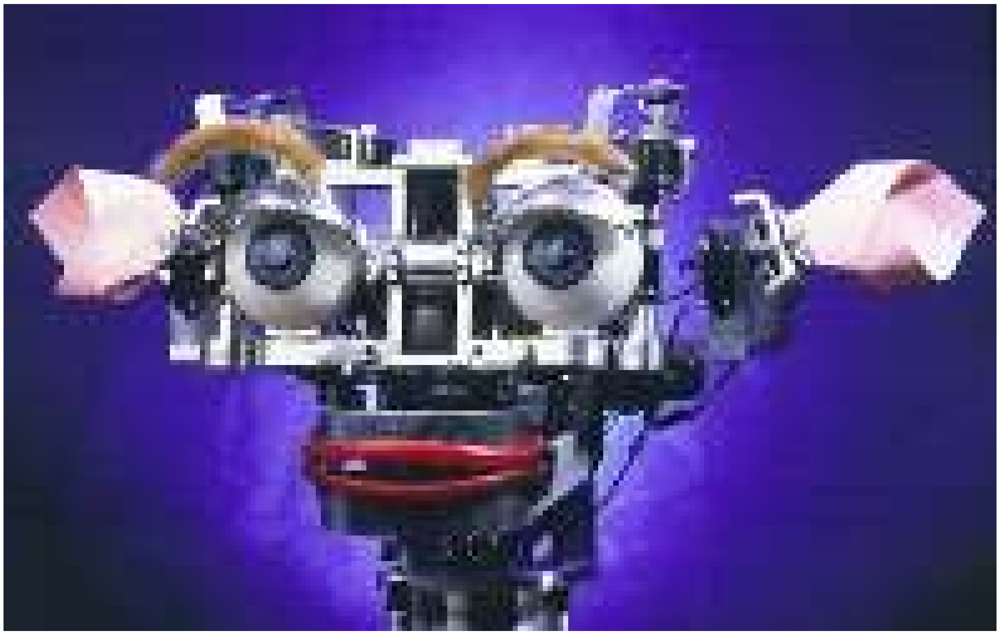

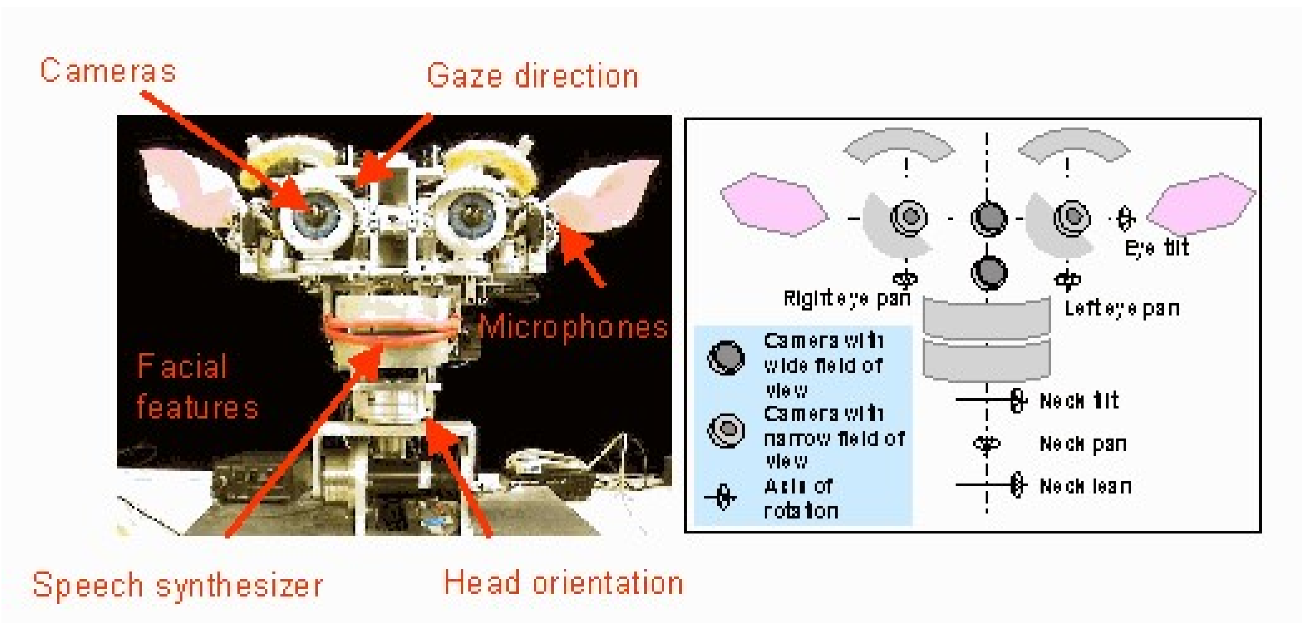

MIT Kismet: Expressions, Socialization, Emotions

ai.mit.edu

10. Bipedal Locomotion

"Everybody's doin' a brand new dance now (c'mon baby do the locomotion)
I know you'll get to like it if you give it a chance now (c'mon baby do the locomotion)
My little baby sister can do it with ease, it's easier than learning your A-B-C's
So come on come on and do the locomotion with me."
–Gerry Goffin and Carole King (recorded by Little Eva)

10.1 Introduction

- Walking is the main form of animal locomotion on land, distinguished from running and crawling.
- The word walk is descended from the Old English wealcan, "to roll".
- Walking is generally distinguished from running in that only one foot at a time leaves contact with the ground. For humans and other bipeds running begins when both feet are off the ground with each step.
- The average human child achieves independent walking ability between nine and fifteen months.
- For humans, walking is the main form of transportation without a vehicle or riding animal.
- An average walking speed is about 4 to 5 km/h although this depends on factors such as height, weight, age, and terrain.

Human walking is accomplished with a strategy called the double pendulum. During forward motion, the leg that leaves the ground swings forward from the hip. This sweep is the first pendulum. Then the leg strikes the ground with the heel and rolls through to the toe in a motion described as an inverted pendulum. The motion of the two legs is coordinated so that one foot or the other is always in contact with the ground. The process of walking recovers approximately sixty per cent of the energy used due to pendulum dynamics and ground reaction force.

Walking differs from a running gait in a number of ways. The most obvious is that during walking one leg always stays on the ground while the other is swinging. In running there is typically a ballistic phase where the runner is airborne with both feet in the air. Another difference concerns the movement of the center of mass of the body. In walking the body 'vaults' over the leg on the ground, raising the center of mass to its highest point as the leg passes the vertical, and dropping it to the lowest as the legs are spread apart. Essentially kinetic energy of forward motion is constantly being traded for a rise in potential energy. This is reversed in running where the center of mass is at its lowest as the leg is vertical. This is because the impact of landing from the ballistic phase is absorbed by bending the leg and consequently storing energy in muscles and tendons. In running there is a conversion between kinetic, potential, and elastic energy.

There is an absolute limit on an individual's speed of walking (without special techniques such as those employed in speed walking) due to the velocity at which the center of mass rises or falls - if it's greater than the acceleration due to gravity the person will become airborne as they vault over the leg on the ground. Typically however, animals switch to a run at a lower speed than this due to energy efficiency.
en.wikipedia.org

10.2 Walking Anatomy/Physiology Overview

Walking involves alternating action of the two legs. This translation motion is caused by rotary motion of the leg joints. Walking involves periodic, pendulum-like motion. Assuming we start with the right leg, in the first step from the vertical position of the humanoid, the right leg is moved forward and placed on the ground with support of the left leg. The first steady walking step involves lifting the left leg with single leg support of the right leg until the left leg is planted on the ground again. The second steady walking step is similar to the first steady walking step, but this step has single leg support of the left leg until the right leg is lifted and planted on the ground again. The consecutive repetitions of steady walking steps after the implementation of first step result in a continued locomotion in the sagittal plane. At the end of each step the biped has two legged support (as opposed to a running gait). Walking can be defined as one starting step and a repetition of steady walking steps with left and right feet alternately switched for supports. For more walking anatomy details, see Hamilton et al. (2008).

In walking, each leg goes through two phases:

- **stance (support) phase**
  - heel-strike
  - foot-flat
  - midstance
  - heel-off
  - toe-off
- **swing (recovery) phase**

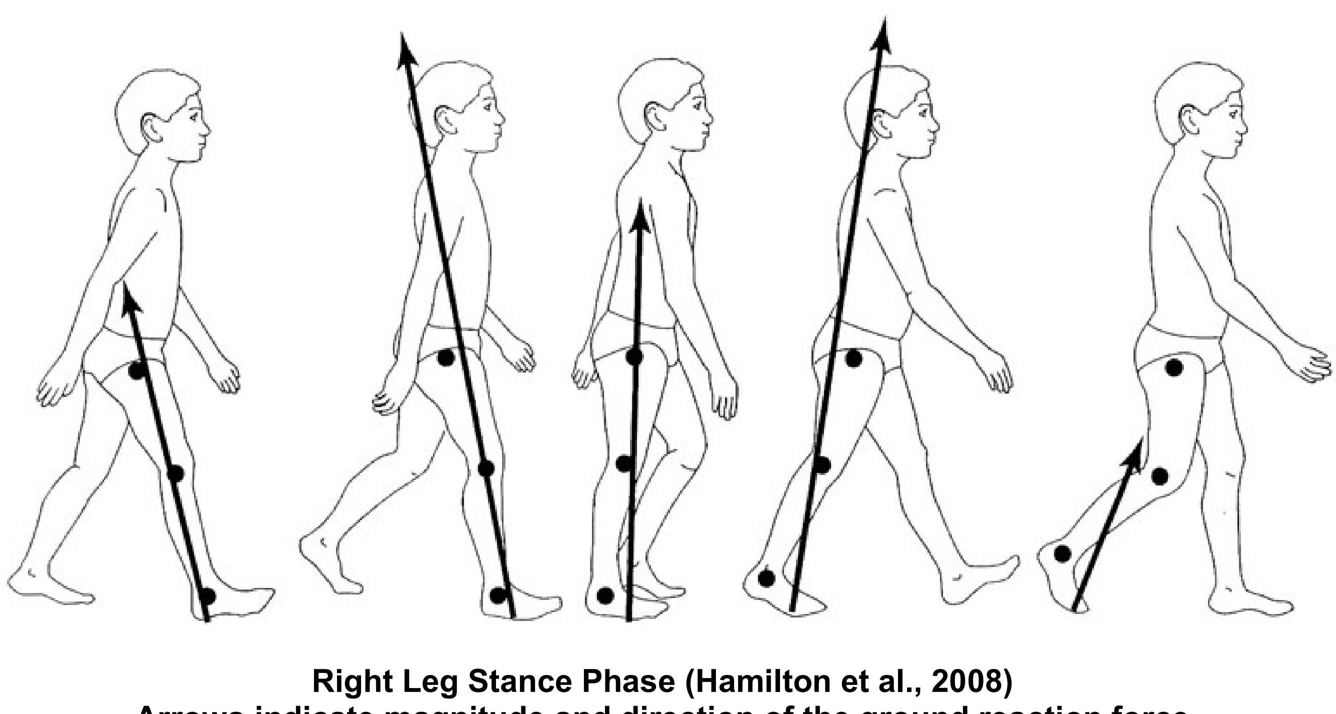

Right Leg Stance Phase (Hamilton et al., 2008)
Arrows indicate magnitude and direction of the ground reaction force

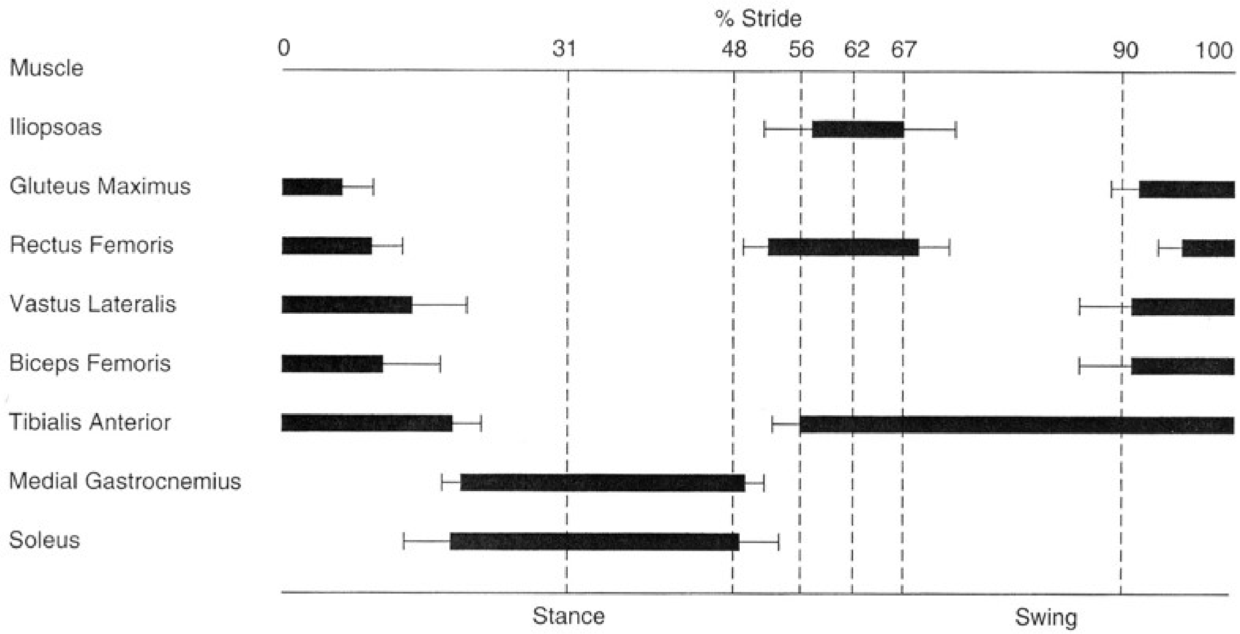

Active Muscles during Stance and Swing Phases (Hamilton et al., 2008)

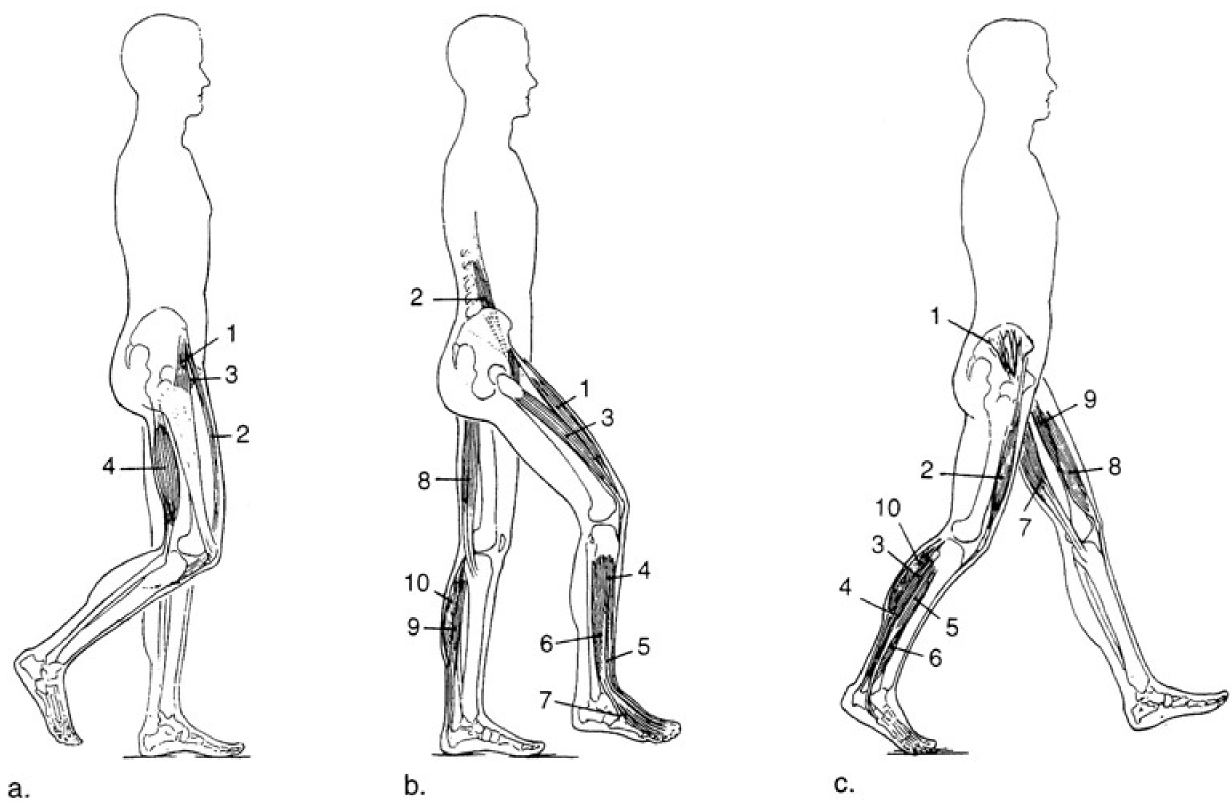

Leg Muscles for Walking (Hamilton et al., 2008)

a	b		c	
1. tensor fasciase latae 2. sartorius 3. pectineus 4. biceps femoris	1. rectus femoris 2. iliopsoas 3. vastus lateralis 4. tibialis anterior 5. extensor hallucis longus	6. extensor digitorum longus 7. peroneus tertius 8. semitendinosus and semimembranous 9. soleus 10. gastrocnemius	1. gluteus medius 2. rectus femoris 3. soleus 4. tibialis posterior 5. peroneus longus	6. peroneus brevis 7. semimembranous and semitendinosus 8. vastus medialis and intermedius 9. adductor longus 10. gastrocnemius

10.3 Biomechanics of the Human Walking Gait

Motion of the Body

As a human walks forward the body center of mass moves in a complex 3D pathway. From the side, it is seen as an undulating excursion with an amplitude of approximately 50 mm. The human's head also moves up and down as forward movement takes place.

This is mirrored in the sequence for the "stick diagram" which shows the points of the markers joined up with straight lines. The ankle, knee and hip markers form a straight line when the leg is fully extended but the angle of knee flexion and of hip flexion can be obtained from these stick diagram data points. Taking the hip markers (greater trochanter) you can see the excursion in the vertical direction and during the changeover you can see that the hip markers move forward and backward relative to each other. This is rotation of the pelvis and trunk about a vertical axis and varies greatly between individuals.

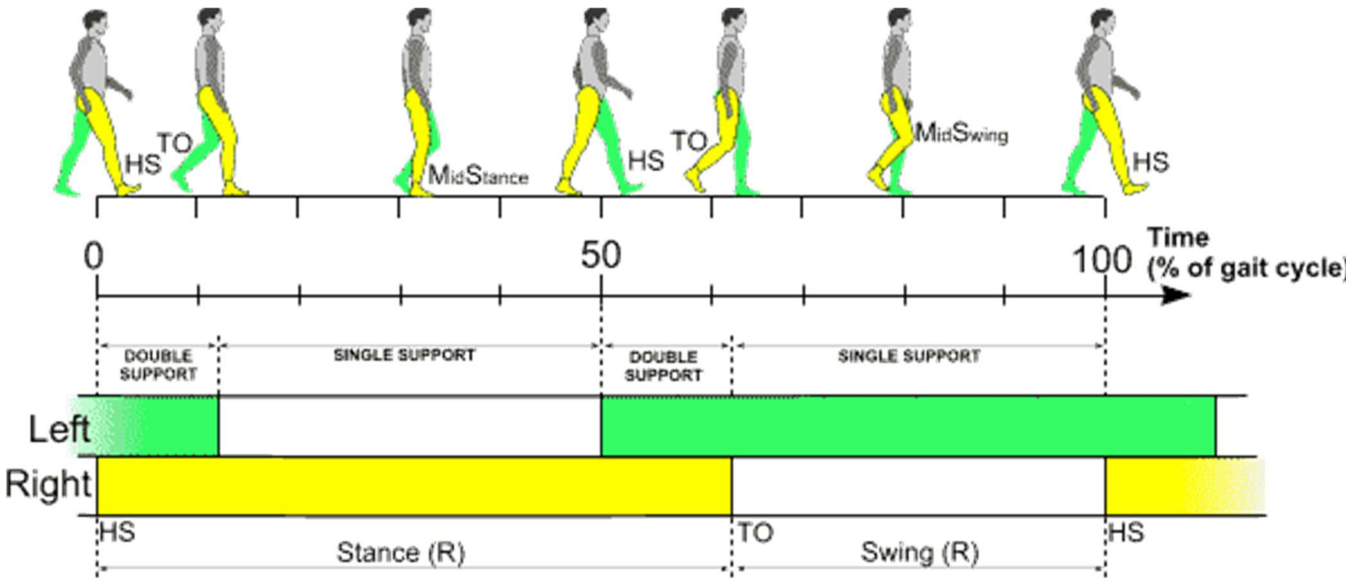

The Human Walking Gait Cycle

The biped gait cycle is split into two separate regions representing the period of time when the foot is in contact with the ground (**stance phase**) and the period of time when the limb is not in contact with the ground (**swing phase**) as it moves forward for the next cycle of events.

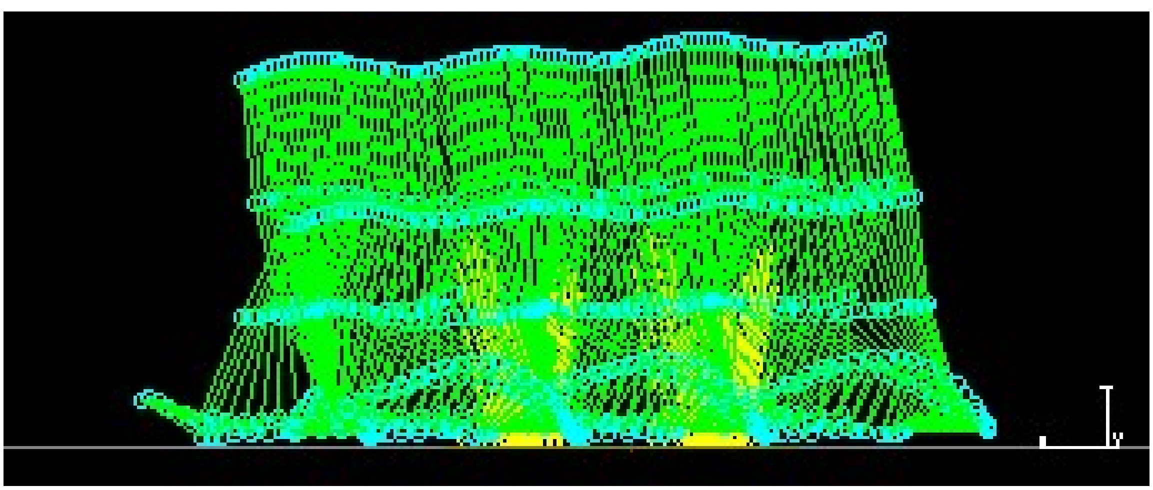

Gait Cycle Animation

This section will not consider the **swing phase** since the loadings on the joints of the body are much less during swing than they are during the support period of **stance**. During **stance phase** the foot contacts the ground, the mass of the body is supported, and then the body is propelled forward during the later stages of stance. The **stance phase** is split into discrete events as shown below.

Heel-strike. The instant when contact is made with the ground usually occurs with the heel touching the ground first. In pathological gait, the foot may come down with the metatarsal heads contacting the ground in which case ground contact is the correct nomenclature to use.	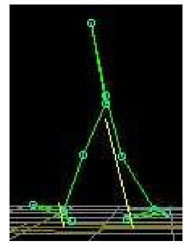	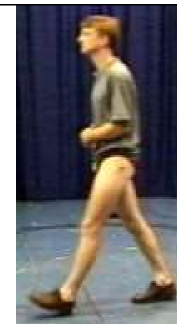
Foot-flat. The instant that the rest of the foot comes down to contact the ground and usually is where full body weight is being supported by the leg (just preceding single leg stance).	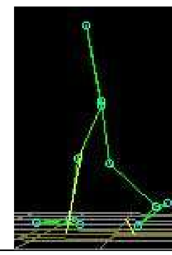	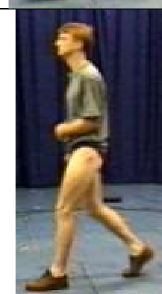
Midstance is defined when the center of mass is directly above the ankle joint center. This is also used as the instant when the hip joint center is above the ankle joint since it is very difficult to evaluate the precise location of the center of mass as the segments of the body move relative to the trunk.	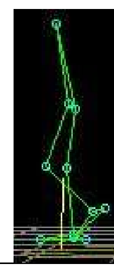	
Heel-off occurs when the heel begins to lift off the ground in preparation for the forward propulsion of the body.	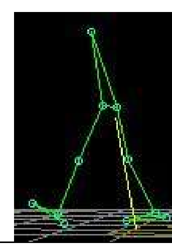	
Toe-off occurs as the last event of contact during the stance phase.	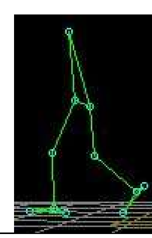	

The frontal plane shows that the body also experiences motion in the vertical and mediolateral directions. As the body moves forward, only one leg will be supporting the mass of the body during the central part of the stance phase. This means that the body is liable to topple because the body mass will be medial to the support point generated by the foot. In reality, this does not happen, because of the inertial forces occurring in the mediolateral direction.

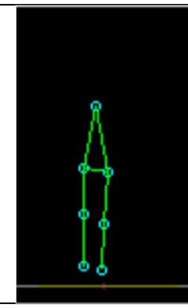

gla.ac.uk

Force Actions on the Foot

Since the body mass is being moved in all three directions; forward, vertically up and down and horizontally side to side, it will take a combination of force actions in order to accelerate and decelerate the body mass to provide the motion seen during gait. If any mass is accelerated, then the relationship $F=mA$ applies to the mass system. The calculation of acceleration is difficult, therefore, it is usual to measure the forces directly by using a force platform mounted in the floor. As the foot contacts the force platform it is able to sense the forces in each of the three directions and these are presented in this section.

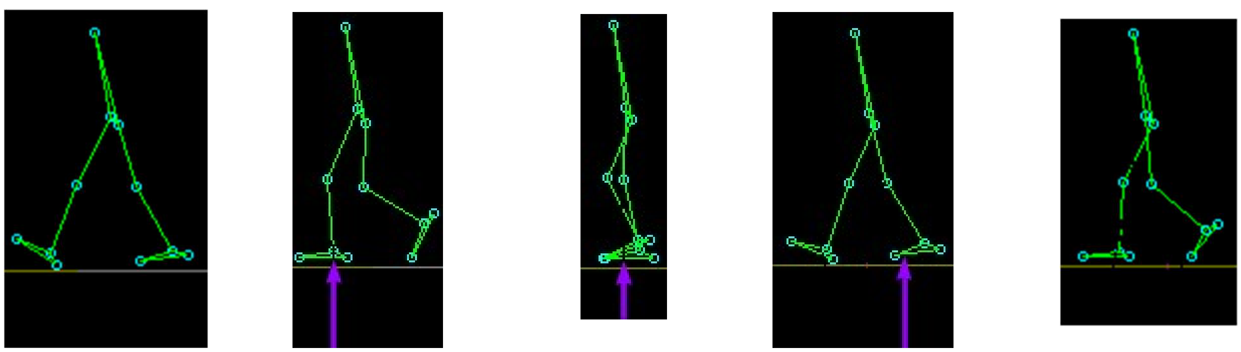

Heel-strike **Foot-flat** **Midstance** **Heel-off** **Toe-off**

__Vertical Component of Force__

Taking the vertical force first, it will be easy to understand that at some point during the stance phase, the subject must at least support full body weight. It is easier to talk in percentages of body weight for a particular subject rather than to discuss certain Newton values. Taking the sequence of events in the same order as previously described, we can start the series of vertical force measurements at heel strike. Since **heel-strike** is the beginning of contact, the vertical force will be zero at the instant of contact with the ground. This vertical force will rise very steeply up to almost body weight in a fraction of a second. The data points were recorded at 50 points per second which is sufficiently fast to capture the variation in force during stance.

At the time point of **foot-flat**, the body mass is moving downwards and landing on the leg as seen by the motion of the hip centers from the stick diagrams. In order to decelerate this downward motion and at the same time support the body weight, it will be necessary to apply a force larger than body weight on the foot. This instant for the subject shows 116% body weight being applied to the foot.

At **midstance** the motion of the center of the body is actually in an upward arc just like driving a car over a hump-backed bridge. The upward motion of the body is being decelerated and then allowed to accelerate downwards at the second half of stance. This acceleration allows a force of less than body weight to support the body but the value of this force is highly variable. This subject shows 59% body weight at mid stance but it is likely that people with a "springy" style of gait could go as low as 20-30% body weight. This may appear very surprising but if you think about the motion of the body as a series of jumps connected together with foot contacts, then it is possible to experience very small contact forces between the ground and the foot during these linked jumps.

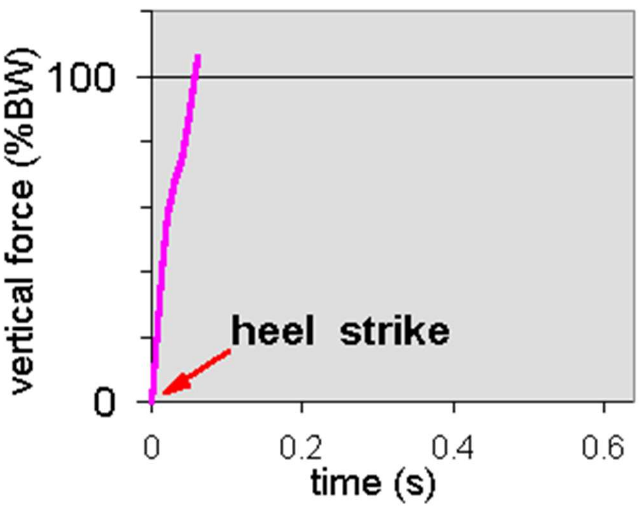

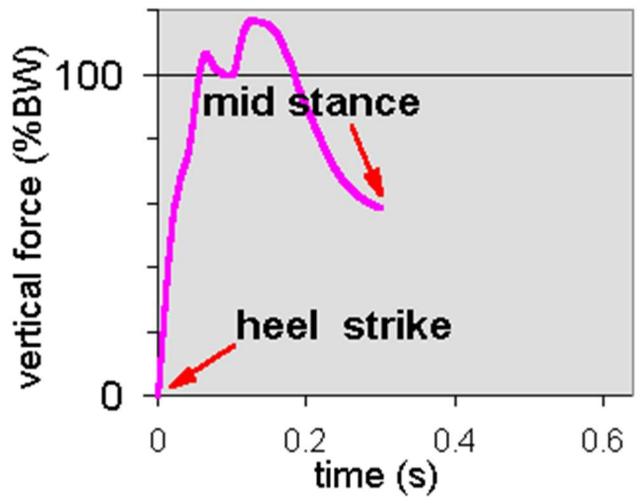

At **heel-off**, the body mass is accelerated forward and upwards ready for the stance phase of the other leg. This means that more than body weight will be required to support the body and as such a force of 117% is experienced by a subject in this section.

Finally, **toe-off** is an instant where contact with the ground is lost and the force returns to zero.

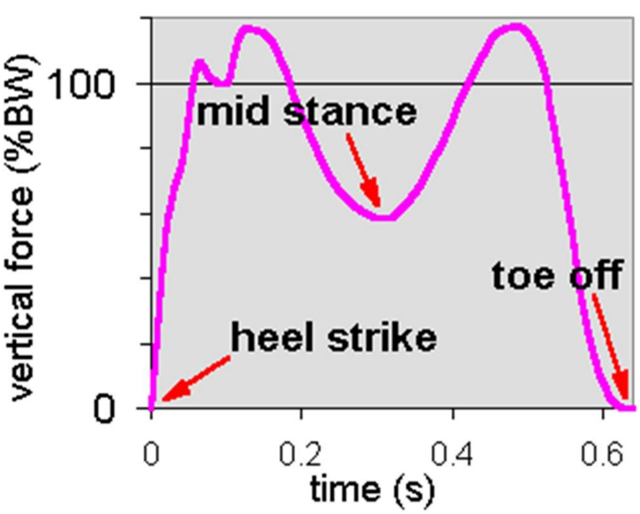

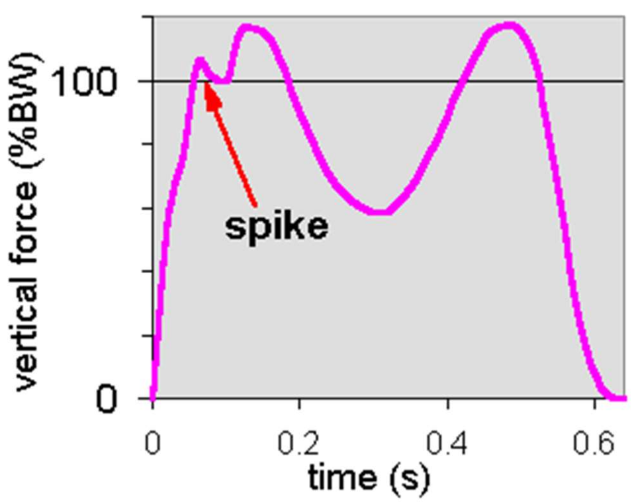

If these contact force points are joined up with the other force points at 50 samples per second, the graph is formed as follows. The M-shaped graph, or double peak graph is typical for normal gait and shows the fluctuation of force relative to 100% body weight.

One particular point of interest is the discontinuity, or spike, on the initial rapid rise of the vertical force from heel strike. This spike is due to the two-stage landing of the body on the ground. Although we said that the body lands on the leg during early stance at foot flat, there is an event preceding this where the leg strikes the ground like a hammer being swung from the hip as a pivot point. The mass and inertial properties of the leg (rather than the whole body) will come to rest more abruptly than the larger mass of the body. This abrupt velocity change in the mass of the leg represents a shock which is no more than a very quick force application due to a change in velocity.

There are several implications about this value of force and since biological tissues such as tendon, cartilage and bone will respond differently to different rates of loading, the rate of loading of shock is very important for the long term survival of these tissues. It is, therefore, useful to reduce the value of shock force to as small a value as possible. Unfortunately, several devices and concepts have been popularized as absorbing shock. It is impossible to absorb shock but it is possible to change the motion of the leg so that the abruptness of the landing is reduced. This means that the accelerations will be reduced and since force is equal to mass multiplied by acceleration, then the shock force will also be reduced. The shock will be reduced by allowing a certain distance for the leg to strike the ground and this can be achieved by soft shoe heels, by shoe inserts or by a small change in the style of leg motion during landing of leg on the floor. As the activity speeds up to running then shock will be a more serious parameter and the reduction of shock is an element which requires serious attention.

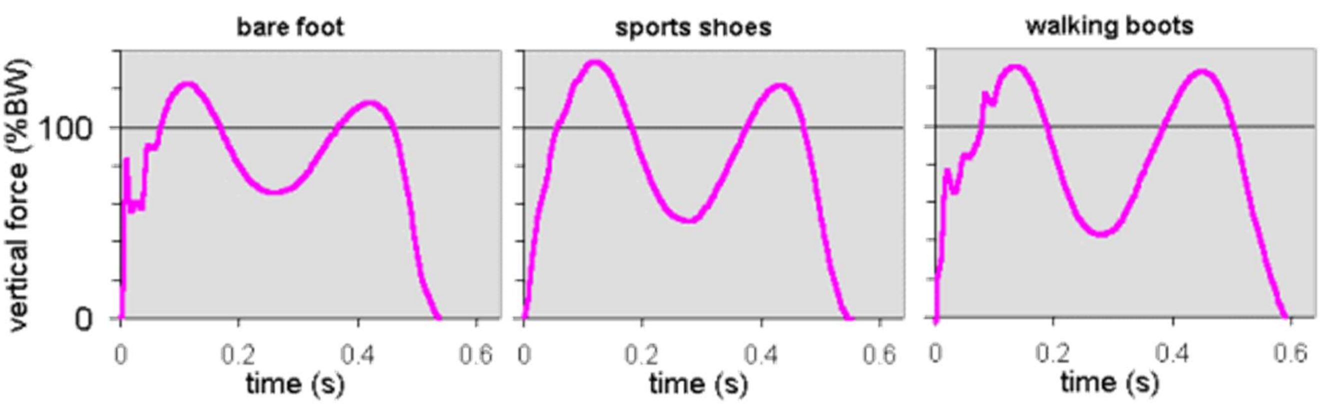

Vertical force profiles for the same subject walking in different footwear

<u>Anterior/Posterior Force</u>

As the body moves forward and up and down, the mass of the body can be considered to be like a trolley moving along and undulating up and down surface. As the body mass moves down the surface it will tend to speed up and as the body mass moves upwards it will tend to slow down. Again, there will be accelerations forwards and backwards in order to achieve these changes in velocity forward. Like any mass on the move, these accelerations will require forces on the mass.

During the stance phase, the forces applied to the foot will be backwards as the body lands and then forwards in late stance as the body lifts up and moves more rapidly in the forward direction.

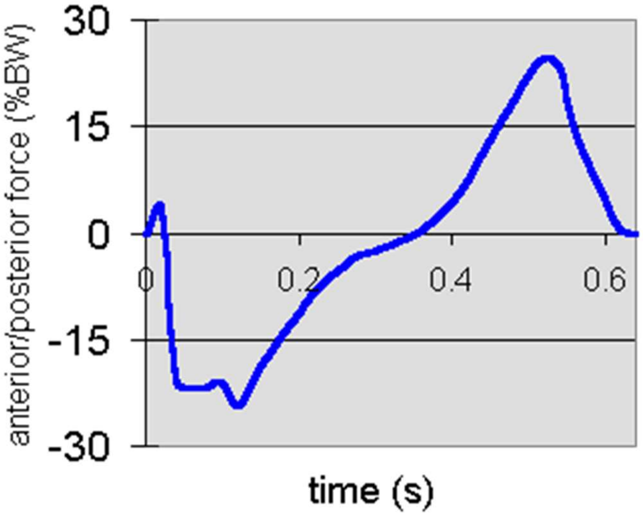

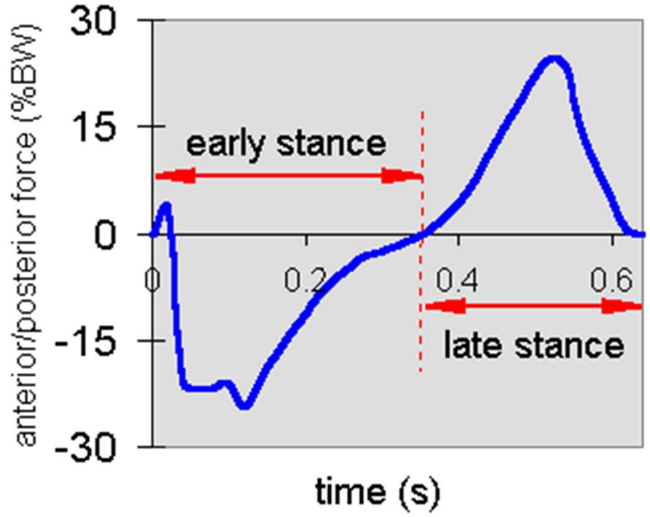

This oscillation from backwards to forwards is important and represents the control of the forward velocity within certain variations. It is normal for the velocity of the mass to fluctuate by 15% of the average velocity of forward progression. During early stance the force applied to the foot will be backwards and can reach 20% body weight at foot flat. During the propulsion phase after heel-off, the force forward on the foot will reach approximately 20% again.

During mid stance the velocity of forward progression should be not changing and as such there will be no requirement for a horizontal anterior/posterior force. Therefore, the force will be zero and represents the point of changeover between the deceleration phase and the acceleration phase. When these data points are combined we obtain the graph shown opposite and the areas representing the negative and positive parts of this force should be equal in order to maintain a forward velocity of the same value from step to step. If the negative portion is larger in area than the positive portion, the body will be slowing down and conversely the body will accelerate forward if the positive portion is larger than the negative one.

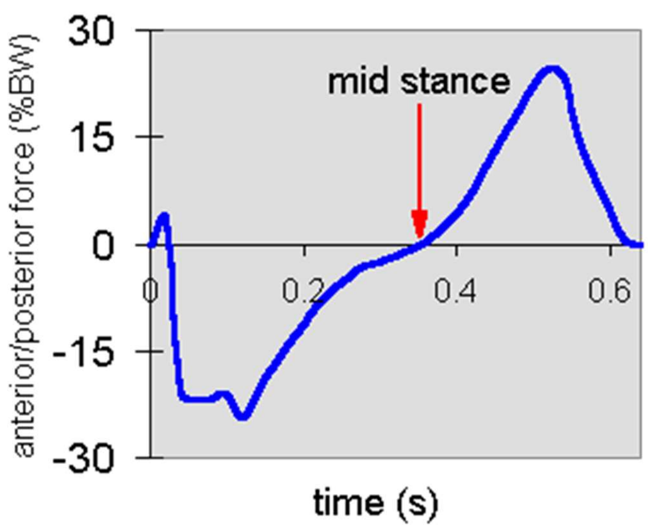

Combined Forces in the Sagittal Plane

The horizontal and vertical forces applied to the foot will happen at the same time. In order to combine the horizontal and vertical force components, it is a straightforward procedure to generate a triangle of forces or to generate a rectangle where the diagonal is the resultant of the two force components. If this is done for the subject walking, the combined actions are as shown in the stick diagram where the yellow line represents the direction of the force. The length of this line is scaled and the longer the line, the larger the force.

At foot flat the force will be positioned around the heel and angled backwards whereas mid stance will see a small force more or less vertical, but the position of the force on the foot has moved forward to the center and at heel-off the force will be around the metatarsal heads and angled forwards on the foot with a combined value more than body weight. Since the whole body mass is not rotating with significant angular accelerations, it is logical to assume that the line of action of the resultant force will pass through the position of the body center of mass and, therefore, produce no accelerations in the angular direction.

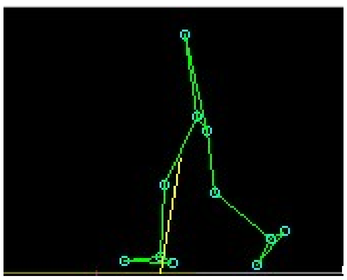

Foot-flat

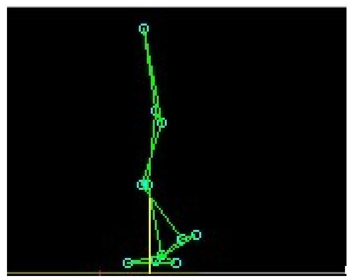

Midstance

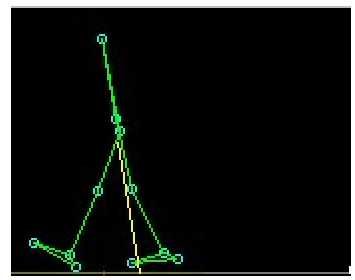

Heel-off

Combined Forces in the Frontal Plane

The same concept applies for balance of the mediolateral force and any tendency to spin in the frontal plane. This means that the line of action of the resultant force from the foot must also pass through the position of the center of mass of the body seen in the frontal plane. Since the vertical force applied to the foot will fluctuate around body weight, it will be necessary to have a horizontal force directed medially in order to swing the line of action of the resultant force inward to pass through the center of mass. This happens with the subject in this section and during the course of the stance phase, this force reaches a maximum of body weight percentage. For the sequences of foot-flat, midstance and heel-off the positions of the resultant force are shown in the three images.

gla.ac.uk

Joint Moments

It is interesting to note the fluctuating value of force on the foot but control of the joints of the leg is done by muscles which will react against the turning effect of these forces around the joints in question.

Taking the ankle joint first, the ground force will produce a tendency to dorsiflex the ankle if the force passes forward of the ankle center. The opposite happens in early stance when the force passes just behind the ankle center tending to plantarflex the foot around the shank. The force moves forward along the foot where the line of action will then pass in front of the ankle. This action is complicated by the fact that the force will tilt backwards in early stance and then forwards in late stance. The effectiveness of turning the ankle joint will be related to a combination of the distance between the ankle center, the line of action of the resultant force and the value of force itself. Since these parameters vary dramatically throughout the time of stance, it is necessary to calculate the individual moments for the samples throughout stance. This has been done and the graph of ankle moment is shown opposite. The important feature here is the large moment tending to dorsiflex the ankle during the propulsion phase of gait stance. This value of 100 Nm is large but is typical for most normal healthy individuals. The large value of moment is due to the force being greater than body weight, being forward from the ankle by a distance and being tilted forward by an angle.

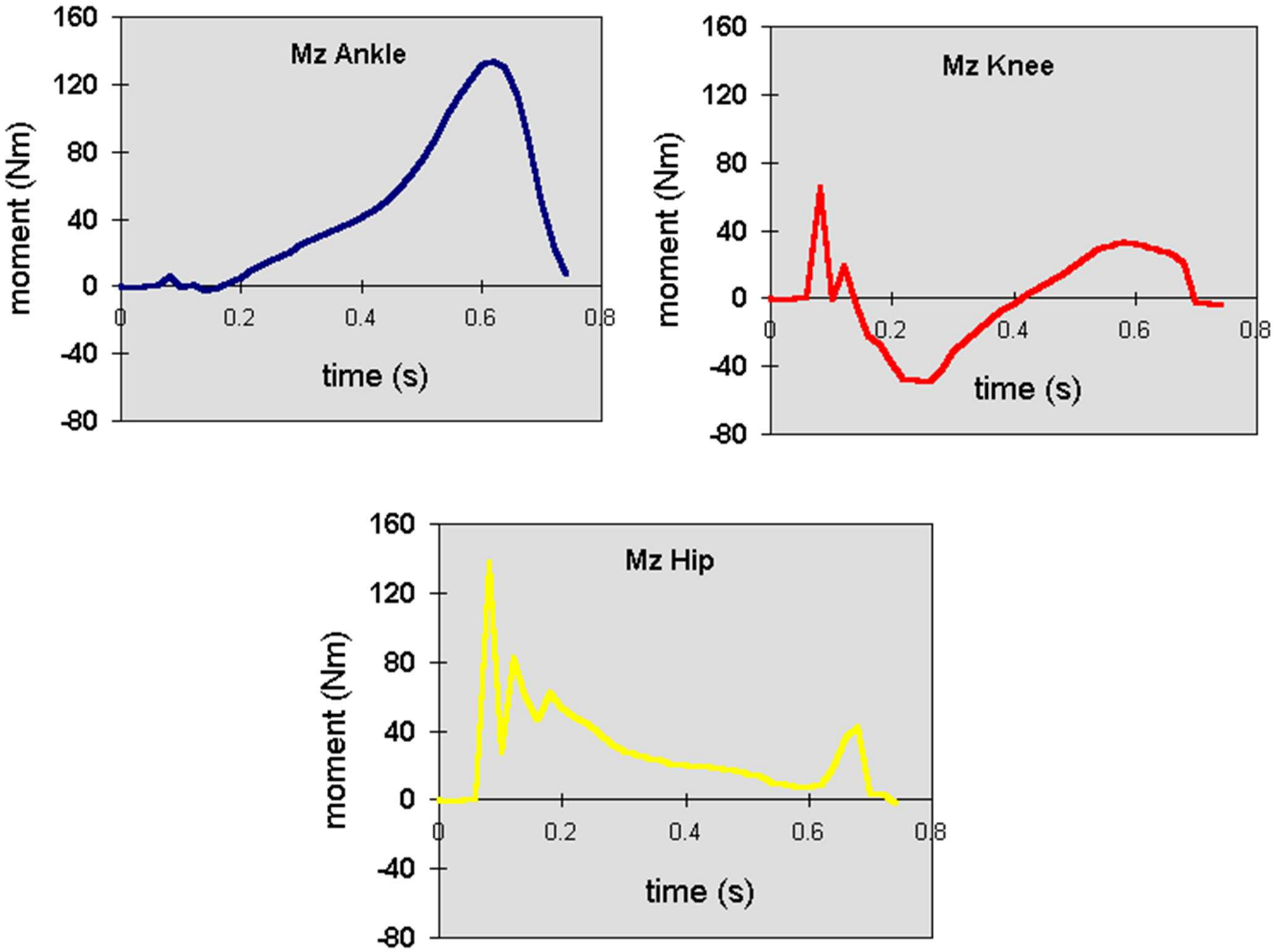

Keeping with the sagittal plane, it is possible to extend the line of action of the force so that the turning moment around the knee joint can be estimated. Since the knee joint is moving forward as the stance situation continues, we have a more complicated pattern of moment.

gla.ac.uk

10.4 Human Walking/Running Engineering Models (Dr. Biknevicius)

A common and effective model for human walking involves an inverted pendulum for the human body CG during the gait trajectory.

At **heel-strike**, the potential energy is minimum while the kinetic energy is maximum.

At **midstance**, the potential energy is maximum while the kinetic energy is minimum.

At **toe-off**, the potential energy is again minimum while the kinetic energy is again maximum.

A popular model for human running involves an inverted mass-spring (m-k) model, for the human body CG during the running trajectory.

The spring element is largely the tendons, used to store strain energy with each pace.

The kangaroo combines the inverted pendulum and *m*-*k* models in its hopping gait. It gets an amazing nearly 100% spring energy release which means the kangaroo needs practically zero muscle input for horizontal motions.

10.5 Humanoid Robot Walking Simulation

The results are provided in the form of graphs with joint angles against time, mimicking the human walking gait trajectory, adapted from Lum (1999). The link lengths (m) of the humanoid robot were obtained by measuring a human subject (see figure below).

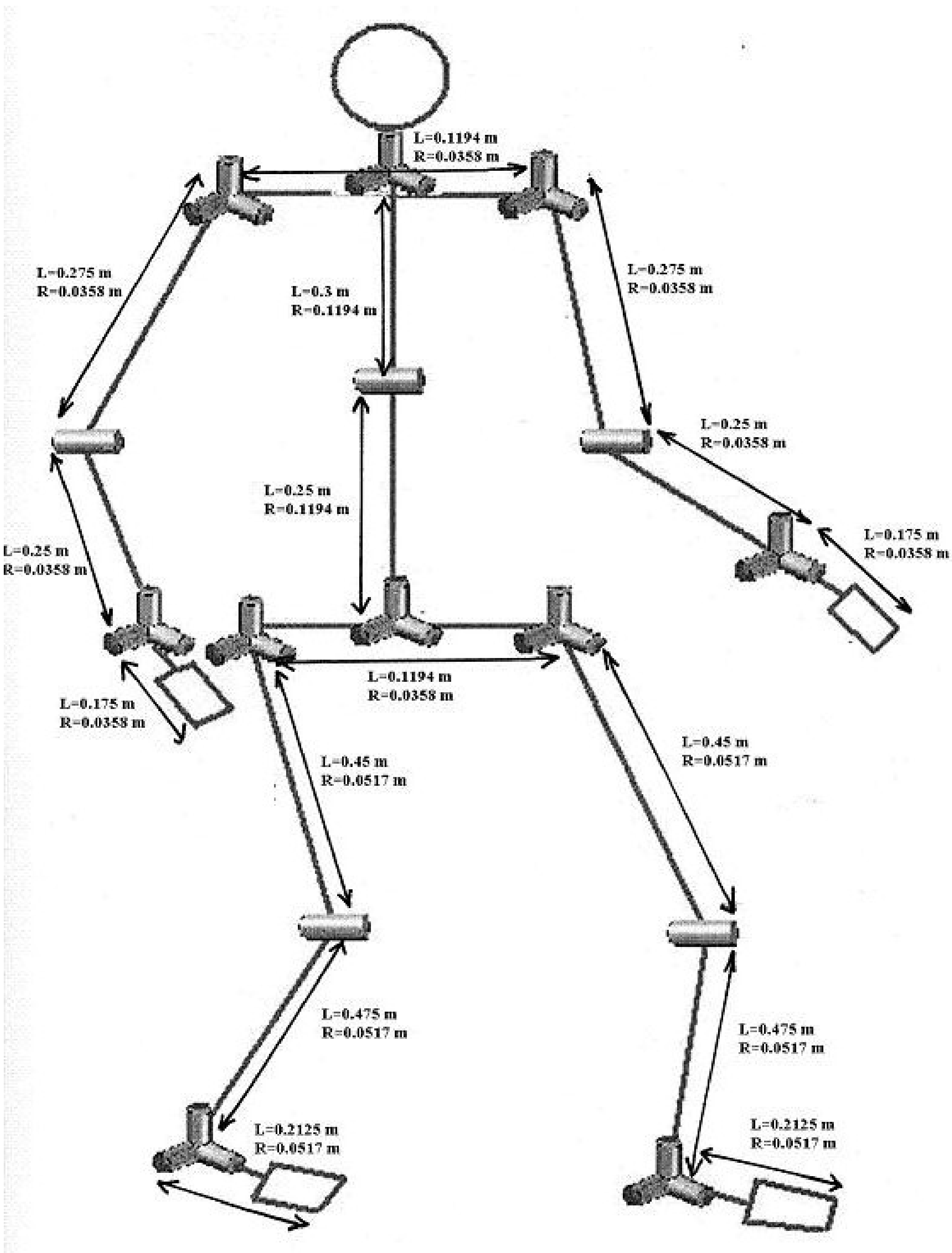

Lengths and Radii of the Links of the Humanoid

The notations for the leg joints angles q_1 (left knee), q_2 (left hip), q_3 (right hip), and q_4 (right knee) are shown in the figure below. The trajectories of these joint angles for simulation of humanoid walking are shown in the following figure.

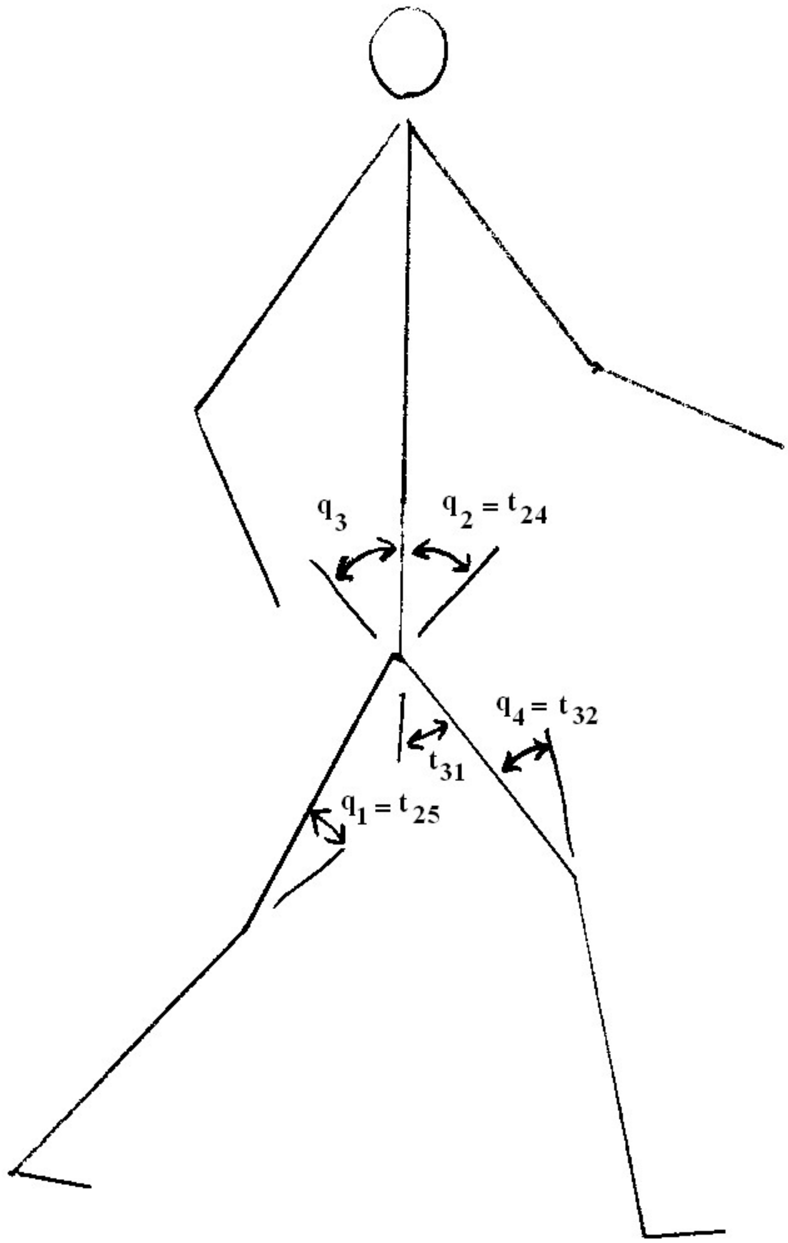

Leg Joint Angles Notation

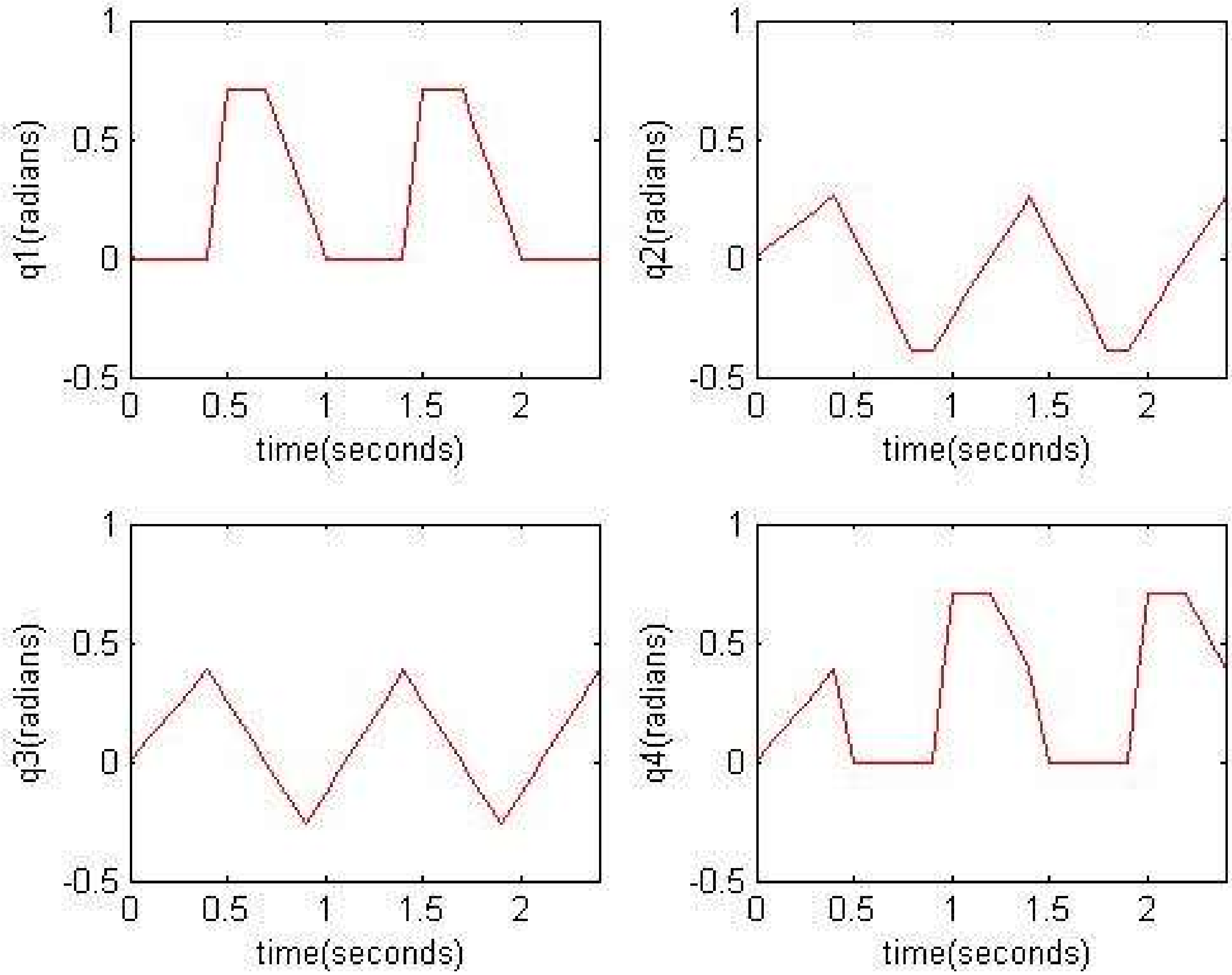

Joint Angles q_1, q_2, q_3, and q_4 vs. time for Simulated Humanoid Walking (adapted from Lum, 1999)

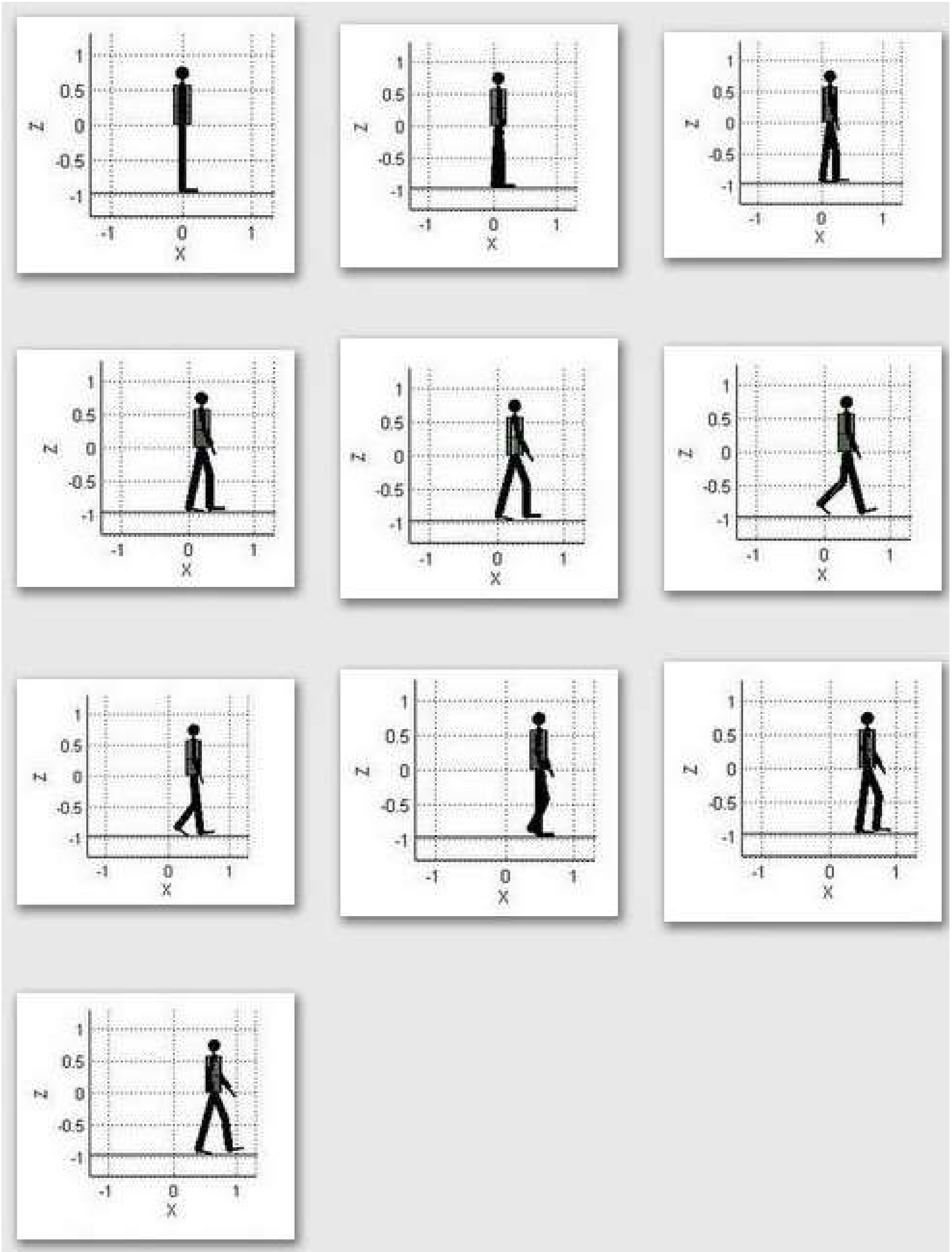

Humanoid Robot, one Complete Gait Cycle

Chandana Ventayogi

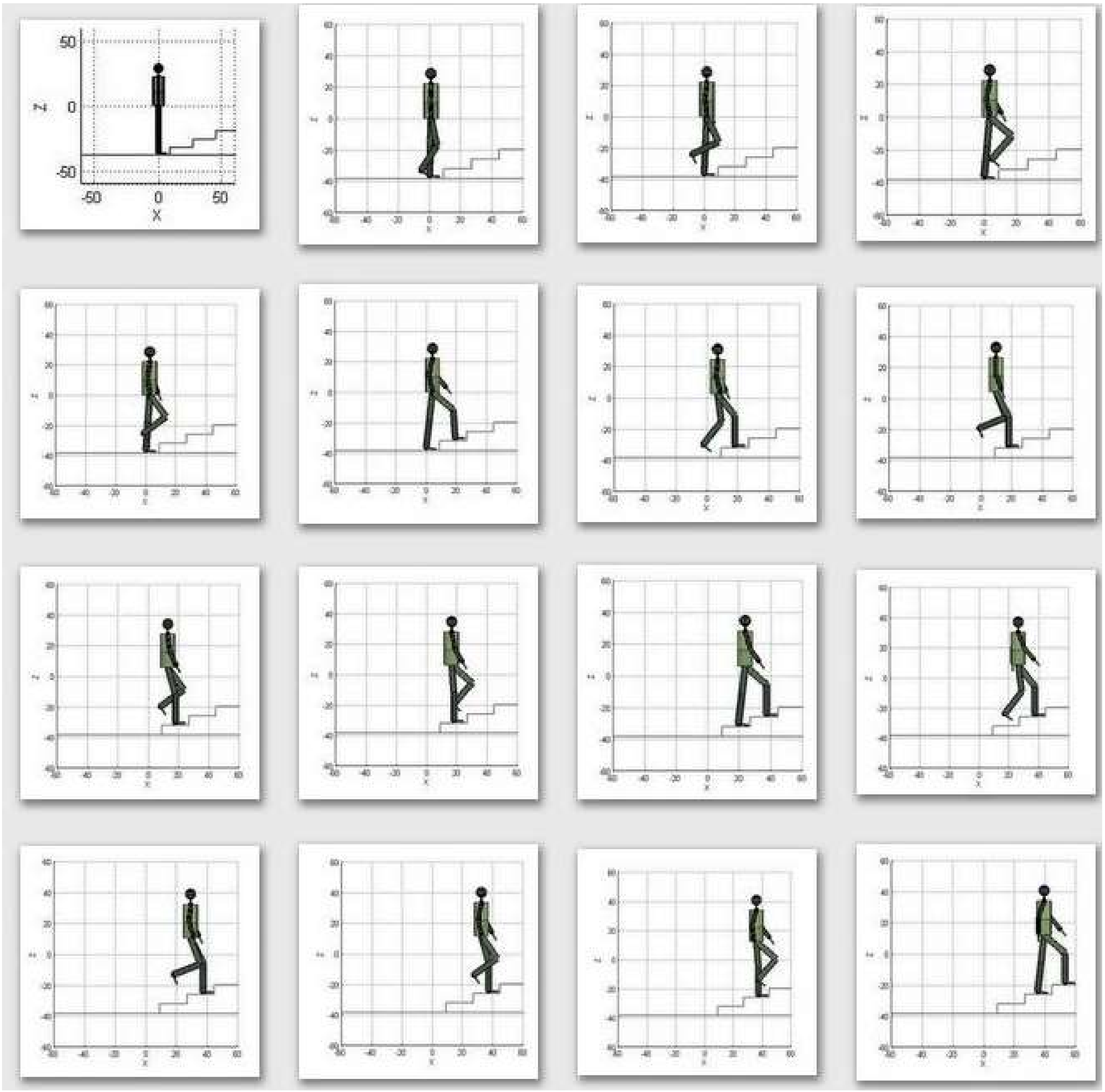

Humanoid Robot Climbing Stairs

Chandana Ventayogi

Appendices

These four appendices augment the material in the ME 4670 / 5670 NotesBook:

http://www.lulu.com/content/e-book/engineering-biomechanics-of-human-motion/20853532

Included here are:

Appendix A. Main Joints of the Human Body

Appendix B. Human Synovial Joint Motion Ranges

Appendix C. Skeletal Muscles for the Major Joints

Appendix D. Human Body Anthropomorphic Parameters

Appendix A. Main Joints of the Human Body

This appendix presents the main joints of the human body, with joint, joint type, and movement listed in tabular form. (adapted from Spence, 1982). dof stands for degrees-of-freedom for each joint. Dr. Bob added that column.

Joint	Type	Movement	dof
cranial bones (skull)	suture	none	0
distal tibia / fibula (ankle)	syndesmosis	slight give	0
mid radius / ulna (forearm)	syndesmosis	slight give	0
ribs / sternum (breastbone)	synchondrosis	slight movement	0
pubic bones (pelvis)	symphysis	slight movement	0
vertebrae (spine)	symphysis	slight movement	0
sacrum / ilium (spine base)	synchondrosis / gliding	slight gliding movement	0
articular processes of vertebrae	plane	gliding	2
rib / vertebrae (back)	plane	gliding	2
occipital / atlas (neck)	ellipsoidal	flexion / extension abduction / adduction	2
atlas / axis (neck)	pivot	rotation about odontoid process	1
sternum / clavicle (shoulder)	plane	gliding	2
scapula / clavicle (shoulder)	plane	gliding	2
scapula / humerus (shoulder)	ball and socket	flexion / extension abduction / adduction medial / lateral rotation	3
humerus / ulna (elbow)	hinge	flexion / extension	1
end radius / ulna (wrist)	pivot	pronation / supination	1
radius / carpals (wrist)	ellipsoidal	flexion / extension abduction / adduction	2
carpals (hand)	plane	gliding	2

Joint	**Type**	**Movement**	**dof**
first metacarpal / carpal (thumb)	saddle	flexion / extension abduction / adduction	2
second through fifth metacarpal / carpal	plane	gliding	2
metacarpals / phalanges (hand)	ellipsoidal	flexion / extension abduction / adduction	2
phalanges (fingers)	hinge	flexion / extension	1
os coxae / femur (hip)	ball and socket	flexion / extension abduction / adduction medial / lateral rotation	3
femur / tibia (knee)	hinge	flexion / extension some rotation	1
tibia / proximal fibula (knee)	plane	gliding	2
distal fibula / tibia and talus (ankle)	hinge	flexion / extension	1
tarsals (ankle)	plane	gliding	2
tarsals / metatarsals (foot)	plane	gliding	2
metatarsals / phalanges (foot)	ellipsoidal	flexion / extension abduction / adduction	2
phalanges (toes)	hinge	flexion / extension	1

Appendix B. Human Synovial Joint Motion Ranges

This appendix presents some average angular motion ranges for human synovial joints in table form from four different sources, in units of *degrees*. Many factors affect joint range (flexibility) including age, gender, body type, disease, level of activity, and past injury, among other factors. Therefore, the data in this appendix is approximate for any individual. Note the spine motion ranges given are for gross motion and not individual vertebrae. The first two pages of this appendix were adapted from Hamilton et al. (2008).

The four sources are 1. AMA (1990); 2. Smith and Lehmkuhl (1983); 3. Kendall (1971); and 4. Gerhardt and Russe (1975). Not all sources have data for each category.

The individual vertebrae rotation limits (lumbar and thoracic) are given last, from Kapandji (1974b) and White and Panjabi (1990).

This joint range data is for active motions, i.e. caused by the subject (as opposed to passive motions, i.e. caused by an external source – e.g. force from another person).

		Source			
Joint	**Direction**	**1**	**2**	**3**	**4**
elbow	flexion	140	145	145	145
	hyperextension	0	0	0	0–10
forearm	pronation	80	90	90	80
	supination	80	85	90	90
wrist	extension	60	70	70	50
	flexion	60	90		60
	radial flexion	20	20	20	20
	ulnar flexion	30	30	35	30
shoulder	flexion	180	170	130	180
	hyperextension	50	30	80	60
	abduction	180	170	180	180
	adduction	50			
	horizontal flexion				135
	horizontal extension				45
	inward	90	90	70	60–90
	outward	90	90	70	90

		Source			
Joint	**Direction**	**1**	**2**	**3**	**4**
hip	flexion	100	120	125	120
	hyperextension	30	10	10	30
	abduction	40	45	45	45
	adduction	20		10	0–25
	inward	40	35	45	40–45
	outward	50	45	45	45
knee	flexion	150	120	140	130
ankle	plantar flexion	20	45	45	50
	dorsiflexion	30	15	20	20
spine	flexion	60			40
(cervical)	hyperextension	75			40
	lateral flexion	45			45
	rotation	80			50
spine	flexion	45–50			45
(thoracic and	hyperextension	25			20–35
lumbar)	lateral flexion	25			30
	rotation	30			45

Now we present individual vertebra rotation limits, about all three rotation axes, as shown in the figure below.

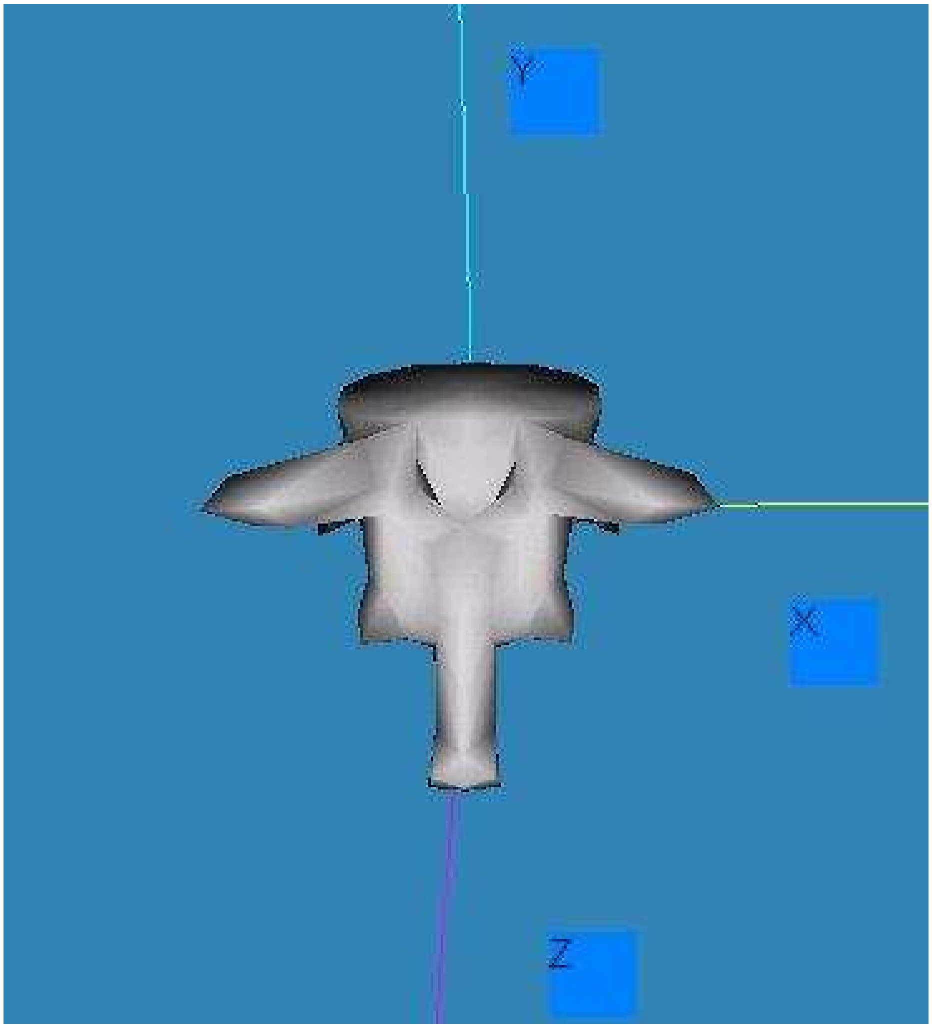

Vertebra with the three rotation axes

Individual Vertebral Joint Limits (deg)

Vertebra	X		Y		Z	
	Max	**Min**	**Max**	**Min**	**Max**	**Min**
L5	8.5	-8.5	1.0	-1.0	3.0	-3.0
L4	8.0	-8.0	2.0	-2.0	6.0	-6.0
L3	7.5	-7.5	2.0	-2.0	8.0	-8.0
L2	7.0	-7.0	2.0	-2.0	6.0	-6.0
L1	6.0	-6.0	2.0	-2.0	6.0	-6.0
T12	2.0	-2.0	9.0	-9.0	5.0	-5.0
T11	2.0	-2.0	8.0	-8.0	6.0	-6.0
T10	2.0	-2.0	8.0	-8.0	5.0	-5.0
T9	2.0	-2.0	8.0	-8.0	6.0	-6.0
T8	2.0	-2.0	8.0	-8.0	6.0	-6.0
T7	2.5	-2.5	7.0	-7.0	6.0	-6.0
T6	3.0	-3.0	7.0	-7.0	6.0	-6.0
T5	3.0	-3.0	6.0	-6.0	6.0	-6.0
T4	3.0	-3.0	4.0	-4.0	6.0	-6.0
T3	4.5	-4.5	2.0	-2.0	7.0	-7.0
T2	6.0	-6.0	2.0	-2.0	9.0	-9.0
T1	6.0	-6.0	2.0	-2.0	8.0	-8.0
C7	3.0	-3.0	8.0	-8.0	4.0	-4.0
C6	8.0	-8.0	9.0	-9.0	7.0	-7.0
C5	8.5	-8.5	10.0	-10.0	8.0	-8.0
C4	6.0	-6.0	12.0	-12.0	11.0	-11.0
C3	6.5	-6.5	11.0	-11.0	11.0	-11.0
C2	4.0	-4.0	9.0	-9.0	10.0	-10.0
C1	5.0	-5.0	47.0	-47.0	8.0	-8.0

Kapandji (1974b)

Appendix C. Skeletal Muscles for the Major Joints

This appendix presents tables from Hall (2007) that summarize the skeletal muscles moving the major joints. This could be considered functional anatomy. Covered are the muscle names, proximal and distal attachments, primary motion actions, and innervation for the major muscles of the shoulder, elbow, hand and fingers, hip, knee, ankle and foot, and the spine.

Muscles of the Shoulder

MUSCLE	PROXIMAL ATTACHMENT	DISTAL ATTACHMENT	PRIMARY ACTION(S)	INNERVATION
Deltoid	Outer third of clavicle, top of acromion, scapular spine	Deltoid tuberosity of humerus		Axillary (C_5, C_6)
(Anterior)			Flexion, horizontal adduction, medial rotation	
(Middle)			Abduction, horizontal abduction	
(Posterior)			Extension, horizontal abduction, lateral rotation	
Pectoralis major		Lateral aspect of humerus just below head		
(Clavicular)	Medial two-thirds of clavicle		Flexion, horizontal adduction, medial rotation	Lateral pectoral (C_5–T_1)
(Sternal)	Anterior sternum and cartilage of first six ribs		Extension, adduction, horizontal adduction, medial rotation	Medial pectoral (C_5–T_1)
Supraspinatus	Supraspinous fossa	Greater tuberosity of humerus	Abduction, assists with lateral rotation	Suprascapular (C_5, C_6)
Coracobrachialis	Coracoid process of scapula	Medial anterior humerus	Flexion, adduction, horizontal adduction	Musculocutaneous (C_5–C_7)
Latissimus dorsi	Lower six thoracic and all lumbar vertebrae, posterior sacrum, iliac crest, lower three ribs	Anterior humerus	Extension, adduction, medial rotation, horizontal abduction	Thoracodorsal (C_6–C_8)
Teres major	Lower, lateral, dorsal scapula	Anterior humerus	Extension, adduction, medial rotation	Subscapular (C_5, C_6)
Infraspinatus	Infraspinous fossa	Greater tubercle of humerus	Lateral rotation, horizontal abduction	Subscapular (C_5, C_6)
Teres minor	Posterior, lateral border of scapula	Greater tubercle, adjacent shaft of humerus	Lateral rotation, horizontal abduction	Axillary (C_5, C_6)
Subscapularis	Entire anterior surface of scapula	Lesser tubercle of humerus	Medial rotation	Subscapular (C_5, C_6)
Biceps brachii		Radial tuberosity		Musculocutaneous (C_5–C_7)
(Long head)	Upper rim of glenoid fossa		Assists with abduction	
(Short head)	Coracoid process of scapula		Assists with flexion, adduction, medial rotation, horizontal adduction	
Triceps brachii (Long head)	Just inferior to glenoid fossa	Olecranon process of ulna	Assists with extension, adduction	Radial (C_5–T_1)

Hall (2007)

Muscles of the Elbow

MUSCLE	PROXIMAL ATTACHMENT	DISTAL ATTACHMENT	PRIMARY ACTION(S)	INNERVATION
Biceps brachii		Radial tuberosity	Flexion, assists with supination	Musculocutaneous (C_5–C_7)
(Long head)	Upper rim of glenoid fossa			
(Short head)	Coracoid process of scapula			
Brachioradialis	Upper two-thirds of lateral supracondylar ridge of humerus	Styloid process of radius	Flexion, pronation from supinated position to neutral, supination from pronated position to neutral	Radial (C_5, C_6)
Brachialis	Anterior lower half of humerus	Anterior coronoid process of ulna	Flexion	Musculocutaneous (C_5, C_6)
Pronator Teres		Lateral midpoint of radius	Pronation, assists with flexion	Median (C_6, C_7)
(Humeral head)	Medial epicondyle of humerus			
(Ulnar head)	Coronoid process of ulna			
Pronator quadratus	Lower fourth of anterior ulna	Lower fourth of anterior radius	Pronation	Anterior interosseous (C_8, T_1)
Triceps brachii		Olecranon process of ulna	Extension	Radial (C_6–C_8)
(Long head)	Just inferior to glenoid fossa			
(Lateral head)	Upper half of posterior humerus			
(Medial head)	Lower two-thirds of posterior humerus			
Anconeus	Posterior, lateral epicondyle of humerus	Lateral olecranon and posterior ulna	Assists with extension	Radial (C_7, C_8)
Supinator	Lateral epicondyle of humerus and adjacent ulna	Lateral upper third of radius	Supination	Posterior interosseou (C_5, C_6)

Hall (2007)

Major Muscles of the Hand and Fingers

MUSCLE	PROXIMAL ATTACHMENT	DISTAL ATTACHMENT	PRIMARY ACTION(S)	INNERVATION
		EXTRINSIC MUSCLES		
Extensor pollicis longus	Middle dorsal ulna	Dorsal distal phalanx of thumb	Extension at MP and IP joints of thumb, adduction at MP joint of thumb	Radial (C_7, C_8)
Extensor pollicis brevis	Middle dorsal radius	Dorsal proximal phalanx of thumb	Extension at MP and CM joints of thumb	Radial (C_7, C_8)
Flexor pollicis longus	Middle palmar radius	Palmar distal phalanx of thumb	Flexion at IP and MP joints of thumb	Median (C_8, T_1)
Abductor pollicis longus	Middle dorsal ulna and radius	Radial base of 1st metacarpal	Abduction at CM joint of thumb	Radial (C_7, C_8)
Extensor indicis	Distal dorsal ulna	Ulnar side of extensor digitorum tendon	Extension at MP joint of 2nd digit	Radial (C_7, C_8)
Extensor digitorum	Lateral epicondyle of humerus	Base of 2nd and 3rd phalanges, digits 2–5	Extension at MP, proximal and distal IP joints, digits 2–5	Radial (C_7, C_8)
Extensor digiti minimi	Proximal tendon of extensor digitorum	Tendon of extensor digitorum distal to 5th MP joint	Extension at 5th MP joint	Radial (C_7, C_8)
Flexor digitorum profundus	Proximal three-fourths of ulna	Base of distal phalanx, digits 2–5	Flexion at distal and proximal IP joints and MP joints, digits 2–5	Ulnar and median (C_8, T_1)
Flexor digitorum superficialis	Medial epicondyle of humerus	Base of middle phalanx, digits 2–5	Flexion at proximal IP and MP joints, digits 2–5	Median (C_7, C_8, T_1)
		INTRINSIC MUSCLES		
Flexor pollicis brevis	Ulnar side, 1st metacarpal	Ulnar, palmar base of proximal phalanx of thumb	Flexion and adduction at MP joint of thumb	Median (C_8, T_1)
Abductor pollicis brevis	Trapezium and schaphoid bones	Radial base of 1st phalanx of thumb	Abduction at 1st CM joint	Median (C_8, T_1)
Opponens pollicis	Schaphoid bone	Radial side of 1st metacarpal	Flexion and abduction at CM joint of thumb	Median (C_8, T_1)
Adductor pollicis	Capitate, distal 2nd and 3rd metacarpals	Ulnar proximal phalanx of thumb	Adduction and flexion at CM joint of thumb	Ulnar (C_8, T_1)
Abductor digiti minimi	Pisiform bone	Ulnar base of proximal phalanx, 5th digit	Abduction and flexion at 5th MP joint	Ulnar (C_8, T_1)
Flexor digiti minimi brevis	Hamate bone	Ulnar base of proximal phalanx, 5th digit	Flexion at 5th MP joint	Ulnar (C_8, T_1)
Opponens digiti minimi	Hamate bone	Ulnar metacarpal of 5th metacarpal	Opposition at 5th CM joint	Ulnar (C_8, T_1)
Dorsal interossei (four muscles)	Sides of metacarpals, all digits	Base of proximal phalanx, all digits	Abduction at 2nd and 4th MP joints, radial and ulnar deviation at 3rd MP joint, flexion at MP joints 2–4	Ulnar (C_8, T_1)
Palmar interossei (three muscles)	2nd, 4th, and 5th metacarpals	Base of proximal phalanx, digits 2, 4, and 5	Adduction and flexion at MP joints, digits 2, 4, and 5	Ulnar (C_8, T_1)
Lumbricales (four muscles)	Tendons of flexor digitorum profundus, digits 2–5	Tendons of extensor digitorum, digits 2–5	Flexion at MP joints of digits 2–5	Median and ulnar (C_8, T_1)

Hall (2007)

Muscles of the Hip

MUSCLE	PROXIMAL ATTACHMENT	DISTAL ATTACHMENT	PRIMARY ACTION(S) ABOUT THE HIP	INNERVATION
Rectus femoris	Anterior inferior iliac spine (ASIS)	Patella	Flexion	Femoral (L_2–L_4)
Iliopsoas		Lesser trochanter of femur	Flexion	L_1 and femoral
(Iliacus)	Iliac fossa and adjacent sacrum			(L_2–L_4)
(Psoas)	12th thoracic and all lumbar vertebrae and lumbar discs			(L_1–L_3)
Sartorius	Anterior superior iliac spine	Upper medial tibia	Assists with flexion, abduction, lateral rotation	Femoral (L_2, L_3)
Pectineus	Pectineal crest of pubic ramus	Medial, proximal femur	Flexion, adduction, medial rotation	Femoral (L_2, L_3)
Tensor fascia latae	Anterior crest of ilium and ASIS	Iliotibial band	Assists with flexion, abduction, medial rotation	Superior gluteal (L_4–S_1)
Gluteus maximus	Posterior ilium, iliac crest, sacrum, coccyx	Gluteal tuberosity of femur and iliotibial band	Extension, lateral rotation	Inferior gluteal (L_5–S_2)
Gluteus medius	Between posterior and anterior gluteal lines on posterior ilium	Superior, lateral greater trochanter	Abduction, medial rotation	Superior gluteal (L_4–S_1)
Gluteus minimus	Between anterior and inferior gluteal lines on posterior ilium	Anterior surface of greater trochanter	Abduction, medial rotation	Superior gluteal (L_4–S_1)
Gracilis	Anterior, inferior pubic symphysis	Medial, proximal tibia	Adduction	Obturator (L_3, L_4)
Adductor magnus	Inferior ramus of pubis and ischium	Entire linea aspera	Adduction, lateral rotation	Obturator (L_3, L_4)
Adductor longus	Anterior pubis	Middle linea aspera	Adduction, assists with flexion	Obturator (L_3, L_4)
Adductor brevis	Inferior ramus of the pubis	Upper linea aspera	Adduction, lateral rotation	Obturator (L_3, L_4)
Semitendinosus	Medial ischial tuberosity	Proximal, medial tibia	Extension	Tibial (L_5–S_1)
Semimembranosus	Lateral ischial tuberosity	Proximal, medial tibia	Extension	Tibial (L_5–S_1)
Biceps femoris (long head)	Lateral ischial tuberosity	Posterior lateral condyle of tibia, head of fibula	Extension	Tibial (L_5–S_2)
The six outward rotators	Sacrum, ilium, ischium	Posterior greater trochanter	Outward rotation	(L_5–S_2)

Hall (2007)

Muscles of the Knee

MUSCLE	PROXIMAL ATTACHMENT	DISTAL ATTACHMENT	PRIMARY ACTION(S) ABOUT THE KNEE	INNERVATION
Rectus femoris	Anterior inferior iliac spine (ASIS)	Patella	Extension	Femoral (L_2–L_4)
Vastus lateralis	Greater trochanter and lateral linea aspera	Patella	Extension	Femoral (L_2–L_4)
Vastus intermedius	Anterior femur	Patella	Extension	Femoral (L_2–L_4)
Vastus medialis	Medial linea aspera	Patella	Extension	Femoral (L_2–L_4)
Semitendinosus	Medial ischial tuberosity	Proximal medial tibia at pes	Flexion, medial rotation	Sciatic (L_5–S_2)
Semimembranosus	Lateral ischial tuberosity	Proximal medial tibia	Flexion, medial rotation	Sciatic (L_5–S_2)
Biceps femoris		Posterior lateral condyle of tibia, head of fibula	Flexion, lateral rotation	Sciatic (L_5–S_2)
(Long head)	Ischial tuberosity			
(Short head)	Lateral linea aspera			
Sartorius	Anterior superior iliac spine	Proximal medial tibia at pes	Assists with flexion and lateral rotation of thigh	Femoral (L_2, L_3)
Gracilis	Anterior, inferior symphysis pubis	Proximal medial tibia at pes	Adduction of thigh, flexion of lower leg	Obturator (L_2, L_3)
Popliteus	Lateral condyle of the femur	Posterior medial tibia	Medial rotation, flexion	Tibial (L_4, L_5)
Gastrocnemius	Posterior medial and lateral femoral condyles	Tuberosity of calcaneus via Achilles tendon	Flexion	Tibial (S_1, S_2)
Plantaris	Distal posterior femur	Tuberosity of calcaneus	Flexion	Tibial (S_1, S_2)

Hall (2007)

Muscles of the Ankle and Foot

MUSCLE	PROXIMAL ATTACHMENT	DISTAL ATTACHMENT	PRIMARY ACTION(S)	INNERVATION
Tibialis anterior	Upper two-thirds of lateral tibia	Medial surface of first cuneiform and first metatarsal	Dorsiflexion, inversion	Deep peroneal (L_4–S_1)
Extensor digitorum longus	Lateral condyle of tibia, head of fibula, upper two-thirds of anterior fibula	Second and third phalanges of four lesser toes	Toe extension, dorsiflexion, eversion	Deep peroneal (L_4–S_1)
Peroneus tertius	Lower third anterior fibula	Dorsal surface of fifth metatarsal	Dorsiflexion, eversion	Deep peroneal (L_4–S_1)
Extensor hallucis longus	Middle two-thirds of medial anterior fibula	Dorsal surface of distal phalanx of great toe	Dorsiflexion, inversion, hallux extension	Deep peroneal (L_4–S_1)
Gastrocnemius	Posterior medial and lateral condyles of femur	Tuberosity of calcaneus via Achilles tendon	Plantar flexion	Tibial (S_1–S_2)
Plantaris	Distal, posterior femur	Tuberosity of calcaneus via Achilles tendon	Assists with plantar flexion	Tibial (S_1–S_2)
Soleus	Posterior proximal fibula and proximal two-thirds of posterior tibia	Tuberosity of calcaneus via Achilles tendon	Plantar flexion	Tibial (S_1–S_2)
Peroneus longus	Head and upper two-thirds of lateral fibula	Lateral surface of first cuneiform and first metatarsal	Plantar flexion, eversion	Superficial peroneal (L_4–S_1)
Peroneus brevis	Distal two-thirds lateral	Tuberosity of fifth fibula	Plantar flexion, eversion metatarsal	Superficial peroneal (L_4–S_1)
Flexor digitorum longus	Middle third of posterior tibia	Distal phalanx of four lesser toes	Plantar flexion, inversion, toe flexion	Tibial (L_5–S_1)
Flexor hallucis longus	Middle two-thirds of posterior fibula	Distal phalanx of great toe	Plantar flexion, inversion, toe flexion	Tibial (L_4–S_2)
Tibialis posterior	Posterior upper two-thirds tibia and fibula and interosseous membrane	Cuboid, navicular, and second to fifth metatarsals	Plantar flexion, inversion	Tibial (L_5–S_1)

Hall (2007)

Muscles of the Spine

MUSCLE	PROXIMAL ATTACHMENT	DISTAL ATTACHMENT	PRIMARY ACTION(S) ABOUT THE HIP	INNERVATION
Prevertebral muscles (rectus capitis anterior, rectus capitis lateralis, longus capitis, longus coli)	Anterior aspect of occipital bone and cervical vertebrae	Anterior surfaces of cervical and first three thoracic vertebrae	Flexion, lateral flexion, rotation to opposite side	Cervical nerves (C_1–C_6)
Rectus abdominis	Costal cartilage of ribs 5–7	Pubic crest	Flexion, lateral flexion	Intercostal nerves (T_6–T_{12})
External oblique	External surface of lower eight ribs	Linea alba and anterior iliac crest	Flexion, lateral flexion, rotation to opposite side	Intercostal nerves (T_7 –T_{12})
Internal oblique	Linea alba and lower four ribs	Inguinal ligament, iliac crest, lumbodorsal fascia	Flexion, lateral flexion, rotation to same side	Intercostal nerves (T_7–T_{12}, L_1)
Splenius (capitis and cervicis)	Mastoid process of temporal bone, transverse processes of first three cervical vertebrae	Lower half of ligamentum nuchae, spinous processes of seventh cervical and upper six thoracic vertebrae	Extension, lateral flexion, rotation to same side	Middle and lower cervical nerves (C_4–C_8)
Suboccipitals (obliquus capitus superior and inferior, rectus capitis posterior major and minor)	Occipital bone, transverse process of first cervical vertebra	Posterior surfaces of first two cervical vertebrae	Extension, lateral flexion, rotation to same side	Suboccipital nerve (C_1)
Erector spinae (spinalis, longissimus, iliocostalis)	Lower part of ligamentum nuchae, posterior cervical, thoracic, and lumbar spine, lower nine ribs, iliac crest, posterior sacrum	Mastoid process of temporal bone, posterior cervical, thoracic, and lumbar spine, twelve ribs	Extension, lateral flexion, rotation to opposite side	Spinal nerves (T_1–T_{12})
Semispinalis (capitis, cervicis, thoracis)	Occipital bone, spinous processes of thoracic vertebrae 2–4	Transverse presses of thoracic and seventh cervical vertebrae	Extension, lateral flexion, rotation to opposite side	Cervical and thoracic spinal nerves (C_1–T_{12})
Deep spinal muscles (multifidi, rotatores, interspinales, intertransversarii, levatores costarum)	Posterior processes of all vertebrae, posterior sacrum	Spinous and transverse processes and laminae of vertebrae below those of proximal attachment	Extension, lateral flexion, rotation to opposite side	Spinal and intercostal nerves (T_1–T_{12})
Sternocleidomastoid	Mastoid process of temporal bone	Superior sternum, inner third of clavicle	Flexion of neck, extension of head, lateral flexion, rotation to opposite side	Accessory nerve and C_2 spinal nerve
Levator scapulae	Transverse processes of first four cervical vertebrae	Vertebral border of scapula	Lateral flexion	Spinal nerves (C_3–C_4), dorsal scapular nerve (C_3–C_5)
Scaleni (scalenus anterior, medius, posterior)	Transverse processes of cervical vertebrae	Upper two ribs	Flexion, lateral flexion	Cervical nerves (C_3–C_7)
Quadratus lumborum	Last rib, transverse processes of first four lumbar vertebrae	Iliolumbar ligament, adjacent iliac crest	Lateral flexion	Spinal nerves (T_{12}–L_4)
Psoas major	Sides of twelfth thoracic and all lumbar vertebrae	Lesser trochanter of the femur	Flexion	Femoral nerve (L_1–L_3)

Hall (2007)

Appendix D. Human Body Anthropomorphic Parameters

This appendix presents some average anthropomorphic parameters for the adult human body. Included are segment lengths (based on body height), segment weights (based on body weight), segment center of gravity (based on segment length) and segment radius of gyration (based on segment length), from which mass moments of inertia may be calculated given segment mass. These parameters are adapted from Hall (2007), which is based on Plagenhoef et al. (1983). This information is required for kinematics, statics, and dynamics modeling of human motion.

An alternative method (not presented here) to find anthropomorphic parameters for the human body is the software **Generator of Body** (**GEBOD**) preprocessing program, used with the **Articulated Total Body** (**ATB**) software of the USAF, for adult males, adult females, children, or test dummies, all of different sizes (dtic.mil).

Segment Lengths as a Percentage of Body Height

Segment	Males	Females
head and neck	10.75	10.75
trunk	30.00	29.00
upper arm	17.20	17.30
forearm	15.70	16.00
hand	5.75	5.75
thigh	23.20	24.90
lower leg	24.70	25.70
ankle-to-floor height	4.25	4.25
foot length*	14.84	14.59

*Measured in ME 4670 / 5670 Spring 2008, n = 37, 9 (Internet searches yielded 15.0% and 15.2%, for average male and female populations, respectively).

Segment Weights as a Percentage of Body Weight

Segment	Males	Females
head and neck	8.26	8.20
trunk	46.84	45.00
upper arm	3.25	2.90
forearm	1.87	1.57
hand	0.65	0.50
thigh	10.50	11.75
lower leg	4.75	5.35
foot	1.43	1.33

In elbow flexion simulations of ME 4670 / 5670 the biceps and triceps insertion points are required, which requires the lengths along the forearm r_B and r_T. These were simply scaled from a forearm musculoskeletal figure (where L_2 is the forearm segment length, male or female):

$$r_B = \left[\frac{3/8}{1\,7/8}\right] L_2 \qquad\qquad r_T = \left[\frac{3/16}{1\,7/8}\right] L_2$$

Segment Center of Gravity as a Percentage of Segment Length (from the proximal end)

Segment	Males	Females
head and neck	56.7	56.7
trunk	56.2	56.9
upper arm	43.6	45.8
forearm	43.0	43.4
hand	46.8	46.8
thigh	43.3	42.8
lower leg	43.4	41.9
foot	50.0	50.0
whole body (from ground)	56.0	54.3

See the figure on the following page.

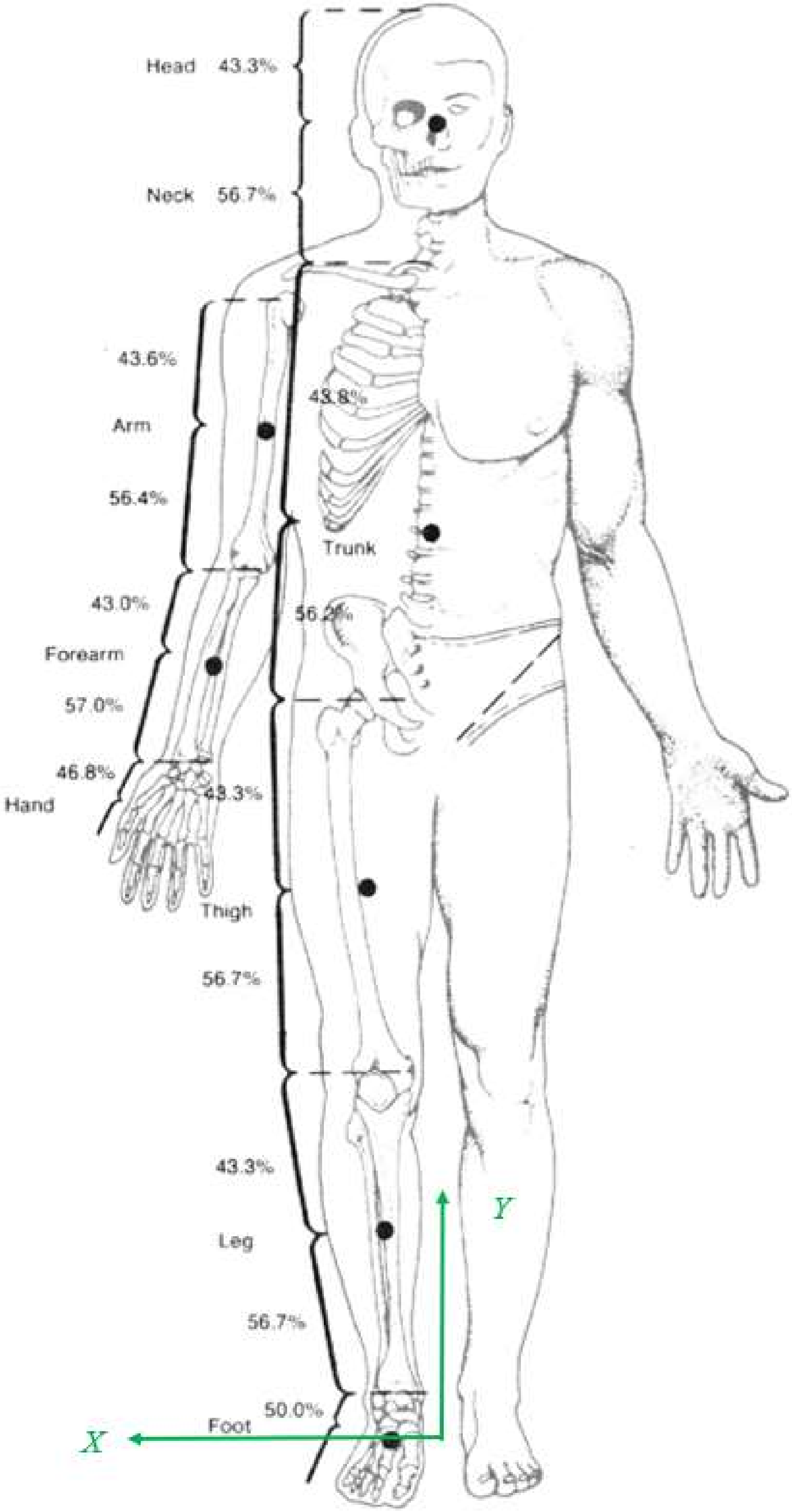

Adult Male Human Body Segment CGs

Hamilton et al. (2008)

Segment Radii of Gyration as a Percentage of Segment Length

	Males		Females	
Segment	**Proximal r_p**	**Distal r_d**	**Proximal r_p**	**Distal r_d**
upper arm	54.2	64.5	56.4	62.3
forearm	52.6	54.7	53.0	64.3
hand	54.9	54.9	54.9	54.9
thigh	54.0	65.3	53.5	65.8
lower leg	52.9	64.2	51.4	65.7
foot	69.0	69.0	69.0	69.0

See the figure on the previous page.

To use this table to find the mass moments of inertia about axes through the link ends, use the following equations.

$$I_p = mr_p^2 \qquad\qquad I_d = mr_d^2$$

where r_p is the radius of gyration referred to the proximal segment end and r_d is the radius of gyration referred to the distal segment end. Both r_p and r_d must have units of length (m), but they are given in terms of percentage of segment length above. Note only the most significant I_{ZZ} is given in this appendix, via the radii of gyration for each segment. One can assume a cylinder or ellipsoid for most human body segment shapes to find I_{XX} and I_{YY} for 3D dynamics.

The mass moments of inertia about the CG are calculated by using the parallel axis theorem:

$$I_p = I_{CG} + mr_{CG}^2 \qquad\qquad I_d = I_{CG} + m\left(L - r_{CG}\right)^2$$

$$I_{CG} = I_p - mr_{CG}^2 \qquad\qquad I_{CG} = I_d - m\left(L - r_{CG}\right)^2$$

where r_{CG} is the length from the proximal segment end to the CG and L is the segment length. Both formulae above will yield the same answer. Note that since I_{CG} is always a positive number, we must necessarily have:

$$r_p > r_{CG} \qquad\qquad r_d > L - r_{CG}$$

Note the mass moments of inertia of the head/neck and trunk were not given in the table above. How do we estimate these values?

Earlier tables give the weight percentages for these segments, from which we can easily find the mass of each segment. Then assume simple geometric shapes (sphere/cylinder for the head/neck and cylinder or rectangular parallelepiped for the trunk) and use their known mass moment of inertia formulae. For a powerful alternative, use CAD software.

Now, for convenience, this anthropomorphic data is used to tabulate the various parameters in SI units for two specific adult humans.

- Male 6’0” 200 lbs (1.829 m, 889.6 N, 90.7 kg).
- Female 5’2” 100 lbs (1.575 m, 444.8 N, 45.3 kg).

Segment Lengths (m)

Segment	Male	Female
head and neck	0.197	0.169
trunk	0.549	0.457
upper arm	0.315	0.272
forearm	0.287	0.252
hand	0.105	0.091
thigh	0.424	0.392
lower leg	0.452	0.405
ankle-to-floor height	0.078	0.067
foot length	0.271	0.230

Biceps/triceps insertion lengths

$r_{Bm} = 0.057$ $r_{Tm} = 0.029$ $r_{Bf} = 0.050$ $r_{Tf} = 0.025$

Segment Weights (N)

Segment	Male	Female
head and neck	73.48	36.47
trunk	416.69	200.16
upper arm	28.91	12.90
forearm	16.64	6.98
hand	5.78	2.22
thigh	93.41	52.26
lower leg	42.26	23.80
foot	12.72	5.92

Segment Masses (kg)

Segment	Male	Female
head and neck	7.490	3.718
trunk	42.476	20.404
upper arm	2.947	1.315
forearm	1.696	0.712
hand	0.589	0.227
thigh	9.522	5.328
lower leg	4.307	2.426
foot	1.297	0.603

Segment Center of Gravity Lengths (m)

(r_{CG}, measured from proximal end)

Segment	Male	Female
head and neck	0.112	0.096
trunk	0.309	0.260
upper arm	0.137	0.125
forearm	0.123	0.109
hand	0.049	0.043
thigh	0.184	0.168
lower leg	0.196	0.170
foot	0.039	0.034

Segment Radii of Gyration (m)

(r_p, about proximal end)

Segment	Male	Female
upper arm	0.171	0.153
forearm	0.151	0.134
hand	0.058	0.050
thigh	0.229	0.210
lower leg	0.239	0.208
foot	0.054	0.046

Mass Moment of Inertia (kg-m²)

(I_p, about proximal end)

Segment	Male	Female
upper arm	0.0859	0.0309
forearm	0.0387	0.0127
hand	0.0020	0.0006
thigh	0.4992	0.2343
lower leg	0.2462	0.1051
foot	0.0038	0.0013

Mass Moment of Inertia (kg-m²)

(I_{CG}, about CG)

Segment	Male	Female
upper arm	0.0303	0.0105
forearm	0.0128	0.0042
hand	0.0005	0.0002
thigh	0.1782	0.0844
lower leg	0.0805	0.0353
foot	0.0018	0.0006